SPATIAL REGULATION OF CELL DIVISION BY THE MIN SYSTEM IN *ESCHERICHIA COLI*

BY

Bang Shen

Submitted to the graduate degree program in Microbiology, Molecular Genetics and Immunology and the Graduate Faculty of the University of Kansas in partial fulfillment of the requirements for the degree of Doctor of Philosophy.

Dissertation Committee:

_____
Joe Lutkenhaus, Ph.D., Chairman

_____
Indranil Biswas, Ph.D.

_____
Kee Jun Kim, Ph.D.

_____
Kenneth Peterson, Ph.D.

_____
Wolfram Züeckert, Ph.D.

Date defended: April 1st, 2010

The Dissertation Committee for Bang Shen

certifies that this is the approved version of the following dissertation:

SPATIAL REGULATION OF CELL DIVISION BY THE MIN SYSTEM IN *ESCHERICHIA COLI*

_____

Joe Lutkenhaus, Ph.D., Chairperson

Acknowledgements

I want to take this opportunity to thank my mentor Joe Lutkenhaus for his guidance and support of my research all these years. His scientific sense and knowledge are invaluable for my studies and his mentoring stytle makes it a very pleasant experience working in the lab. I also want to thank him for his help in getting me into the graduate school at KU Medical Center.

Thanks also go to the previous and current members of the Lutkehaus lab for their help and support. Sebastien Pichoff is a great resource for suggestions regarding bacterial genetics. Alex Dajković and Christina Hester offered valuable advices and discussions throughout this study.

Drs. Indranil Biswas, Kee Jun Kim, Kenneth Peterson and Wolfram Zueckert also deserve gratitude for serving on my thesis committee. I am also grateful to Dr. Yi, who introduced me into this wonderful lab.

Lastly, I want to extend my appreciation to my parents and my wife, their support and encouragement is critical to this work.

Table of Contents

List of Figures

List of Tables

Abbreviations

ADP: adenosine diphosphate

ATP: adenosine triphosphate

DNA: deoxyribonucleic acid

GFP: green fluorescent protein

IPTG: isopropyl-β-thiogalactopyranoside

LB: Luria-Bertani medium

OD: optical density

GDP: guanosine diphosphate

GTP: guanosine triphosphate

HEPES: N-(2-hydroxymethyl)piperazine-N'-(2-ethanesulfonic acid)

MES: 2-Morpholinoethanesulfonic acid

PAGE: polyacrylamide gel electrophoresis

SDS: sodium dodecyl sulfate

Amp^R: ampicillin resistance

Abstract

The *E. coli* Min system contributes to spatial regulation of cell division by preventing Z ring assembly at cell poles. Critical to our understanding of this spatial regulation by the Min system is the mechanism of action of MinC, an inhibitor of Z ring formation. Even though the Min system has been extensively studied, the molecular mechanism by which MinC antagonizes Z ring assembly is still not very clear, which is the goal of this study. MinC has two functional domains, both of which are able to block cell division in the proper context---$MinC^N$ can do so by itself whereas $MinC^C$ requires MinD. In this work, we describe the inhibitory mechanism of each domain of MinC on Z ring assembly.

First, we show that the septal localization and division inhibitory activity of $MinC^C$/MinD requires the conserved C-terminal tail of FtsZ. Using a genetic screen we identified four mutations in FtsZ that significantly decrease the $MinC^C$/MinD-FtsZ interaction and the toxivity of $MinC^C$/MinD. These mutations are clustered at the conserved C-terminal tail of FtsZ, a region critical for FtsZ-FtsA and FtsZ-ZipA interactions and therefore Z ring assembly. Using this as a clue, we were able to show that the toxicity of $MinC^C$/MinD in blocking division is due to its competition with FtsA and/or ZipA for the tail of FtsZ. In the presence of overexpressed $MinC^C$/MinD, such competition displaces FtsA and/or ZipA from the Z ring to disrupt the integrity and functionality and eventually totally destroy the structure of the Z ring.

Second, we studied the interaction between FtsZ and the N terminal domain of MinC. $MinC^N$ has been shown to be the anti-FtsZ part of MinC but the detailed mechanism regarding this activity is not known. Previous studies lead to the puzzling observation that $MinC^N$ blocks FtsZ polymer sedimentation but does not affect its GTPase. Because the GTPase activity of FtsZ

is linked to its polymerization, $MinC^N$ is believed to act after the polymerization of FtsZ to shorten FtsZ polymers. Using a similar genetic screen as above, we identified the residues in FtsZ that are critical for the $MinC^N$-FtsZ interaction. These important residues are clustered at the FtsZ dimerization interface, indicating that $MinC^N$ attacks FtsZ polymers at the dimer interface. Based on this, a "wedge" model for the action of $MinC^N$ on FtsZ is proposed.

Collectively, this study encourages us to suggest a more detailed model for how MinC/MinD antagonizes the Z ring formation: MinC/MinD localizes to the Z ring or membrane-associated FtsZ polymers through $MinC^C$/MinD interacting with the conserved C-terminal tail of FtsZ. By directly contacting FtsZ, MinC/MinD prevents Z ring formation in at least two ways: first, $MinC^C$/MinD disrupts the function and structural integrity of the Z ring by interfering with the recruitment of FtsA and/or ZipA; second, this targeting of MinC/MinD to the Z ring brings $MinC^N$ in close proximity to FtsZ polymers, which then severs these FtsZ polymers so that the Z ring is completely destroyed. By targeting different regions of FtsZ the two domains of MinC affect different aspects of Z ring formation to achieve synergy in disrupting Z rings.

Normally the activity of MinC/MinD is spatially regulated by MinE so that it works only at cell poles to block the formation of any potential polar Z rings. During the course of this study, we discovered another layer of spatial regulation of cytokinesis by MinC/MinD independent of MinE. The accumulated evidence shows that polar Z rings are more sensitive to MinC/MinD than midcell Z rings even in the absence of MinE. In some cases such as in the FtsZ-I374V strain, wild type morphology can be achieved by MinC/MinD without MinE. The mechanism of this differential MinC/MinD sensitivity between polar and midcell Z rings is unknown but it suggests that another layer of spatial regulation of cytokinesis by MinC/MinD exists other than oscillation induced by MinE.

Chapter I: Introduction

Bacterial cell division.

As one of the most fundamental processes in biology, cell division is essential for the propagation of all living organisms. The ultimate goal of cell division is to reproduce cells with intact genetic materials and other components required for viability and functionality. In bacteria, cells divide through a process called "binary fission", which occurs by the ingrowth of the cell envelope to form a septum that splits the mother cell into two daughter cell compartments (Fig 1). The daughter cells are then separated and released through the hydrolysis of the septal cell wall materials that connect them.

In the past, bacterial cells were looked at as "amorphous bags of enzymes" without any intracellular organization or specified structures. However, in recent years with the development of protein tracking techniques such as green fluorescent protein (GFP) fusion and immunofluorescence microscopy, it has become crystal clear that bacterial cells are highly organized at least at the level of protein localization. Cell division is an excellent example to elucidate this point. Bacterial cell division requires the coordination of more than a dozen proteins, which localize to the division site with a more or less defined linear hierarchy of dependency. The site of division and therefore the destination of the cell division machinery assembly are usually well defined. In addition to cell division, many other fundamental processes in bacterial cells such as DNA replication, chromosome segregation and cell growth require the localization of specific proteins to specific sites at the right time. With the application of these emerging technologies, huge progress has been made during the last 20 years in understanding

Fig. 1. Cell cycle and cell division in bacteria. Cells start the cell cycle by increasing their size and then replicate and segregate the chromosomal DNA. As this is going on, the early form of the division machinery---Z ring is assembled at midcell. Then the cells further increase their size and finish the chromosome segregation, at the same time the divisome matures as more division proteins localize to the Z ring. Once the division machinery (divisome) is fully assembled, cell division/cell envelop constriction starts and a septum is made to separate the two daughter cell compartments. After the septum is sealed to completely separate the daughter cells, the septal peptidoglycan is hydrolyzed at some time point to release the daughter cells.

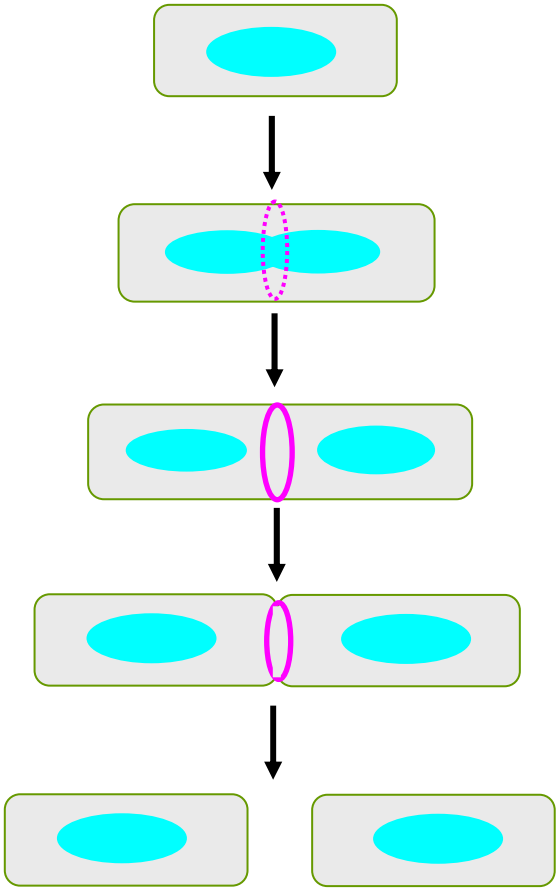

Chromosome replication and segregation, Z ring formation

Divisome maturation, division initiation

Septum formation and constriction

Septal cell wall hydrolysis and daughter cell release

bacterial cell division and its regulation (Harry *et al.*, 2006, Margolin, 2005, Dajkovic & Lutkenhaus, 2006, Adams & Errington, 2009).

In the 1960s, researchers obtained a large collection of thermosensitive *E. coli* mutants that affect different aspects of the cell. Among them are mutants that are specifically defective in cell division because they generate extremely filamentous cells at high temperature (Hirota *et al.*, 1968, Van De Putte *et al.*, 1964). These mutants replicate and segregate their chromosomes and accumulate mass normally but fail to divide, thus exhibiting a characteristic filamentation phenotype. Characterization of these conditional mutants allows the identification of a set of genes (*fts*, filamentation temperature sensitive) that are essential for cell division (Goehring & Beckwith, 2005). Nowadays with the more sophisticated genetical and biochemical (even bioinformatical) tools, the list of bacterial cell division genes is still growing. It is amazing to see how many proteins are involved in this process. However, the core components (essential ones) of the division machinery seem to be mostly identified as most of the newly identified ones are nonessential and they mainly play accessory roles (Gueiros-Filho & Losick, 2002, Ebersbach *et al.*, 2008).

Among all the cell division proteins, FtsZ is believed to be the first one to localize to the division site (Dajkovic & Lutkenhaus, 2006, Bi & Lutkenhaus, 1991, Beall & Lutkenhaus, 1991, Adams & Errington, 2009, Harry et al., 2006). FtsZ polymerizes to form a ring like structure (Z ring) on the cytoplasmic membrane with the help of other division proteins such as FtsA, ZipA and ZapA (Pichoff & Lutkenhaus, 2002, Bi & Lutkenhaus, 1991, Hale & de Boer, 1997, Gueiros-Filho & Losick, 2002). The Z ring marks the site for division and functions as scaffold for the recruitment of downstream division proteins (Goehring & Beckwith, 2005). These proteins localize to the Z ring to form a complex called the cytokinetic ring (C ring) or divisome

Fig. 2. Assembly of the cell division complex in *E. coli*. Divisome assembly starts with the Z ring formation, which involves FtsZ polymerization into filaments and subsequent attachment of these FtsZ filaments to the cytoplasmic membrane by FtsA and ZipA to make the Z ring. After the Z ring is formed, it functions as a scaffold and recruits other division proteins to make a mature divisome. These downstream proteins are recruited to the Z ring in a somewhat linear hierarchy (as indicated by the arrows).

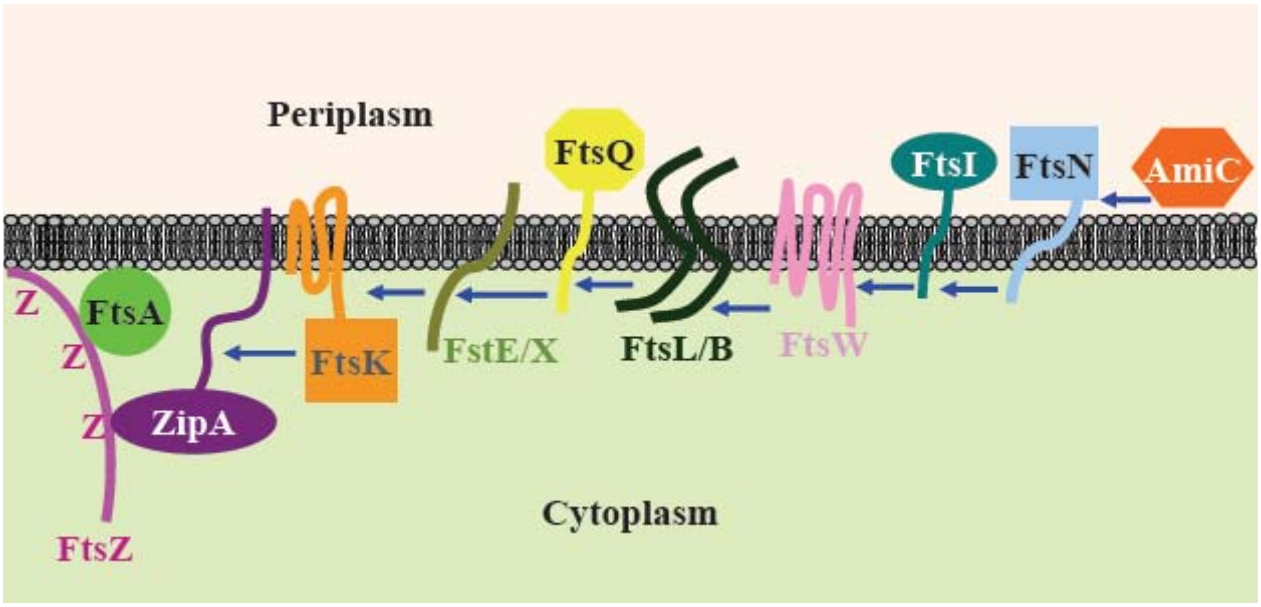
Periplasm
FtsQ
FtsI
FtsN
AmiC
Z
FtsA
Z
FtsK
FstE/X
FtsL/B
FtsW
Z
ZipA
Cytoplasm
FtsZ

(Dajkovic & Lutkenhaus, 2006), which is able to drive the division process (Fig. 2). The Z ring recruited proteins include FtsK, FtsE, FtsX, FtsQ, FtsL, FtsB, FtsW, FtsI, FtsN and AmiC (Goehring & Beckwith, 2005) in *E. coli*. They are recruited to the Z ring according to a somewhat defined linear hierarchy (Harry et al., 2006), which means that a given protein requires the presence of all upstream proteins to localize to the Z ring and is in turn required for the localization of all downstream proteins. Homologs of many of these proteins are present in other bacteria such as *B. subtilis*. The function of most of these proteins is not known even though they are thought to be involved in 1) Z ring stabilization, 2) clear the replicated chromosome from the division site, 3) direct peptidoglycan (PG) synthesis and ingrowth of the cell wall at the septum, and 4) hydrolyze the cell wall materials connecting the two daughter cells to separate and release the daughter cells.

FtsZ and Z ring

Over the last 20 years, research in the bacterial cell division field has been dominated by the FtsZ protein. One of the reasons is that FtsZ assembles into what is known as the Z ring and it is thought to be the first protein to localize to the future division site (Bi & Lutkenhaus, 1991). What properties FtsZ has so that it can assemble the Z ring and how the Z ring formation is regulated temporally and spatially are the most frequently asked questions ever since its discovery.

FtsZ is thought to be the tubulin homologue in bacteria even though the sequence similarity between FtsZ and tubulin is very low [<10% identity] (Mukherjee *et al.*, 1993). However, FtsZ shares many biochemical properties with tubulin and its 3D structure (Fig. 3) is

very close to that of tubulin (Mukherjee & Lutkenhaus, 1998a, de Boer *et al.*, 1992a, Mukherjee et al., 1993, Mukherjee & Lutkenhaus, 1994, Lowe & Amos, 1998, Lowe, 1998, Michie & Lowe, 2006), suggesting they are indeed homologues. Like tubulin, FtsZ binds and hydrolyzes GTP (de Boer et al., 1992a, Mukherjee et al., 1993). GTP binding induces FtsZ assembly into protofilaments which consists of a head to tail linear polymer of FtsZ (Mukherjee & Lutkenhaus, 1994). These protofilaments are able to arrange into higher order structures: in the case of tubulin, they are laterally associated to produce a well defined structure called the microtubule, which contains 13 tubulin protofilaments arranged around a hollow core; with FtsZ, lateral association of protofilaments does occur but does not generate a specific structure like the microtubule even though a variety of structures such as bundles, sheets and mini rings can be fromed depending on the *in vitro* experimental conditions (Mukherjee & Lutkenhaus, 1994, Erickson *et al.*, 1996, Bramhill & Thompson, 1994). FtsZ polymers generated by GTP are very dynamic because the bound GTP may be hydrolyzed and subsequently the subunits in the GDP form may be disassociated from the polymer (Stricker *et al.*, 2002, Anderson *et al.*, 2004, Chen & Erickson, 2005, Mukherjee & Lutkenhaus, 1998a). These disassociated subunits can undergo nucleotide exchange to the GTP form and join the polymer again. GTP hydrolysis of FtsZ requires polymerization because the GTPase active site is formed by the association of two monomers, with the catalytic loop (T7 loop or synergy loop, Fig. 3, purple) at the bottom of one monomer inserting into the GTP binding pocket of the other monomer (Lowe & Amos, 1998, Oliva *et al.*, 2004).

One important feature of FtsZ assembly is that it assembles cooperatively, with a critical concentration of about 1 μM. That means FtsZ polymerization occurs only when the FtsZ protein concentration in the pool is above 1 μM and any solution of FtsZ + GTP contains FtsZ polymers

Fig. 3. Structure of the α/β-tubulin heterodimer and the FtsZ dimer, showing the position of the nucleotide (GTP, blue) at the dimer interface and the T7 synergy loop (purple). The α/β-tubulin heterodimer is from zinc-induced sheets stabilized with taxol [PDB ID# 1JFF] (Lowe *et al.*, 2001) and the FtsZ dimer is from *Methanocaldococcus jannaschii* [PDB entry 1W5B] (Oliva et al., 2004).

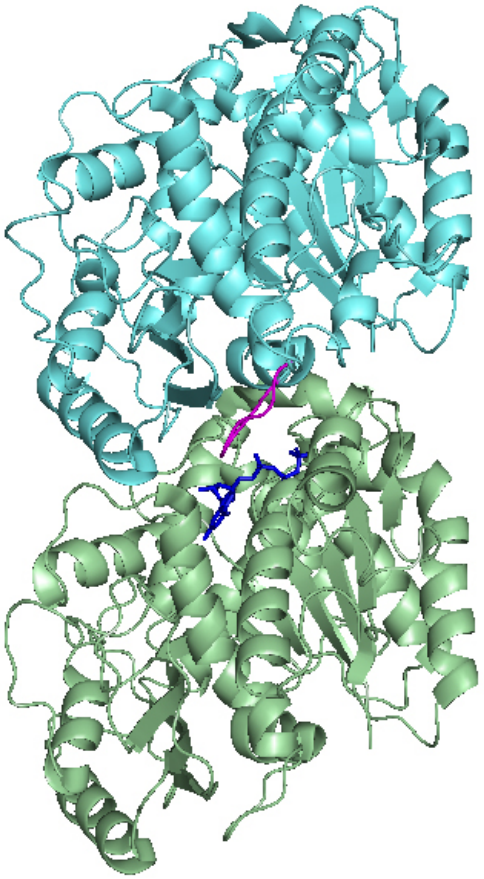

αβ-tubulin dimer

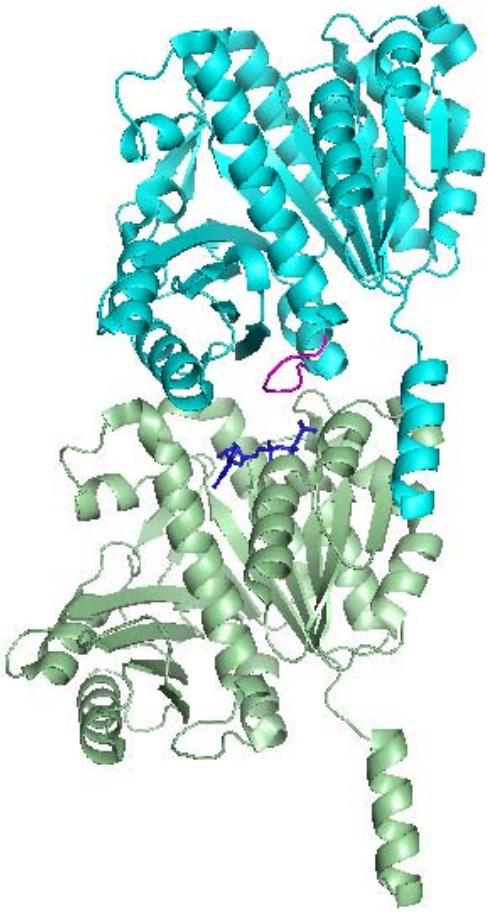

FtsZ dimer

and a pool of unpolymerized FtsZ that equals the critical concentration (Chen *et al.*, 2005, Chen & Erickson, 2005, Mukherjee & Lutkenhaus, 1998a). Although the presence of a critical concentration for FtsZ polymerization has been verified repeatedly, which indicates that the FtsZ polymer assembly is a cooperative process, the origin of this cooperativity is still in question. The theory of cooperative polymerization was originally developed for actin polymers where an incoming subunit makes more than one contact with the surrounding subunits in an elongating polymer (Oosawa & Kasai, 1962), which does not happen during the nucleation phase when two subunits get together to start a polymer de novo. However the basic assembly unit for FtsZ is the protofilament, which means that addition of subunits involves the same contacts during nucleation and polymer elongation, therefore this cooperatively is not driven by variation in the number of subunit contacts. Different models have been proposed to explain the source of this cooperatvity, but no reliable conclusion has been drawn yet (Dajkovic & Lutkenhaus, 2006, Gonzalez *et al.*, 2005).

As mentioned above, FtsZ is the first protein to localize to and mark the future division site. This was first shown by immunoelectron microscopy (Bi & Lutkenhaus, 1991) and later confirmed by fluorescence microscopy in live and fixed cells (Ma *et al.*, 1996). All these studies suggest that FtsZ was in a ring like structure at the leading edge of the septum, which was referred to as the Z ring (Bi & Lutkenhaus, 1991). Even though the Z ring was discovered more than 20 years ago, the nature and the structure of the Z ring is still not very clear. It is known that the Z ring contains FtsZ polymers but how these polymers are arranged in the Z ring is not known. FtsZ polymers assembled *in vitro* hydrolyze GTP very fast [10 GTP per FtsZ molecule per minute under optimal conditions] (Chen & Erickson, 2005, Mukherjee & Lutkenhaus, 1998a). Calculations based on this high GTPase activity associated with FtsZ assembly suggest that on

average an FtsZ protofilament contains only 30 subunits [~ 120 nm in length], which is similar to what was observed *in vitro* experimentally (Chen & Erickson, 2005). Given the fact that wild type *E. coli* cells have a circumference between 2000 and 3000 nm at the division site, this would suggest that the Z ring consists of a network of short protofilaments that are laterally associated and partially overlapped. Even though this theory has been accepted by many people, however, it has never been conclusively confirmed by microscopy due to the lack of high resolution.

Although the Z ring seems like a static structure in fluorescence microscopy, it is actually very dynamic. FRAP (fluorescence recovery after photobleaching) studies in live *E. coli* and *B. subtilis* cells revealed that the FtsZ subunits in the Z ring are constantly exchanging with the FtsZ outside of the Z ring (Anderson et al., 2004, Stricker et al., 2002). The half life of individual FtsZ subunits in the Z ring is estimated to be 8-9 seconds. Another aspect of the Z ring dynamics revealed by FtsZ-GFP is the rapid movement of the helix-like structures of FtsZ along the membrane in the cell (Margolin, 2002). These structures are likely to be FtsZ polymers attached to the membrane (see below) and are the precursors/turnover products of the Z ring because they are observed to join and leave the Z ring constantly.

Fts Z is a highly conserved protein that is almost universally found in the bacterial world. It is also found in the major groups of archaea and has an active role in the division of the chloroplasts and mitochondria of several groups of the eukarya (Adams & Errington, 2009, Margolin, 2005). However there are bacteria that do not have FtsZ, it is of great interest to know how these cells divide without FtsZ.

Z ring and the membrane

An essential requirement for Z ring assembly is the attachment of FtsZ to the cell membrane. FtsZ by itself does not have any affinity for the membrane, but all models for Z ring formation require its attachment to the membrane to maintain its structural integrity and to generate and transmit the force constricting the cell envelop during division. In *E. coli*, two proteins called FtsA and ZipA collaborate to anchor FtsZ polymers to the membrane (Pichoff & Lutkenhaus, 2002). Both proteins are essential for cell division although either one of them is sufficient to support Z ring formation even thought such rings are not functional for division (Pichoff & Lutkenhaus, 2002, Hale & de Boer, 1997). When both FtsA and ZipA are depleted, Z rings do not form.

Both FtsA and ZipA bind to the extreme C-terminal tail of FtsZ (Ma & Margolin, 1999, Haney *et al.*, 2001), which is not involved in FtsZ polymerization (Liu *et al.*, 1999), to link FtsZ filaments to the membrane. ZipA is a bitopic protein with three domains: an N-terminal transmembrane anchor, a long and flexible linker and a large, globular C-terminal domain (Hale & de Boer, 1997, Mosyak *et al.*, 2000, Moy *et al.*, 2000). Interestingly, the transmembrane domain of ZipA does not seem to be simply a membrane anchor because it can not be functionally replaced by transmembrane segments of other membrane proteins (Hale *et al.*, 2000), suggesting that it has a specific role in cell division. The cytoplasmic C-terminal domain of ZipA mediates its interaction with FtsZ. This domain of ZipA has also been shown to be able to bundle FtsZ polymers (Hale et al., 2000), consistent with its role in promoting Z ring formation. FtsA, which is thought to be an actin homolog (van den Ent & Lowe, 2000), associates with the membrane through an amphipathic helix called membrane targeting sequence [MTS] (Pichoff &

Lutkenhaus, 2005). This membrane targeting sequence does not seem to be very specific as it can be replaced by the MTS from other proteins such as MinD (Pichoff & Lutkenhaus, 2005). Purified FtsAs from a couple of species have been studied *in vitro*, but they seem to behave differently. Some can form polymers (Lara *et al.*, 2005) and some can bind ATP/ADP with or without ATPase activity (Sanchez *et al.*, 1994, Feucht *et al.*, 2001, Lara et al., 2005). The biochemical activities of FtsA are largely unknown and deserve further investigation. Unlike ZipA, which is conserved only in the γ-proteobacteria, FtsA is widely conserved throughout most bacteria and is often found in the same operon as *ftsZ* (Pichoff & Lutkenhaus, 2005). This suggests that FtsA may play a more important role in linking FtsZ to the membrane than ZipA during evolution. In support of this idea, a single gain-of-function mutation in FtsA is able to bypass ZipA, allowing efficient cell division in the absence of ZipA (Geissler *et al.*, 2003). In *E. coli* cells, the ratio of FtsZ to FtsA or ZipA is very critical for cell division. Depletion or overproduction of any of these proteins will block division because unbalanced FtsZ/ZipA and/or FtsZ/FtsA ratio destroys the integrity and structure of the Z ring (Hale & de Boer, 1997, Dai & Lutkenhaus, 1992).

Z ring assembly can also be aided by other factors such as ZapA and ZapB, which are positive but nonessential modulators of Z ring formation and stability (Gueiros-Filho & Losick, 2002, Low *et al.*, 2004, Small *et al.*, 2007, Ebersbach et al., 2008). When Z ring is successfully established on the membrane, it functions as scaffold to recruit other division proteins to make a mature division machine that drives cytokinesis (Fig. 2). The Z ring may also directly generate force to constrict the cell envelop (Osawa *et al.*, 2008).

Spatial and temporal regulation of Z ring assembly

The Z ring is the structure that marks and eventually determines the future division site; therefore its assembly has to be regulated in a way that it forms in the right place and at the proper time. Indeed, Z ring formation must be regulated temporally so that division is occurring in accordance with the cell physiological status such as cell size, chromosome replication and segregation, genetic material integrity and so on (Dajkovic & Lutkenhaus, 2006). It must also be regulated spatially to make sure that the subsequent cell division gives rise to two equally sized daughter cells.

Although in some bacteria such as Caulobacter crescentus both FtsZ synthesis and its stability are tightly regulated during a cell cycle (Quardokus *et al.*, 1996, Kelly *et al.*, 1998, Rueda *et al.*, 2003), in the two best studied model bacteria---*E. coli* and *B. subtilis*, the cellular FtsZ level (and most other division proteins too) seems to be constant over time (Rueda et al., 2003, Weart & Levin, 2003). Therefore in these bacterial cells, the timing of Z ring formation must be regulated at the level of FtsZ assembly into higher order structures. Z ring formation seems to respond to cell cycle signals, but the nature of these signals is not known. They could be signals from DNA replication and chromosome segregation as there seems to be a correlation between Z ring formation and them. However on the other hand, some of these temporal signals may actually be the same as the spatial signals originating from the Min and NOC systems (see below). Over the years, a couple of factors have been discovered to regulate Z ring assembly in according to cell cycle and cell physiological status: 1), SulA, which is a potent division inhibitor that is produced in response to DNA damage as part of the SOS response. In *E. coli* when DNA is extensively damaged and the SOS response in initiated, SulA will be induced to rapidly stall

cell division by both preventing the assembly of nascent Z rings and facilitating the disassembly of existing Z rings (Bi & Lutkenhaus, 1990, Bi & Lutkenhaus, 1993, Dajkovic *et al.*, 2008b, Huisman *et al.*, 1984, Mukherjee *et al.*, 1998). 2), UgtP, a terminal sugar transferase that coordinates cell division with growth rate and cell size in *B. subtilis* (Weart *et al.*, 2007). This protein has been shown to be an inhibitor of FtsZ assembly to delay cell division until cells reach a sufficient length. 3), MciZ, a small peptide found in *B. subtilis*, contributes to the inhibition of Z ring assembly after the initiation of sporulation (Handler *et al.*, 2008). This protein was predicted to bind close to the GTP binding pocket of FtsZ to block FtsZ polymerization.

Spatial regulation of Z ring assembly involves positioning the Z ring at the correct place in the cell, which is the midpoint of the long axis of the cell in rod-shaped bacteria such as *E. coli* and vegetative growing *B. subtilis*. The center positioned Z ring then guides cell division to produce two equally-sized daughter cells. In these bacteria, how a cell finds its geometric center to assemble the division machinery is a fundamental question and has been being studied for quite some time. So far, two negative regulatory systems, NOC (Nucleoid Occlusion) and Min, are known to be involved in the spatial control of Z ring assembly (Rothfield *et al.*, 2005, Lutkenhaus, 2007). These systems position division inhibitors within the cell in such a way that Z ring formation is restricted to the middle of the long axis of the cell (Fig. 4). Although neither system is essential, inactivation of both is synthetic lethal due to an inability to assemble functional Z rings (Wu & Errington, 2004, Bernhardt & de Boer, 2005).

NOC inhibits Z ring formation over the nucleoid and prevents guillotining of the chromosome by the cell division apparatus. It is based on the well established observation that Z ring formation, and therefore cell division, normally does not occur in the regions of the cell

Fig. 4. Spatial control of Z ring assembly by negative regulators. The placement of the Z ring at midcell is regulated by the Min and NOC systems, which are Z ring inhibitors at off-center sites. These systems establish Z ring inhibitor gradients in the cell such that their negative effects are lowest at midcell, allowing the Z ring to form there. The effect of the Min system (red color) is highest at cell poles and lowest at midcell due to the rapid oscillation of the Min proteins. The effect of the NOC (blue color) system is highest near the replication origin region of the chromosome and lowest at the terminus region due to the enrichment of its binding sequences near the origin neighborhood (shown in *B. subtilis*).

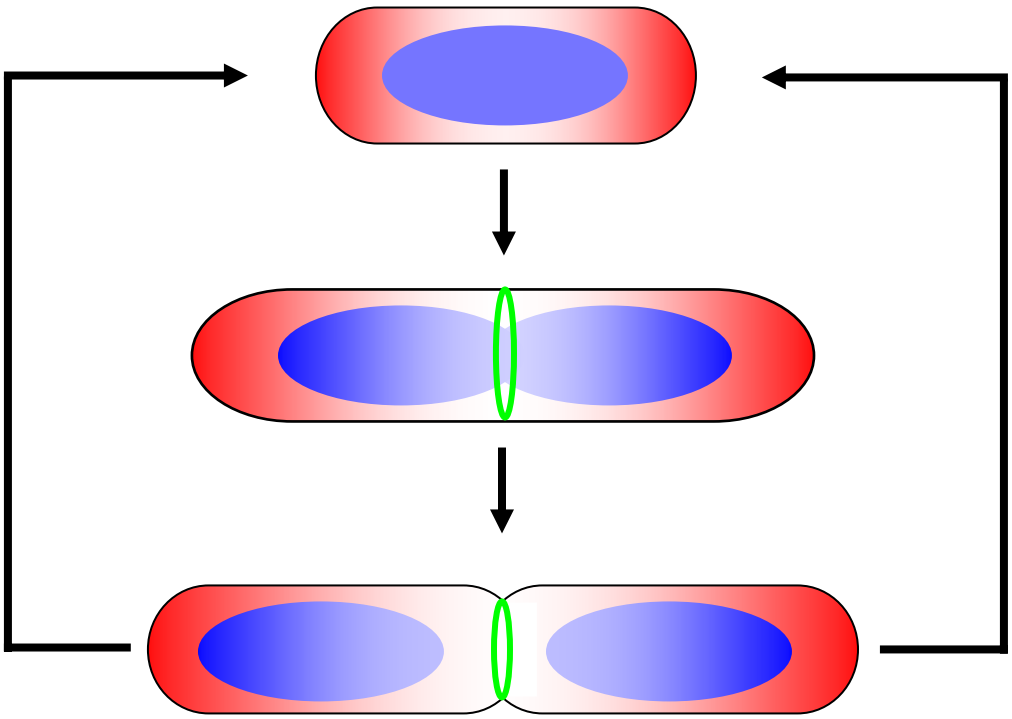

occupied by the nucleiod (Mulder & Woldringh, 1989, Yu & Margolin, 1999). The NOC phenotype has been noticed for a long time but the molecular basis was unknown until recently when the important players of this system are being identified (Bernhardt & de Boer, 2005, Wu & Errington, 2004). In *B. subtilis*, a parB homolog called Noc, is the effector of the NOC system. Because of its DNA binding and Z ring inhibitory activity, Noc was originally proposed to block division over the chromosome as a NOC factor (Wu & Errington, 2004). More recently, the cellular location of Noc has been shown to be restricted through binding to specific DNA sequences that are scattered around the chromosome but absent from the terminus region. As the replicating chromosome segregates, a Noc free space is generated around the terminus region at midcell, allowing the Z ring to assemble (Wu *et al.*, 2009). In *E. coli*, nucleoid occlusion is mediated by a protein called SlmA, which is a TetR like DNA binding protein with no homology to Noc. SlmA was identified in a screen for mutants which are synthetic lethal with loss of the Min system (Bernhardt & de Boer, 2005). Like Noc, SlmA interacts with both FtsZ and DNA to inhibit Z ring assembly over the nucleoid. Interestingly, under normal conditions, inactivation of Noc or SlmA does not have any detectable phenotype, indicating that the NOC system may be partially redundant and play a less important role than other systems such as *min*.

The other system involved in spatial regulation of Z ring positioning is Min, which blocks Z ring formation at cell poles, so named because its inactivation results in polar division and production of chromosomeless minicells [Fig. 5 and (Adler *et al.*, 1967)]. In *E. coli*, the Min system consists of three proteins (MinC, MinD and MinE), which are encoded by the minB operon (de Boer *et al.*, 1989). The effector of the Min system is MinC, which blocks cell division by preventing Z ring formation (de Boer et al., 1989, Hu *et al.*, 1999, de Boer *et al.*, 1990). MinC requires MinD for full activity; in part, because MinD recruits MinC to the membrane

Fig. 5. Cell division in Δmin cells. A: a cartoon showing the potential divisions in a Δmin cell, essentially cell division can occur anywhere in the nucleoid free area. If it occurs between nucleoids, it will generate two normal sized daughter cells. If it occurs at the cell poles, it will produce a minicell without chromosomal DNA and a big cell containing more than one nucleoid. B: morphology of Δmin cells under the microscope compared with WT cells.

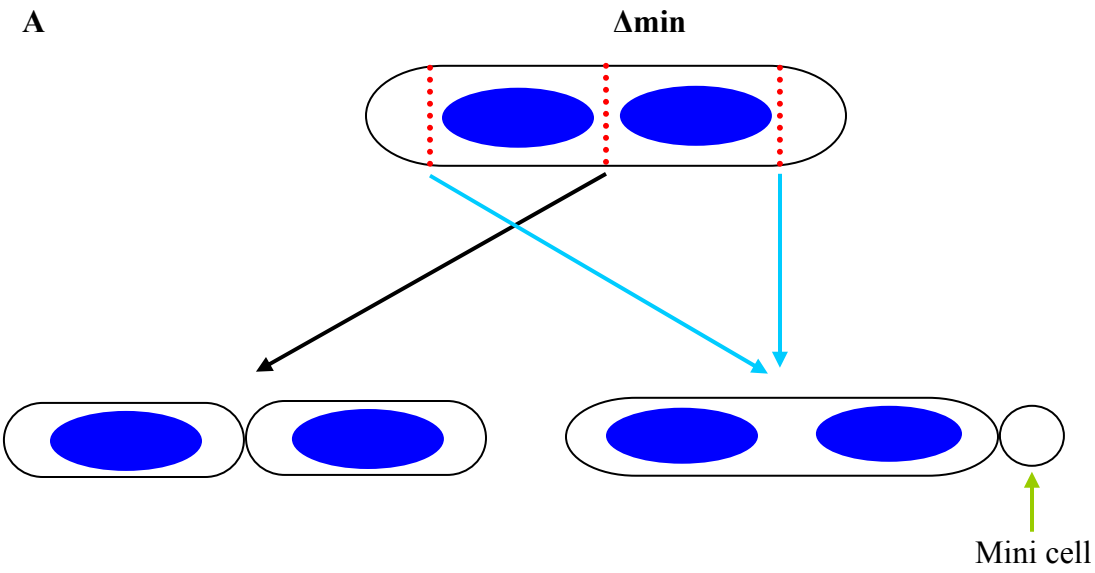
A
Δmin
Mini cell

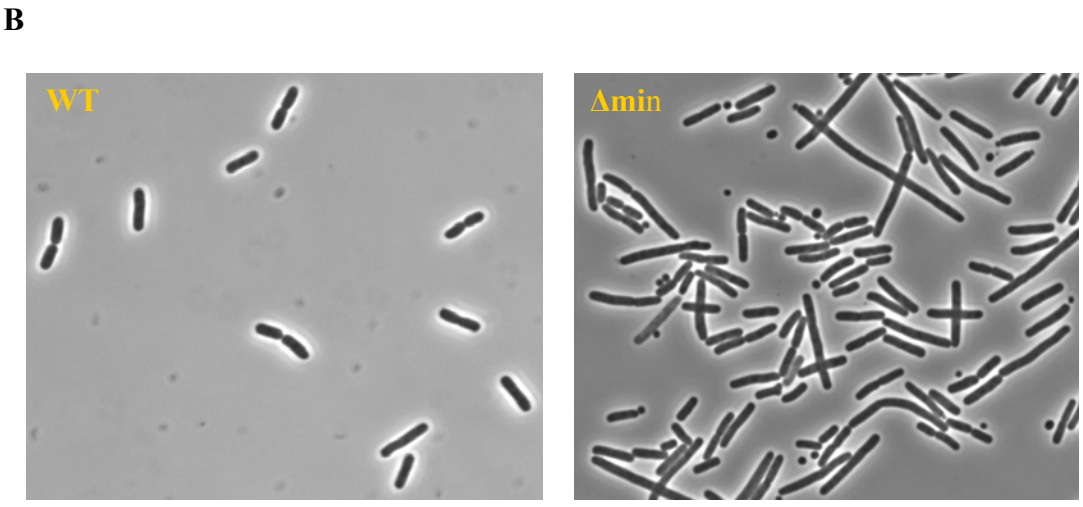
B
WT
Δmin

(Hu & Lutkenhaus, 2001, Hu *et al.*, 2003, Hu & Lutkenhaus, 2003). MinD is a membrane associated ATPase which plays a central role in the Min system (Lackner *et al.*, 2003, de Boer *et al.*, 1991). When bound to ATP, MinD dimerizes and binds to the membrane (Hu & Lutkenhaus, 2003). The subsequent recruitment of MinC leads to a cell division inhibitory complex (MinC/MinD) that is evenly distributed on the membrane (Hu et al., 2003, de Boer *et al.*, 1992b). The activity of the MinC/MinD complex is spatially regulated by MinE, a small protein that restricts the MinC/MinD complex to the poles of the cell. MinE does this by stimulating the pole to pole oscillation of MinC/MinD due to its ability to stimulate the ATPase activity of MinD and thus, the release of MinD from the membrane (Raskin & de Boer, 1999b, Raskin & de Boer, 1999a, Hu & Lutkenhaus, 1999, Hu & Lutkenhaus, 2001, Fu *et al.*, 2001, Hu *et al.*, 2002, Hale *et al.*, 2001). Such dynamic behavior of the Min proteins results in a time-averaged concentration of the MinC/MinD division inhibitor that is highest at cell poles and lowest at mid-cell where the Z ring forms (Meinhardt & de Boer, 2001).

The fascinating aspect of the Min system is the way it inhibits Z ring formation at cell poles but allows it to occur at midcell---through a remarkable oscillation of a Z ring inhibitor between the cell poles (Lutkenhaus, 2007). Early models for the Min system were static based on the observation of MinE rings near midcell in fixed cells (Raskin & de Boer, 1997). It was proposed that MinE localized to the midcell independent of FtsZ to prevent the action of MinC/MinD and function as a shield for Z ring formation. However, with the application of GFP-fusion tracking technology in live cells, it was shown that the Min proteins were actually very dynamic instead of static in the cell (Hu & Lutkenhaus, 1999, Raskin & de Boer, 1999b). The breakthrough study using GFP-MinD demonstrated that it undergoes a rapid pole to pole oscillation in the cell with a periodicity of about 40 to 50 seconds per cycle (Raskin & de Boer,

1999b). After this report, numerous studies were done to try to understand the molecular and biochemical basis for the dynamic behavior of the Min proteins.

It turns out that only MinD and MinE are required for the oscillation to occur, MinC just simply follows the pattern of MinD (Raskin & de Boer, 1999a, Hu et al., 2003). During an oscillation cycle (Fig. 6B), MinD forms a polar zone on the membrane extending toward the midcell due to its ability to bind phospholipid membranes in an ATP dependent manner; MinE, on the other hand, forms a ring at the edge of the MinD zone. The MinE at the tip of MinD zone then activates the ATP hydrolysis of MinD and facilitates the release of MinD from the membrane. As MinE is chewing off MinD, the MinD zone shrinks toward the pole and the released MinD accumulates on the membrane at the other pole after nucleotide exchange to the ATP form. By the time this MinD zone disappears, a new polar MinD zone is established at the other end of the cell and a new MinE ring also forms at the edge of the new MinD zone, and the cycle is repeated (Dajkovic & Lutkenhaus, 2006, Lutkenhaus, 2007). As it can be seen from this description, the oscillation is driven by MinE. MinD is evenly on the membrane without MinE; additionally the oscillation frequency is determined by the ratio of MinE to MinD. Decreasing this ratio will slow down the oscillation and induce minicell production (Raskin & de Boer, 1999b, Howard & Kruse, 2005).

Even though it has been extensively studied during the last ten years, there are still many questions left unsolved regarding the mechanism of the dynamic behavior of the Min proteins. Computer simulations have been used to understand it and different models have been generated (Howard & Kruse, 2005, Drew *et al.*, 2005, Huang *et al.*, 2003). Regardless of these, the dynamic behavior of the Min proteins has been reconstituted *in vitro* using just MinD, MinE, ATP and phospholipid membranes (Loose *et al.*, 2008), indicating it can occur without any

Fig. 6. Oscillation of the Min proteins in the *E. coli* cell. A: oscillation pattern of MinD in a live cell as revealed by GFP-MinD (Hu & Lutkenhaus, 2001). In this experiment, gfp-minD/minE was induced in a Δmin strain, time-lapse microscopy was used to track the localization of GFP-MinD over time, and cells were photographed every 25 seconds. B: a model explaining the oscillation of the Min system [see text for details] (Lutkenhaus, 2007).

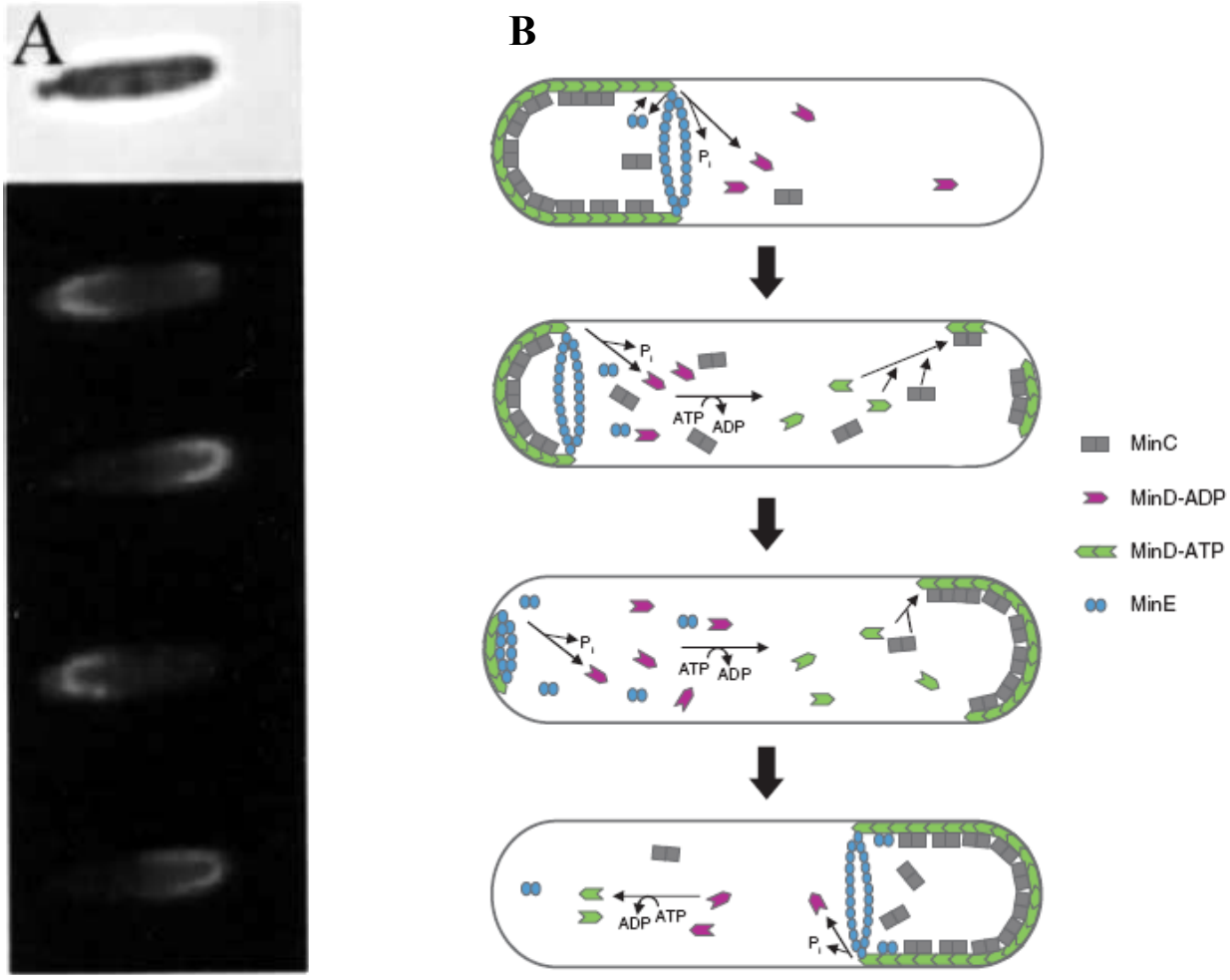
A
B
P
i
ATP
ADP
MinC
MinD-ADP
MinD-ATP
MinE

additional factors. Min oscillation has also been studied in long filamentous cells (Raskin & de Boer, 1999b), round cells such as *mreB* and *rodA* mutants (Corbin *et al.*, 2002, Varma *et al.*, 2008) and Y-shaped cells (Varma et al., 2008), and conserved patterns are observed in all cases.

Even though MinC is only a passenger and plays no role in the oscillation, it is actually the effector of the Min system responsible for antagonizing FtsZ assembly at cell poles (de Boer et al., 1989, de Boer et al., 1990, Bi & Lutkenhaus, 1993, Hu et al., 1999). Structural, sequence and functional analyses of MinC reveal that it has two domains of approximately equal size (Hu & Lutkenhaus, 2000, Cordell *et al.*, 2001). Both domains are required for the proper function of the Min system as mutations inactivating either domain inactivate Min as evidenced by minicell production (Hu et al., 1999, Zhou & Lutkenhaus, 2005). The two domains have been studied separately to elucidate their activites (Hu & Lutkenhaus, 2000). The N-terminal domain of MinC ($MinC^{1-115}$ [$MinC^{N}$]) interacts with FtsZ and is able to block cell division when overexpressed, even in the absence of MinD. It prevents the sedimentation of FtsZ polymers in vitro, which is thought to be the basis of its inhibitory activity in vivo. $MinC^{N}$ blocks FtsZ polymer sedimentation but it does not affect the GTPase activity of FtsZ, therefore it is thought to act after polymerization to shorten FtsZ polymers (Hu & Lutkenhaus, 2000, Dajkovic *et al.*, 2008a). The C-terminal domain of MinC ($MinC^{116-231}$ [$MinC^{C}$]) mediates homodimerization and interaction with MinD. In contrast to $MinC^{N}$, $MinC^{C}$ does not affect the sedimentation of FtsZ polymers *in vitro* nor does it affect cell division *in vivo* by itself (Hu & Lutkenhaus, 2000). Important residues in MinC that mediate $MinC^{N}$-FtsZ and $MinC^{C}$-MinD interactions are identified, which offer nice tools for subsequent studies (Hu et al., 1999, Zhou & Lutkenhaus, 2005).

Although MinC is able to block Z ring formation on its own, it is a weak inhibitor in the absence of those so called activators (de Boer et al., 1989, de Boer et al., 1990). In *E. coli* MinC can be activated by MinD or DicB (de Boer et al., 1990). MinD is the natural activator for MinC because it is expressed from the same operon as MinC and it always works together with MinC under physiological conditions. DicB, on the other and, is an artificial activator for MinC since it is encoded by a defective prophage in some *E. coli* strains and it is not expressed under normal conditions (de Boer et al., 1990). The mechanism by which MinD activates MinC is not fully understood but it is believed to involve: 1) recruit and concentrate MinC on the membrane where MinC meets FtsZ polymers; and 2) make a complex with MinC and enhance the affinity for the Z ring (Johnson *et al.*, 2002). GFP-$MinC^C$ was shown to localize to the Z ring in the presence of MinD but not by itself (Zhou & Lutkenhaus, 2005, Shiomi & Margolin, 2007). The component in the Z ring that recruits $MinC^C$/MinD was not clearly clarified even though it is suggested to be FtsZ because all other early division proteins required for Z ring formation (FtsA, ZipA and ZapA) are not required for $MinC^C$/MinD localization and the interaction between $MinC^C$/MinD and FtsZ polymers has been reported (Johnson *et al.*, 2004, Dajkovic et al., 2008a). Interestingly, $MinC^C$ does not affect division by itself but it is also able to block cell division in the presence of MinD (Shiomi & Margolin, 2007), however the basis for this is not clear. DicB activates MinC by targeting it to the Z ring directly through the DicB-ZipA interaction and potentially the FtsZ-$MinC^C$ interaction too (Johnson et al., 2004, Zhou & Lutkenhaus, 2005). In addition, the MinC/MinD complex is spatially regulated by the oscillation induced by MinE whereas the MinC/DicB complex is not topologically regulated at all.

The Min system is also found and studied in other bacteria such as *B. subtilis*. By large it functions very similarly as in *E. coli*; however the topological specificity is achieved differently

(Bramkamp & van Baarle, 2009). In *B. subtilis*, the Min system consists of four components---the division inhibitor MinC/MinD, which works the same as the MinC/MinD in *E. coli* and the topology regulator MinJ/DivIVA (Bramkamp *et al.*, 2008, Patrick & Kearns, 2008, Edwards & Errington, 1997, Gregory *et al.*, 2008). It is a more static system than the Min in *E. coli*, with the MinC/MinD being confined at cell poles most of the time and delivered to the septum late in the division by MinJ/DivIVA (Edwards & Errington, 1997). Because MinC/MinD localizes to the septum at a late stage of division, when this division finishes and gives rise to two new cell poles, MinC/MinD is there (new poles) to block another round of division at the newly formed poles (Gregory et al., 2008), which otherwise will promote minicell production as the new poles are supposed to be the preferred place for minicell formation in *B. subtilis*.

In this thesis, I studied the interaction between FtsZ and MinC and tried to understand the molecular mechanism by which MinC antagonizes Z ring assembly. Using a genetic approach, I was able to select for FtsZ mutants that are resistant to each domain of MinC. By analyzing these mutants, we showed that the two domains of MinC interact with different regions of FtsZ and they affect Z ring assembly through different mechanisms. By targeting different regions of FtsZ the two domains of MinC affect different aspects of Z ring formation to achieve synergy in disrupting Z rings. During this study, we also discovered that the polar Z rings are more sensitive to MinC/MinD than midcell Z rings in Δmin cells, which indicates that another layer of spatial regulation of cytokinesis by MinC/MinD exists other than the oscillation induced by MinE.

Chapter II: Materials and Methods

Bacterial strains, plasmids and growth conditions.

Strains and plasmids used in this study are listed in table 1 and 2 respectively. Cells were grown in LB medium at 37^{o}C unless otherwise indicated. When needed, antibiotics were used at the following concentrations: ampicillin= 100 µg/ml; spectinomycin= 25µg/ml; kanamycin= 25µg/ml, tetracycline= 10µg/ml, cephalexin= 20 µg/ml and chloramphenicol= 20µg/ml.

Strain S7 (*ftsZ*^{0} *recA*::Tn*10*)/ pKD3C was constructed in two steps. First the *ftsZ*^{0} allele was introduced into strain S4 (*leu*::Tn*10 ftsZ*$^{+}$ *min::kan*)/pKD3C (*ftsZ*$^{+}$) with P1 phage grown on PB143 (*leu*$^{+}$ *ftsZ*^{0} *recA*::Tn*10*) by selecting Leu^{+} at 30 °C on M9 minimal medium. The resultant transductants were checked for temperature and tetracycline sensitivity. The desired transductants (S6/pKD3C) should have the genotype of *leu*$^{+}$, *ftsZ*^{0}, *min::kan* with the temperature sensitive plasmid pKD3C supplying FtsZ. In a second step, the *recA*::Tn*10* allele from PB143 was transduced into S6/pKD3C by selecting tetracycline resistance on LB plates at 30 °C. The resultant cells S7 (*ftsZ*^{0} *recA::Tn10*)/pKD3C were checked for UV sensitivity to confirm *recA* inactivation. The strain S18/pKD3C was constructed in a similar way except that the starting strain for S18 construction is S3 (which is *min*$^{+}$) instead of S4 (which is *min*$^{-}$).

The strain BSZ374 (*ftsZ-I374V*) was generated by replacing the *ftsZ84* allele (TS) on the chromosome of strain PS106 with *ftsZ-I374V* through recombineering using the lamda RED system (Datsenko & Wanner, 2000). The PCR product of *ftsZ* containing the *I374V* mutation was electroporated into PS106 (*ftsZ84*)/pKD46 induced with arabinose=0.04% for 3 h at 30 °C and recombinants were selected on LB plates with no salt at 42 °C. To determine if the ftsZ-I374V

Table 1. Strains used in this study

Strain	description	source
JS964	*min::kan*, *laq*I^{q}	lab collection
PB143/pCX41	*ftsZ*^{0} *recA*::Tn10/pSC101(*repA*^{TS}) ::*ftsZ*$^{+}$	(Raskin & de Boer, 1997)
PS106	W3110, *ftsZ84*, *leu*::Tn*10*	lab collection
S7	W3110, *ftsZ*^{0}, *min::kan*, *recA*::Tn*10*	this work
S3	W3110 *leu*::Tn*10*	this work
S4	S3, *min::kan*	this work
BSZ374	S3, *ftsZ-I374V*	this work
BSM374	BSZ374, *min::kan*	this work
BSZ280D	S3, *ftsZ-N280D*	this work
BSZ23	S3, *ftsZ-I374V+N280D*	this work
BSM280D	BSZ280D, *min::kan*	this work
BSM23	BSZ23, *min::kan*	this work
S18	W3110 ftsZ^{0}, recA::tn10	this work
S22	S3 *slmA::cat*	this work
BSS374	BSZ374V *slmA::cat*	this work
BSS280D	BSZ280D *slmA::cat*	this work
BSS23	BSZ23 *slmA::cat*	this work
SFY526	yeast strain for Y-T-H test	Clonetech

Table 2. Plasmids used in this study

plasmid	description	source
pKD3C	pGB2 (*repA*^{TS}), *ftsZ*$^{+}$, Cam^{r}	(Dai & Lutkenhaus, 1991)
pBANG112	pACYC184, *ftsZ*$^{+}$, Amp^{r}	this work
pBANG59	pEXT22, P*tac*::*minC/minD*, Spc^{r}	this work
pBANG78	pGB2, P*lac*::*minC/minD*, Spc^{r}	this work
pBANG75	pGB2, P*lac*::*minC*^{C}*/minD*, Spc^{r}	this work
pZH111	pBR322, P*ara*::*malE-minC*^{N}, Amp^{r}	(Hu & Lutkenhaus, 2000)
pHJZ109	pGB2, P*lac*::*gfp-minC*^{C}*/minD*, Spc^{r}	(Zhou & Lutkenhaus, 2005)
pSEB293	pBAD18, P*ara*::*gfp-ftsA*, Amp^{r}	(Pichoff & Lutkenhaus, 2007)
pSEB103	pGB2, P*ara*::*zipA-gfp*, Spc^{r}	(Pichoff & Lutkenhaus, 2001)
pKD46	pSC101(*repA*^{TS}), P*ara::gam bet exo*, Amp^{r}	(Datsenko & Wanner, 2000)
pKD126	pBR322, P*lac*::*ftsZ* , Amp^{r}	(Mukherjee & Lutkenhaus, 1998b)
pZH112	pBR322, P*ara*::*malE-MinC*^{C}, Amp^{r}	(Hu & Lutkenhaus, 2000)
pBS31	pDSW208, P*trc::sulA*, Amp^{r}	this work
pCX53	pGAD424::FtsZ	(Pichoff & Lutkenhaus, 2007)
pSEB347	pGT9::FtsA	(Pichoff & Lutkenhaus, 2007)
pSEB126	pGT9::ZipA	(Liu et al., 1999)
pBANG85	pEXT22, P*trc::gfp-minC/minD*, Spc^{r}	this work
pBANG84	pEX22, P*trc::minC/minD*, Spc^{r}	this work
pBANG76	pGB2, P*lac::minC/minD*, Spc^{r}	this work

mutation was present, 10 colonies were randomly selected and checked for MinC/MinD resistance (about 25% of the randomly streaked colonies showed MinC/MinD resistance). We then did PCR to amplify the *ftsA-ftsZ* region from the chromosome of the MinC/MinD resistant strains and confirmed that *ftsZ I374V* was present and that *ftsZ84* was absent. BSZ280D and BSZ23 were created in the same way. P1 transduction was then used to move the *min::kan* allele into BSZ374, BSM280D and BSZ23 to give BSM374, BSM280D and BSM23 respectively.

The *slmA* mutants were made by P1 phage mediated transduction. The *slmA::cat* (with most of the *slmA* coding sequence replaced by the chloramphenicol resistant gene *cat*) construct from the strain W3110 *slmA::cat* (from S. Pichoff) was transduced into strains S3, BSZ374, BSZ280D, BSZ23, S4, BSM374, BSM280D and BSM23 by P1 transduction and selection of transductants at 42 °C to give the *slmA* knockout of corresponding strains.

The plasmid pBANG112 was constructed by inserting a fragment containing *ftsZ* into a pACYC184 based vector. The *ftsZ* gene was obtained by XmaI and PstI digestion of pKD4 (Dai & Lutkenhaus, 1991). To make pBANG59, *minC/minD* was PCR amplified from pSC104CD using primers 5'-MinC-SstI and 3'-MinD- HindIII. The PCR product was digested with SstI+HindIII and cloned into to a Spc^r version of pEXT22. pBANG75 and pBANG78 were made by replacing *gfp-minC^C/minD* in pHJZ109 (Zhou & Lutkenhaus, 2005) with the properly digested *minC^C/minD* and *minC/minD* PCR product respectively. Both *minC/minD* and *minC^C/minD* were amplified from pCS104CD (Zhou & Lutkenhaus, 2005) using the following primers: 5'-MinC*-SstI (for *minC/minD* on pBANG78), 5'-$MinC^{C116}$-SstI (for *minC^C/minD* on pBANG75)and 3'-MinD- HindIII. Both pBANG75 and pBANG78 contain artificially conserved ribosome binding site (RBS) for $MinC^C$ and MinC translation respectively. The plasmid pBANG85 was constructed in two steps: first the *tac* promoter of the plasmid pBANG59 was

replaced by the *trc* promoter from pDSW210 to give the plasmid pBANG84. The P*trc*+*lacI*^{q} region from pDSW210 (Weiss *et al.*, 1999) was PCR amplified (using 5'-lacIq-BglII and 3'-LacIq-MCS as primers) and cloned into pBANG59 digested with BglII+EcoRI. Second, the region containing *gfp-minCD* from plasmid pMCW71 (M. Wissel and J. Lutkenhaus, unpublished) was cloned into pBANG84 by SstI+HindIII digestion and subsequent ligation. The plasmid pBS31 was constructed by cloning the sulA fragment obtained by SstI and HindIII digestion of pA3 into pDSW208. pBANG76 was made by subcloning minC/minD from pCS104CD into pHJZ109 to replace gfp-minC^{C}/minD. All other plasmids are described previously and all primers for PCR amplification are listed in table 3.

PCR random mutagenesis of ftsZ.

Using pBANG112 as template and 5'- FtsZ-Bsu36I and 3'-FtsZ-PstI as primers, *ftsZ* was PCR amplified using the GeneMorph II Random Mutagenesis kit from Stratagene with a mutagenesis rate of 1-4 bases/Kb. The PCR fragments were then digested with EcoRI + EagI and ligated into EcoRI + EagI digested pBANG112. The ligation product was then electroporated into S7/pKD3C and transformants were selected at 42 °C on plates with ampicillin. All colonies that grew up were pooled to give a library of FtsZ mutants that can still complement the *ftsZ* depletion strain and support cell division. Then pBANG75 was transformed into these cells and colonies resistant to MinC^{C}/MinD were selected with IPTG=200 μM at 42 °C on plates containing Amp and Spc. Plasmids were isolated from the surviving colonies and the *ftsZ* gene was sequenced to identify the mutations. This library was also screened using the plasmid pBANG59 at IPTG=1 mM for MinC/MinD resistant mutants. To select MinC^{N} resistant mutants,

Table 3. PCR primers and their sequences used in this work

Name	sequence
5'-MinC-SstI	GGAGCTCGCTAATTGAGTAAGGCCAGGATG
3'-MinD- HindIII	CATGTCCTGCAGAAGCTTGCATTAAAATCTAGCGAGGGC
5'-MinC*-SstI	CGAGCTCTTTAAGAAGGAGATATACGGATGTCAAACACGCCAATCG
5'-MinC^{C116}-SstI	CGAGCTCTAAGGAGGTTATAAATAATGGCGCAAAATACAACGCCGGTC
5'-lacIq-BglII	GCAGATCTACGATGTCGCAGAGTATGCC
3'-LacIq-MCS	GAATTGGGACAACTCCAGTG
5'- FtsZ-Bsu36I	GCCTCAGGCGACAGGCACAAATCGGAGAG
3'-FtsZ-PstI	GCGAGGGCT TTACTAAGCT TGGCTGCAGA TATTC

an *ftsZ-I374V* based mutant library (random mutagenesis done on the *ftsZ-I374V* allele) was constructed by a similar strategy as above; the resultant library was screened by the plasmid pBANG78 with 100 μM IPTG. Survivors were analyzed by sequencing the *ftsZ* gene.

Analysis of GFP-MinC^{C}/MinD and GFP-MinC/MinD localization.

For GFP-MinC^{C}/MinD analysis, overnight cultures of S4, BSM374 or JS964 (*min::kan*) containing the plasmid pHJZ109 (*gfp-minC^{C}/ minD*) were diluted 1000 fold into LB+Spc and grown at 37 °C until OD_{600}≈0.3. IPTG was then added at the indicated concentrations and the cultures were diluted every 0.5-1 h to keep the OD_{600}<0.4. Samples were taken at different time points and checked by microscopy as previously described (Zhou & Lutkenhaus, 2005). For GFP-MinC/MinD localization studies, Overnight cultures of S7/pBANG112 (*ftsZ^{0} min::kan/ftsZ-*WT), S7/pBANG112-280D (*ftsZ^{0} min::kan/ftsZ-N280D*) and S7/pBANG112-23 (*ftsZ^{0} min::kan/ftsZ-23*) containing the plasmid pBANG85 (P*trc*::*gfp-minCD*) were diluted 1000 fold into LB containing spectinomycin and ampicllin and grown at 37 °C until OD_{600}≈0.05. IPTG was then added at the indicated concentrations and the cultures were grown for another 2-3 hours to reach OD_{600}≈0.4. Samples were taken and analyzed by microscopy in the same way as above.

Yeast two hybrid assay.

To detect FtsZ-FtsA and FtsZ-ZipA interactions, the appropriate plasmids were transformed into the reporter strain SFY526 as described (Huang *et al.*, 1996). The colonies

obtained were analyzed for β-galactosidase production by the colony lift assay described in the CLONTECH manual.

Protein purification and FtsZ recruitment assay.

WT FtsZ, FtsZ-I374V, FtsZ-N280D and FtsZ-23 were expressed and purified from W3110/pKD126 (*ftsZ-WT*), BSZ374/pKD126-I374V (*ftsZ-I374V*), BSZ280D/pKD126-N280D (*ftsZ-N280D*) and BSZ23/pKD126-23(*ftsZ-23*) respectively according to the method described previously (Mukherjee & Lutkenhaus, 1998b). A slight modification was that after ammonium sulfate precipitation, the pellet was dissolved and dialyzed in Buffer A and further purified by chromatography on a Resource Q column (GE healthcare) eluting with 50 mM Tris-HCl (pH 7.9), 1 mM EDTA, 10% glycerol, and a gradient of 50-500 mM KCl. The FtsZ fractions (eluting at 200-300 mmM KCl) were pooled and dialyzed against 50 mM HEPES-NaOH (pH 7.2), 0.1mM EDTA and 10% glycerol, aliquoted and stored at –80°C. The quality of the purified proteins was checked by SDS-PAGE following the standard FtsZ polymerization assay (Dajkovic *et al.*, 2008a). The purification of all other proteins (MalE-MinC^{C}, MalE-MinC^{N}, MalE-MinC and MinD) and the FtsZ recruitment assay as well as the FtsZ sedimentation assay were performed as previously described (Dajkovic et al., 2008a).

Immunofluorescent microscopy.

Overnight cultures of S4/pBANG75 and BSM374/pBANG75 were diluted 1000-fold in LB+Spc and grown at 37 ^{o}C. At OD_{600}≈0.3, samples were taken and fixed with

paraformaldehyde + glutaraldehyde. At the same time the cultures were diluted 10 times to fresh LB+Spc and induced with IPTG=100μM. Samples were taken and fixed every hour and cultures were diluted every hour to maintain the exponential phase. As a control, an exponentially growing culture of S4/pBANG75 was treated with 20 μg/ml cephalexin for 2 hours and then cells were fixed with paraformaldehyde + glutaraldehyde. Fixation of the cells, preparation for immuno-staining and photography of samples were done as described before (Pichoff & Lutkenhaus, 2002). The antisera were used at following concentrations: FtsZ (1/5000), FtsA (1/5000), ZipA (1/4000) and FtsK (1/1000).

Western blot.

To determine the MinC/MinD level in the indicated strains and conditions, in LB medium (supplemented with Spc if necessary and IPTG at indicated concentrations), grow strains S3, S4, S4/pBANG59 (with IPTG=40μM), S4/pBANG78-G10D (with IPTG=30μM), S4 /pBANG78-R172A (with IPTG=30μM), BSM374/pBANG78 (with IPTG=25μM) and BSM374/pBANG78-R172A (with IPTG=40μM) at 37°C for about 3 hours to reach OD_{600}=0.4. Cells are then collected and resuspended in sodium dodecyl sulfate (SDS) sample buffer, boiled for 10min, and subjected to SDS polyacrylamide gel electrophoresis (PAGE). Subsequent immunoblot was done as previously described (Zhou & Lutkenhaus, 2005). For better comparison, the loading volume for these samples is adjusted as: for S3, S4 and S4/pBANG59, the loading volume is equivalent to 300μl of OD_{600}=0.4 cells; for the rest is 60μl of OD_{600}=0.4 cells. To detect the stability and abundance of FtsZ in different mutants, grow the indicated strains (S3, BSZ280D, BSZ374V, BSZ23, S18/pBANG112, S18/pBANG112-280D, S18/pBANG112-374V, S18/pBANG112-23)

to OD600=0.4 and then harvest the cells. Using the same treatment as above, the whole cell lysate was used in an immunoblot analysis to determine the stability and abundance of FtsZ mutants in corresponding strains. For each sample, the loading volume is equivalent to the lysate of 200µl OD600=0.4 cells.

Far western analysis.

MalE-MinC or MalE-MinC^N (or MalE-SulA as control) was run on a 7.5% native PAGE gel (Biorad, cat # 161-1100) following the instructions coming with the gel. 1µg of protein was loaded into each of the 10 wells. The protein was then transferred to the nitrocellulose membrane following the standard western blot protocol (the transfer buffer is the same as the PAGE running buffer). The membrane was then cut into 3 equal pieces. One piece was used for Ponceau-S staining to see the amount and position of the protein on the membrane. The other two pieces were first blocked with 2.5% milk in the FtsZ polymerization buffer (50 mM MES, 50 mM KCl, 10 mM $MgCl_2$, pH=6.5) for 1 hour and then incubated in the same buffer (with milk) containing 5 µM FtsZ (WT or the FtsZ-N280D mutant, one piece of membrane for each) for about 1 hour at room temperature with gentle shaking. After 5min/each X 3 washes with the FtsZ polymerization buffer, the membrane was blotted with FtsZ antiserum and detected with an AP-conjugated secondary antibody as in regular western blots.

Biosensor assay.

The instrument we used is the Biacore X and the sensor chips are the SA chips from GE healthcare. FtsZ (WT or the FtsZ-N280D mutant) was biotinylated using EZ-Link Sulfo-NHS-LC-Biotinylation kit to the level of 1:1 (1 biotin to 1 FtsZ molecule) following the protocol provided by the manufacturer (Pierce, cat # 21435). The biotinylated FtsZ was then immobilized onto the sensor chip by interacting with streptavidin, which was covalently linked to the chip surface. After the sensorgram reached a stabilized signal, MalE-MinC at various concentrations (1, 2, 4, 8, 16, 32 μM) was injected into the sensor flow cells at the rate of 10 μl/min. The response was recorded and analyzed by the BIAevaluation software. The buffer used was the HBS-P buffer from GE healthcare and MalE-MinC dilutions were made in this buffer. After each MalE-MinC injection, the sensor chip was regenerated by HBS-P buffer containing 4M NaCl.

Chapter III: The conserved C terminal tail of FtsZ is required for the septal localization and division inhibitory activity of $MinC^{C}$/MinD.

Abstract

The *E. coli* Min system contributes to spatial regulation of cytokinesis by preventing assembly of the Z ring away from midcell. As the effector of the Min system, MinC is a cell division inhibitor whose activity is spatially regulated by MinD and MinE. It has two functional domains of similar size. The N-terminal domain disrupts FtsZ polymers and therefore inhibits division when overproduced. The C-terminal domain also inhibits cell division when overproduced in the presence of MinD. However, the molecular mechanism of either domain is not very clear. Here, we report that the septal localization and division inhibitory activity of $MinC^{C}$/MinD requires the conserved C-terminal tail of FtsZ. This tail also mediates interaction with two essential division proteins, ZipA and FtsA, to link FtsZ polymers to the membrane. Overproduction of $MinC^{C}$/MinD displaces FtsA from the Z ring and eventually disrupts the Z ring, probably because it also displaces ZipA. These results support a model for the division inhibitory action of MinC/MinD. MinC/MinD binds to ZipA and FtsA decorated FtsZ polymers located at the membrane through the $MinC^{C}$/MinD-FtsZ interaction. This binding displaces FtsA and/or ZipA, and more importantly, positions $MinC^{N}$ near the FtsZ polymers making it a more effective inhibitor.

Introduction

As discussed above, the effector of the Min system--- MinC has two domains of approximately equal size (Cordell *et al.*, 2001, Hu & Lutkenhaus, 2000). Both domains are essential for MinC to spatially regulate division since mutations mapping in either domain lead to minicell formation. The min operon containing the MinC-G10D (located in the N-terminal domain ($MinC^{1-115}$ [$MinC^{N}$])) or MinC-R172A mutation (located in the C-terminal domain ($MinC^{116-231}$ [$MinC^{C}$])) on a single copy plasmid loses the ability to complement the min deletion strain (unpublished data, Wissel and Lutkenhaus and (Zhou & Lutkenhaus, 2005).

The two domains of MinC have been separated to determine the basis for their activity. Overproduction of a MalE-$MinC^{N}$ fusion blocks Z ring formation in vivo and the purified protein disrupts FtsZ polymer sedimentation in vitro without affecting the GTPase activity of FtsZ (Hu & Lutkenhaus, 2000). The C terminal domain of MinC mediates homodimerization and interaction with MinD. Overproduction of $MinC^{C}$ alone does not affect cell division, but it has inhibitory activity in the presence of MinD (Shiomi & Margolin, 2007) and the molecular basis for this is completely unknown. $MinC^{C}$ also limits the bundling of FtsZ filaments In vitro but this does not require MinD (Dajkovic et al., 2008a), indicating that the block of FtsZ polymer bundling may not be able to fully explain the division inhibitory activity of $MinC^{C}$/MinD in vivo.

At low expression levels, GFP-$MinC^{C}$/MinD localizes to the Z ring without disrupting it (Johnson *et al.*, 2002). This localization is dependent upon FtsZ but not other early division proteins such as FtsA, ZipA and ZapA (Johnson *et al.*, 2002, Johnson *et al.*, 2004, Zhou & Lutkenhaus, 2005), suggesting that $MinC^{C}$/MinD interacts with FtsZ directly. An interaction between FtsZ and $MinC^{C}$/MinD was observed in an in vitro assay (Dajkovic et al., 2008a), which

strongly supports this idea. In this paper we further investigate the mechanism by which $MinC^C$/MinD antagonizes Z ring formation. We isolated FtsZ mutants that are resistant to $MinC^C$/MinD and then used these mutants to study the $MinC^C$/MinD-FtsZ interaction and the basis of the toxicity of $MinC^C$/MinD overproduction.

Results

Isolation of FtsZ mutants resistant to $MinC^C$/MinD.

Overproduction of $MinC^C$/MinD disrupts the Z ring and causes filamentation and therefore lethality (Shiomi & Margolin, 2007). There are several lines of evidence suggesting that $MinC^C$/MinD binds FtsZ (Dajkovic et al., 2008a, Johnson et al., 2004, Johnson et al., 2002). To further study the inhibitory mechanism of $MinC^C$/MinD, we exploited the above phenotype in a screen for FtsZ mutants that are resistant to $MinC^C$/MinD. To this end, we performed PCR random mutagenesis over the coding region of *ftsZ* and screened for mutants that still support division and can suppress the toxicity of $MinC^C$/MinD overexpression.

Using the strategy described in "materials and methods", we isolated four FtsZ mutants which are resistant to $MinC^C$/MinD. Each of these mutants contained a single mutation in *ftsZ* - D373E, I374V, L378V and K380M (Fig. 7A). Interestingly, all of these mutations result in amino acid substitutions in the C-terminal conserved tail of FtsZ that is also involved in interaction with the essential division proteins FtsA and ZipA (Fig. 7B). All four mutations, when introduced into pBANG112, do not affect its ability to complement the *ftsZ* depletion

Fig. 7. A: summary of FtsZ mutants that are resistant to $MinC^C$/MinD. In the genetic screen for *ftsZ* mutations that suppress the toxicity of $MinC^C$/MinD overproduction, we obtained four mutations (each of them was obtained multiple times in the screen). A single colony of each mutant was resuspended in LB and serially diluted (10 fold steps) and aliquots spotted on Spc and Amp plates with or without IPTG and incubated overnight at 37 °C. 1, S7 (*ftsZ*^{0} *recA::Tn10*) /pBANG112 (WT-FtsZ) + pBANG75-1 ($MinC^C$-R172A); 2, S7/pBANG112 (WT-FtsZ) + pBANG75 (WT-$MinC^C$/MinD); 3, S7/pBANG112-1 (*ftsZ-D373E*) + pBANG75; 4, S7/pBANG112-2 (*ftsZ-I374V*) + pBANG75; 5, S7/pBANG112-3 (*ftsZ-L378V*) + pBANG75; 6, S7/pBANG112-4 (*ftsZ-K380M*) + pBANG75. B: diagram of FtsZ. A cartoon of FtsZ showing the sequence of the conserved C-terminal tail involved in binding ZipA and FtsA and the location of the mutations isolated in this study.

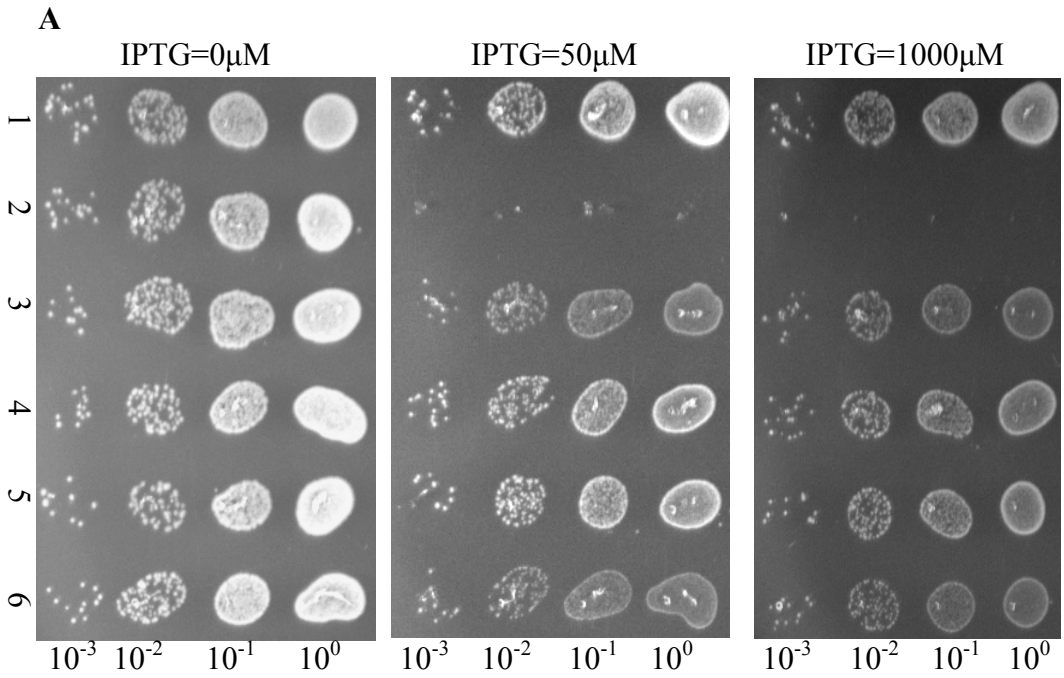
A
IPTG=0μM
IPTG=50μM
IPTG=1000μM
1
2
3
4
5
6
10-3 10-2 10-1 100
10-3 10-2 10-1 100
10-3 10-2 10-1 100

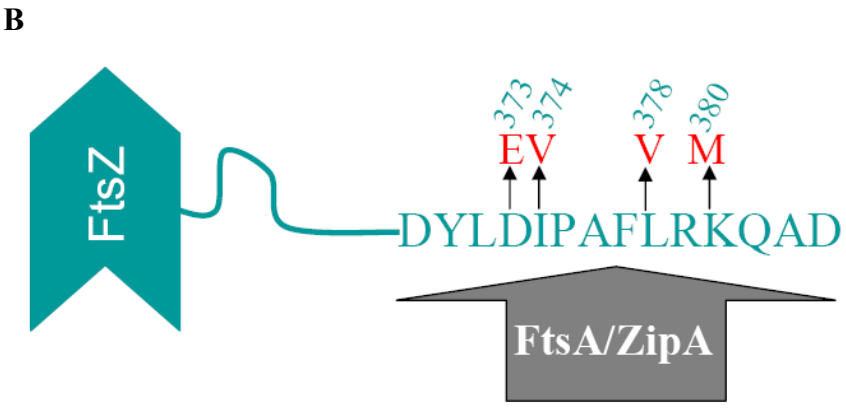
B
FtsZ
373
374
378
380
EV
V
M
DYLDIPAFLRKQAD
FtsA/ZipA

strain (S7 [*ftsZ*^{o} *recA*::Tn*10*]/pKD3C) at 42 ºC or 37 ºC, although the presence of the L378V mutation causes the cells to grow a little slower than the others (data not shown). Since these mutations do not affect complementation of the *ftsZ* depletion strain, they must not disrupt the essential activities of FtsZ required for cell division (see below). Among the four mutants, FtsZ-I374V afforded the greatest resistance to MinC^{C}/MinD (data not shown) and was therefore chosen for subsequent studies. It is likely that the resistance to MinC^{C}/MinD afforded by all four mutants is due to the same mechanism since they map to the same small region of FtsZ.

Characterization of FtsZ-I374V mutant.

E. coli cells are sensitive to the FtsZ protein level since they have different morphologies with different *ftsZ* expression levels. To get a better idea about the effect of this mutation (I374V) on FtsZ function we used the lamda RED recombineering system (Datsenko & Wanner, 2000) to put the *ftsZ-I374V* mutation to the chromosome at its native locus. The resultant strain (BSZ374 [*ftsZ-I374V*]) does not show any significant difference to the control strain (S3 [*ftsZ*-WT]) in terms of growth rate and morphology. The only effect of the mutation was observed when the entire *min* locus was deleted from these strains to give BSM374 (BSZ374 *min::kan*) and S4 (S3 *min::kan*). BSM374 grew similarly to S4 at 30 °C and 37 °C but failed to form isolated colonies at room temperature (20 ºC). S4 grew at room temperature but the cells were filamentous (data not shown).

BSM374 (*ftsZ-I374V, min::kan*) is resistant to MinC^{C}/MinD and also displays resistance to MinC/MinD. As shown in the spot test in Fig. 8, the control strain S4 (*min::kan*) containing plasmids expressing MinC/MinD (pBANG59/P*tac::minCD*) or MinC^{C}/MinD

(pBANG75/*Plac::minC^{C}D*) under control of IPTG-inducible promoters did not grow at or above 50 μM IPTG (Fig. 8, row 1) and 25 μM IPTG (Fig. 8, row 3) respectively. Even though pBANG75 requires less IPTG to prevent the growth of the S4 strain, it is a higher copy number plasmid than pBANG59 (around 10 for pBANG75 and 1-2 for pBANG59) and has a stronger ribosome binding site for MinC^{C} translation (compared to MinC). As will be shown later, the minimal amount of protein required to prevent the growth of this strain is actually higher for MinC^{C}/MinD than for MinC/MinD. In contrast to S4 containing these plasmids, BSM374/pBANG59 (*ftsZ-I374V*, *min::kan*/P*tac::minCD*) and BSM374/pBANG75 (*ftsZ-I374V*, *min::kan*/P*lac::minC^{C}D*) could grow with IPTG as high as 1000μM (Fig. 8, rows 2 and 4) and the cells were not filamentous. Since FtsZ-I374V confers resistance to MinC/MinD in addition to MinC^{C}/MinD, it is surprising to note that the BSZ374 cells have WT morphology and do not produce minicells. We expected it might produce minicells at a frequency comparable to a *min* null strain since FtsZ-I374V displays some resistance to MinC/MinD. Deletion of the *min* locus in BSZ374 did result in a minicell phenotype indicating that FtsZ-I374V could produce polar rings and lead to polar divisions when Min was absent. These observations suggest that FtsZ-I374V still responds to MinC/MinD to some extent and the polar Z rings made from FtsZ-I374V are still susceptible to MinC/MinD (discussed later).

To rule out the possibility that the MinC/MinD resistance of FtsZ-I374V strain is due to an increased steady state protein level or reduced GTPase of the mutant protein, we checked the SulA sensitivity of this strain. SulA is another cell division inhibitor (Bi & Lutkenhaus, 1993) and it is well documented that increased FtsZ level or FtsZ mutants with decreased GTPase activity confers resistance to SulA (Dai *et al.*, 1994, Dajkovic *et al.*, 2008b, Lutkenhaus *et al.*, 1986). A careful spot test revealed that the SulA sensitivity of the BSZ374 (*ftsZ-I374V*) strain

Fig. 8. FtsZ-I374V is resistant to both $MinC^{C}$/MinD and MinC/MinD. One colony of each strain was resuspended in 900 μl of LB medium and serially diluted by 10. Then 3μl culture from each dilution was spotted on plates (with Spc) with or without IPTG (as indicated) and incubated overnight at 37 °C. 1, S4 (*min::kan*)/pBANG59; 2, BSM374 (*ftsZ-I374V, min::kan*)/pBANG59; 3, S4 /pBANG75; 4, BSM374 /pBANG75.

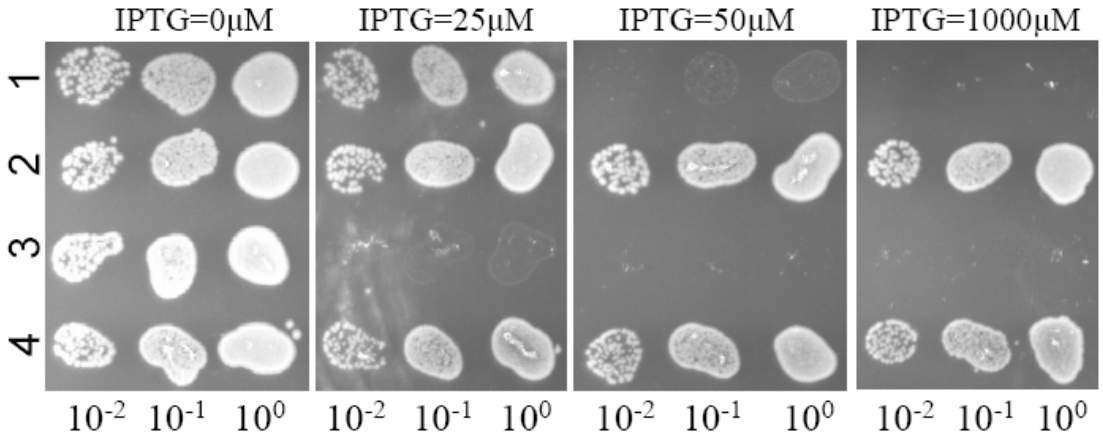
IPTG=0μM
IPTG=25μM
IPTG=50μM
IPTG=1000μM
1
2
3
4
10-2 10-1 100
10-2 10-1 100
10-2 10-1 100
10-2 10-1 100

was not any greater than that of the WT strain S3 (Fig. 20). We also checked the FtsZ protein level in the FtsZ-I374V mutant strain and the result showed that it was indistinguishable from that of the WT strain (Fig. 18). All these indicate that the stability and GTPase activity of the FtsZ protein are not significantly affected by this mutation.

Interaction of FtsZ I374V with FtsA and ZipA.

Previously, a yeast-two-hybrid study showed that the conserved extreme C terminus of FtsZ containing the I374 residue was involved in the FtsZ-FtsA and FtsZ-ZipA interactions (Haney *et al.*, 2001). Here, we asked whether the *ftsZ-I374V* mutation affected these interactions. Using the yeast-two-hybrid system (YTH) to look at these interactions, we found that FtsZ-I374V interacted with ZipA similarly to WT FtsZ but it did not interact with FtsA (Table 4). The loss of the interaction between FtsZ-I374V and FtsA in this assay is somewhat surprising since FtsZ-I374V can fully complement the *ftsZ* depletion strain and support cell division. We therefore examined the effect of the *ftsZ-I374V* mutation on the recruitment of FtsA to the septum by immunofluorescent microscopy.

Immuno-staining of cells from exponentially growing cultures revealed that Z rings were present at similar frequencies in BSZ374 (*ftsZ-I374V*) and the wild type strain S3 (>80% of cells had a Z ring at midcell; no polar rings were observed). FtsA and ZipA were both efficiently recruited to the Z ring in BSZ374 (*ftsZ-I374V*) since FtsA rings and ZipA rings were observed at similar frequencies (> 80%) to Z rings (Table 5). The ability of ZipA and FtsA to localize to Z rings in the FtsZ-I374V mutant strain was also investigated by using green fluorescent protein (GFP) fusions as reported previously (Pichoff & Lutkenhaus, 2001, Pichoff & Lutkenhaus, 2007).

Table 4. Analysis of FtsZ-FtsA and FtsZ-ZipA interaction by yeast-two-hybrid.

For each protein interaction tested, the β-galactosidase assay was done twice with colonies obtained from ten independent transformats using the filter lift assay as described in Clontech manual and results are reproducible. +++, indicates blue color development in less than 1 h; ++, blue color between 1h and 2h; –, indicates no blue color development. N/D, not determined. #The FtsA construct used here is the MTS truncated version as described previously (Pichoff & Lutkenhaus, 2007).

Product fused to AD	Interaction with product fused to BD		
	None	ZipA	FtsA[#]
None	**N/D**	-	-
FtsZ-WT	-	+++	++
FtsZ-I374V	-	+++	-

Table 5. Frequencies of FtsZ, FtsA and ZipA rings in WT and FtsZ I374V mutant strains. Cells from exponentially growing cultures of S3 and BSZ374 were fixed and subjected to immuno-staining to examine the localization of endogenous FtsZ, FtsA and ZipA proteins. The numbers are the number of cells with rings divided by the totally number of cells analyzed.

	S3 (WT)	BSZ374 (*ftsZ-I374V*)
FtsZ ring	97/117=83%	88/101=87%
FtsA ring	103/129=80%	126/156=81%
ZipA ring	108/131=83%	90/105=86%

Although these fusions cause filamentation, at appropriate induction levels both ZipA-GFP and GFP-FtsA formed ring structures in FtsZ-I374V cells that were similar to those in WT cells (Fig. 9), indicating that both of these fusions localized to the Z ring. The results of the FtsA localization appear inconsistent with the YTH result. It is possible, however, that there is an interaction between FtsZ-I374V and FtsA that is sufficient to recruit FtsA to the Z ring even though it can not be detected by YTH.

FtsZ-I374V is unable to recruit $MinC^{C}$/MinD in vivo.

$MinC^{C}$/MinD has been shown to localize to the Z ring as revealed by GFP-tagging of $MinC^{C}$ (Johnson et al., 2002, Zhou & Lutkenhaus, 2005). Several lines of evidence suggest that $MinC^{C}$/MinD interacts with FtsZ directly to achieve this localization (Johnson et al., 2002, Johnson et al., 2004, Dajkovic et al., 2008a). Our results are consistent with this idea since we isolated FtsZ mutants that are resistant to $MinC^{C}$/MinD. We speculated that the $MinC^{C}$/MinD resistance of these mutants is due to the loss of interaction with $MinC^{C}$/MinD. To test this hypothesis, we first checked the ability of GFP-$MinC^{C}$/MinD to localize to the Z ring. We introduced a plasmid (pHJZ109) expressing GFP-$MinC^{C}$/MinD under an IPTG-inducible promoter control into FtsZ WT and FtsZ-I374V strains [the GFP fusion used here is distinct from the GFP-$MinC^{122-231}$ construct described in (Shiomi & Margolin, 2007) since it does not interfere with the activity of $MinC^{C}$]. GFP-$MinC^{C}$/MinD expression was induced with IPTG and fluorescence was monitored over time. As shown in Fig.10, the localization of GFP-$MinC^{C}$/MinD to the Z ring in the S4 (*ftsZ-WT*, *min::kan*) strain was already observed before induction (Fig.10, A1), indicating the basal expression was sufficient to allow visualization of

Fig. 9. Localization of FtsA and ZipA in S4 and BSM374 strains as revealed by GFP-FtsA and ZipA-GFP. The plasmid pSEB293 (*gfp-ftsA*) was transformed into strains S4 and BSM374 and transformants were streaked on plates containing 0.0001% arabinose. After 5 hours growth at 37°C cells were examined by fluorescence microscopy. Exponentially growing S4 or BSM374 cells harboring the plasmid pSEB103 (*zipA-gfp*) were diluted into LB+Amp liquid medium containing 0.05% arabinose for 2 hours at 37°C with shaking. Cells were then removed and checked by fluorescence microscopy.

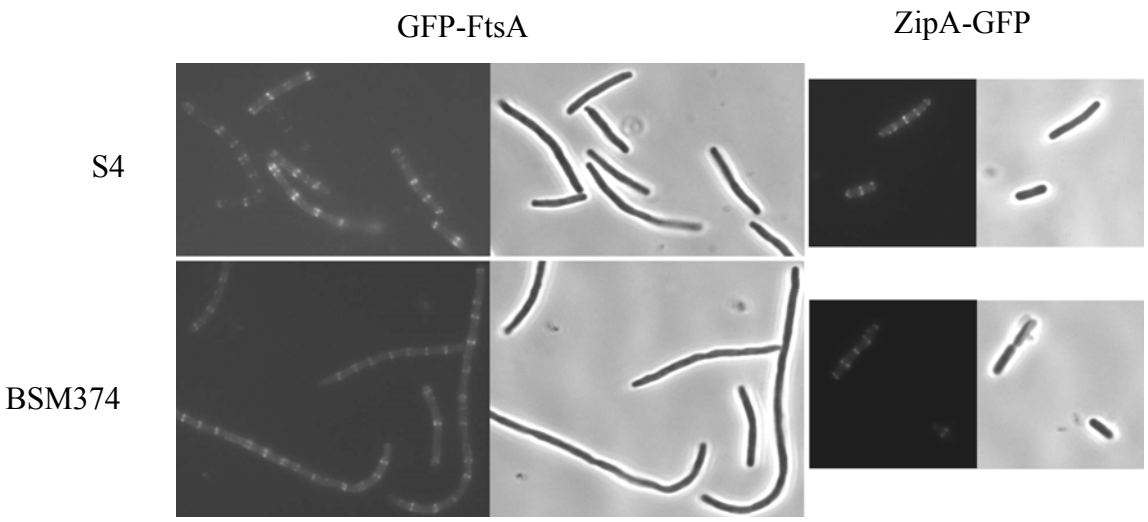
GFP-FtsA
ZipA-GFP
S4
BSM374

fluorescent rings. The GFP-MinC^{C}/MinD rings became brighter (Fig.10, A2) after 40 minutes of induction, however, as the induction time increased further, the GFP-MinC^{C}/MinD rings gradually disappeared indicating that the Z rings were being disrupted. At 70 minutes after induction, cells were longer and only a small fraction still possessed GFP-MinC^{C}/MinD rings (Fig.10, A3); in most filaments the GFP-MinC^{C}/MinD was primarily on the membrane but was also in spiral-like structures in many cells. At 100 minutes of induction, all cells became filamentous and no GFP-MinC^{C}/MinD rings were observed (Fig.10, A4). These results are consistent with previously reported observations that GFP-MinC^{C}/MinD is able to localize to the Z ring but that high levels disrupt the Z ring causing filamentation (Johnson et al., 2002, Shiomi & Margolin, 2007). In contrast, when GFP-MinC^{C}/MinD was induced in the FtsZ mutant strain BSM374 (*ftsZ-I374V min::kan*), cells never became filamentous and GFP-MinC^{C}/MinD never localized as a ring but was evenly distributed on the membrane at both early and late times after induction (Fig. 10B). These observations strongly indicate that FtsZ-I374V does not interact with MinC^{C}/MinD.

FtsZ-I374V does not bind MinC^{C}/MinD in vitro.

To confirm the loss of interaction between FtsZ-I374V and MinC^{C}/MinD, we employed an in vitro recruitment assay described previously (Dajkovic et al., 2008a) to assess the interaction between FtsZ and MinC^{C}/MinD. In this assay FtsZ polymers that are assembled in the presence of GMPCPP are efficiently recruited to MinD and MinC^{C} bound vesicles. MinD binds to phospholipid vesicles (MLVs) in an ATP-dependent manner and this MinD-MLV complex is readily sedimented in a tabletop centrifuge. If MinC^{C} is added to the reaction, it is recruited to

Fig. 10. GFP-MinC^{C}/MinD does not localize to Z rings composed of FtsZ-I374V. Expression of GFP-MinC^{C}/MinD was induced with IPTG in S4 (*min::kan*)/pHJZ109 (A) and BSM374 (*ftsZ-I374V, min::kan*)/pHJZ109 (B) and samples at various times were subjected to fluorescent microscopy. Fluorescence micrographs (A1-A4, B1-B4) and the corresponding phase contrast images (A1'-A4', B1'- B4') showing the localization of GFP-MinC^{C}/MinD over time in these two strains are presented. Cells were grown in the presence of 50 μM IPTG at 37°C for 0 min (A1, B1), 40 min (A2, B2), 70 min (A3, B3) and 100 min (A4, B4). Arrows in panel A indicate GFP-MinC^{C}/MinD localized to rings. The contrast and brightness of these pictures are adjusted unequally for better viewing.

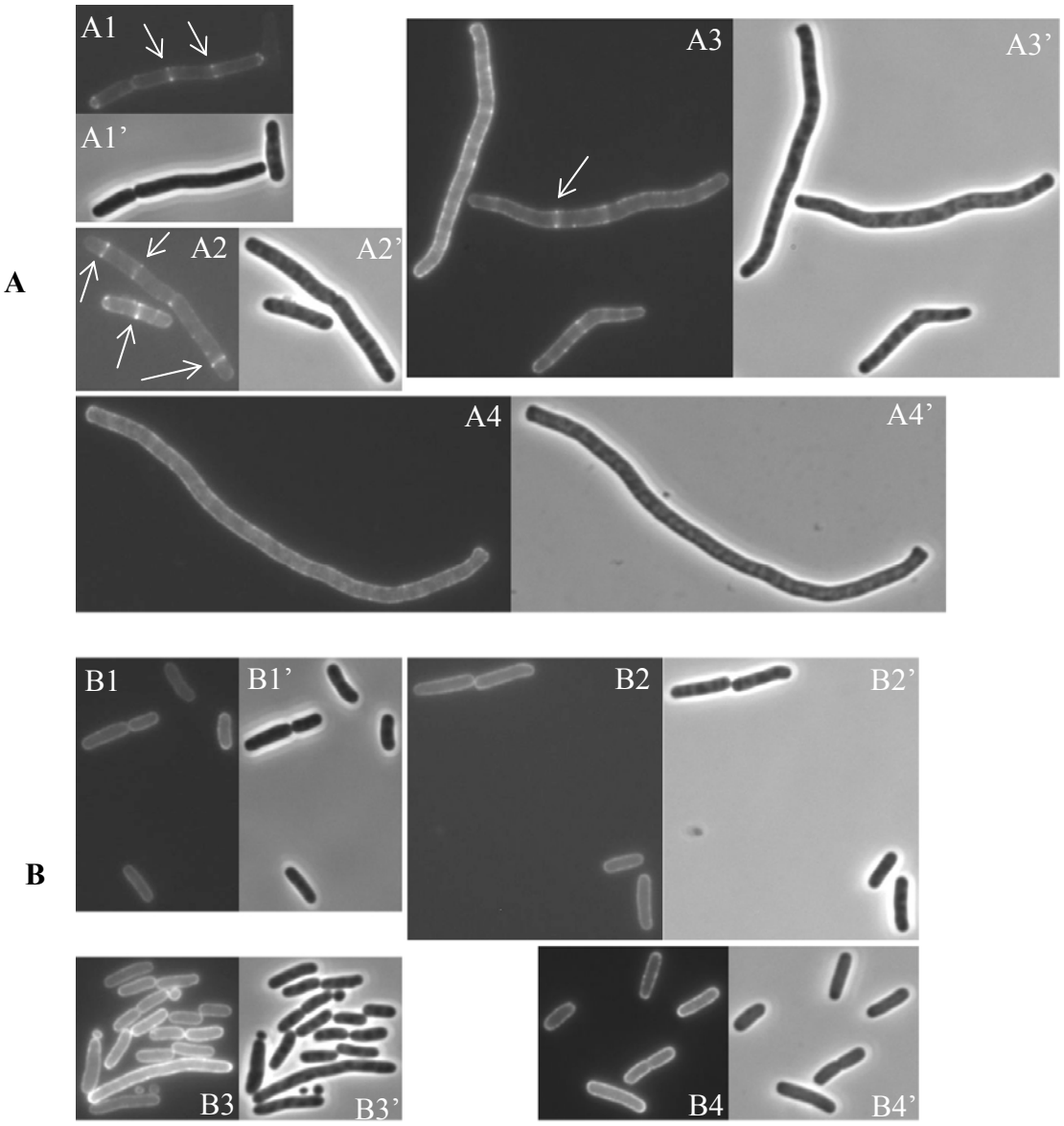
A
A1
A1'
A2
A2'
A3
A3'
A4
A4'
B
B1
B1'
B2
B2'
B3
B3'
B4
B4'

the MinD-MLV complex due to the interaction between $MinC^C$ and MinD (Fig. 11A, lane 4 and 6). If WT FtsZ is polymerized with GMPCPP and included in the reaction with MinD+ATP, $MinC^C$ and MLVs, the FtsZ polymers are recruited to the vesicle-Min complex (Fig 11A, lane 6). This recruitment requires $MinC^C$ as FtsZ polymers are not sedimented when $MinC^C$ is not included (Fig. 11A, lane 2). These results demonstrate that the centrifugation force used here is not sufficient to pellet FtsZ polymers and that there is a direct interaction between the $MinC^C$/MinD complex and FtsZ. We then purified the FtsZ-I374V protein and tested its ability to bind $MinC^C$/MinD using the above recruitment assay. Preliminary results revealed that the FtsZ-I374V protein displayed identical polymerization properties to WT FtsZ; both polymerized with GTP and GMPCPP and not GDP (Fig. 11C). When used in the recruitment assay, FtsZ-I374V polymers did not bind to the $MinC^C$/MinD-phospholipid vesicle complex (Fig 11B, lane 6), confirming that FtsZ-I374V does not interact with $MinC^C$/MinD.

FtsZ-I374V is still sensitive to the N-terminus of MinC.

MinC has two functional domains and each domain affects FtsZ function but the mechanism of action is quite different (Hu & Lutkenhaus, 2000, Shiomi & Margolin, 2007, Hu *et al.*, 1999, Dajkovic et al., 2008a). Although FtsZ-I374V confers resistance to MinC/MinD we speculated that it only suppresses the action of $MinC^C$ and would still be sensitive to $MinC^N$. To test this we introduced a plasmid (pZH111) expressing a MalE-$MinC^N$ fusion under arabinose promoter control into the S4 (*min::kan*) and BSM374 (*ftsZ-I374V min::kan*) strains to determine their sensitivity to arabinose. Neither S4 nor BSM374 containing the plasmid pZH111

Fig. 11. FtsZ-I374V does not bind $MinC^C$/MinD in vitro. The interaction between FtsZ and $MinC^C$/MinD was determined by a sedimentation assay in which the recruitment of FtsZ polymers to a phospholipid vesicle-associated $MinC^C$/MinD complex was assessed. Reactions containing mutilamellar phospholipid vesicles (MLV, 400 μg/mL), MinD (6μM), WT FtsZ (A) or FtsZ-I374V (B) at 6 μM, GMPCPP or GDP (200 μM) with (lane 3 to 6) or without (lane 1 and 2) MalE-$MinC^C$ (6 μM) were incubated at room temperature for 5 min in ATPase buffer (25 mM Tris-HCl [pH 7.5], 50mM KCl, and 5mM $MgCl_2$). ATP or ADP (1 mM) were then added to the reactions and incubated for another 5 min. The reactions were then centrifuged at 10,000×g for 2 min. The pellets were solubilized and analyzed by SDS-PAGE. C: standard polymerization assay of FtsZ and FtsZ-I374V to determine their polymerization property. WT FtsZ or the FtsZ-I374V mutant (5μM) was incubated in polymerization buffer and polymerization was initiated with 1 mM GTP or GMPCPP (GDP as control). The reaction was incubated at room temperature for 5 min and then sedimented at 80,000 rpm for 15 min at 25 °C. Pellets were then dissolved in SDS sample buffer and analyzed on SDS-PAGE gel. With repeated experiments, about 50-60% of the input FtsZ can be sedimented if polymerized with GTP and about 70% with GMPCPP for both proteins.

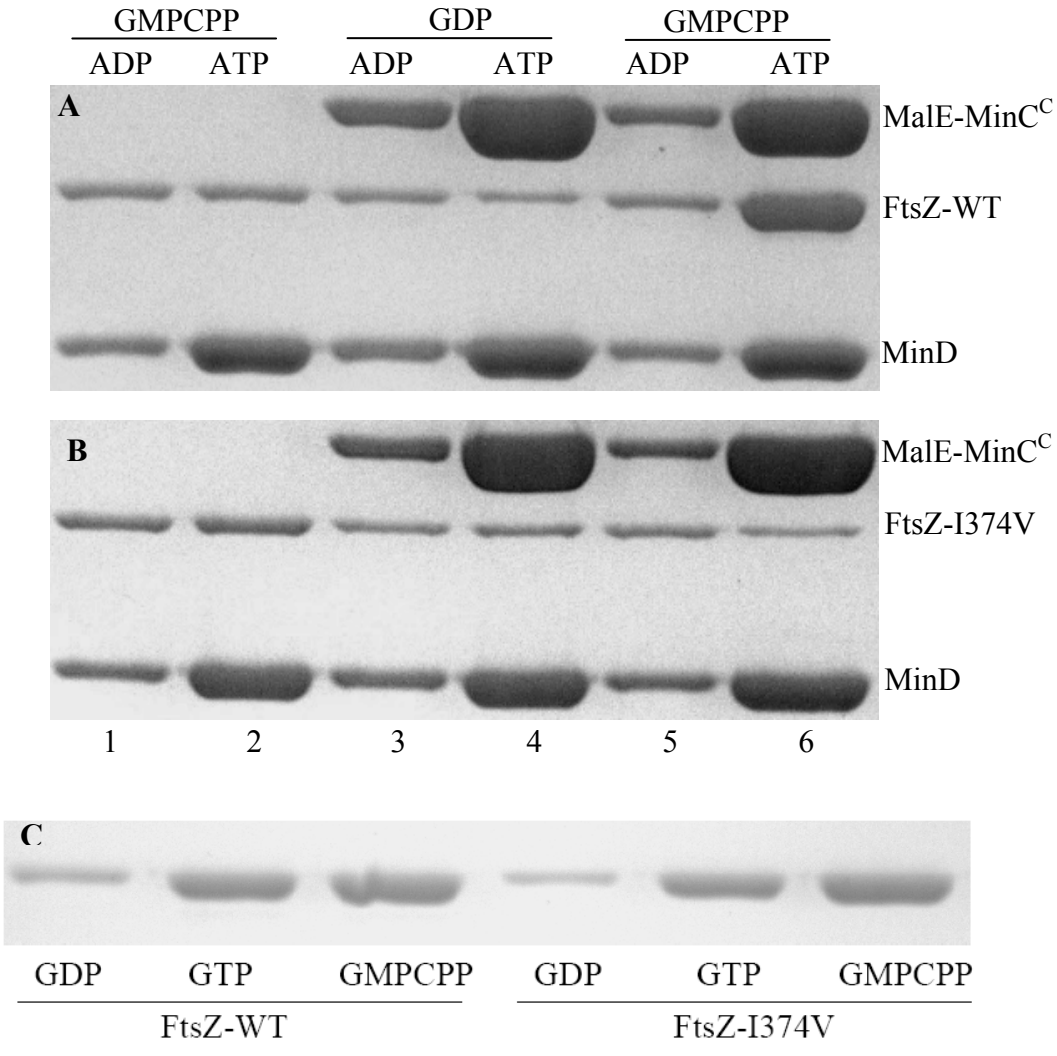
GMPCPP
GDP
GMPCPP
ADP
ATP
ADP
ATP
ADP
ATP
A
MalE-MinC^C
FtsZ-WT
MinD
B
MalE-MinC^C
FtsZ-I374V
MinD
1
2
3
4
5
6
C
GDP
GTP
GMPCPP
GDP
GTP
GMPCPP
FtsZ-WT
FtsZ-I374V

(P*ara::malE-minC*^{N}) formed colonies on plates containing 0.2% arabinose (data not shown). Colony formation was rescued by introduction of a point mutation (G10D) in MinC^{N} [this mutation disrupts the activity of MinC^{N} (Hu et al., 1999)] confirming that MinC^{N} was responsible for the toxicity. At low arabinose concentrations, pZH111 caused filamentation in both strains and no difference in arabinose sensitivity was detected. When grown on plates with 0.05% arabinose for 5 hours, both S4/pZH111 and BSM374/pZH111 became extremely filamentous (Fig. 12, A and B). This filamentation phenotype was not observed if the G10D substitution was present in MinC^{N} (Fig. 12, A' and B'). These observations indicate that the FtsZ-I374V mutant is as sensitive to MinC^{N} as the WT strain.

In the above assay MalE-MinC^{N} is not on the membrane, although it is still toxic if sufficiently overexpressed. To test the MinC^{N} sensitivity of the WT and FtsZ-I374V mutant strains under more physiological conditions, we compared the sensitivity of these two strains to MinC-R172A/MinD. The division inhibitory activity of this mutant form of MinC/MinD is from the N-terminal domain of MinC as the inhibitory activity of the C terminal domain is abolished by the R172A mutation (Zhou & Lutkenhaus, 2005). As shown in Fig. 13A rows 2 and 5, the growth of both S4 (*min::kan*) and BSM374 (*ftsZ-I374V, min::kan*) bearing the plasmid (pBANG78-R172A) expressing MinC-R172A/MinD under *lac* promoter control was blocked at similar IPTG concentrations (20 μM for S4 and 30 μM for BSM374, data not shown). A Western blot showed that a similar level of the MinC-R172A protein (with MinD) was required to cause uniform filamentation in these two strains in liquid cultures (Fig. 13B, lane c and f), suggesting similar toxicity in both strains. We also tested the sensitivity of FtsZ-WT and FtsZ-I374V to MinC^{N} in vitro. Sedimentation of both WT FtsZ and FtsZ-I374V in the presence of GTP was

Fig. 12. The FtsZ-I374V mutant strain is sensitive to $MinC^N$. (A) BSM374 (*ftsZ-I374V, min::kan*) and(B) S4 (*min::kan*) harboring the plasmid pZH111 (Para::*malE-minC*^{N}) were grown on plates containing 0.05% arabinose at 37°C. The morphology of these cells was then checked at 5 hours by phase contrast microscopy. As a control, a point mutation (G10D) that inactivates $MinC^N$ was introduced into pZH111 and the mutant protein was expressed in BSM374 (A') and S4 (B') with the above conditions.

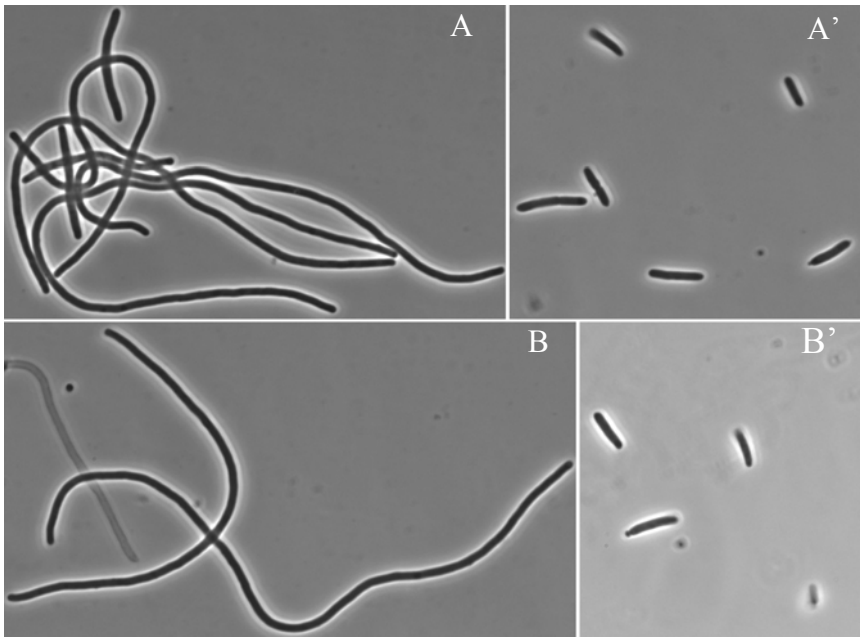
A
A’
B
B’

Fig. 13. Comparison of the killing efficiency of MinC/MinD and its mutants in FtsZ-WT and FtsZ-I374V strains. A: Plasmids pBANG78 (P*lac::minC/minD*), pBANG78-G10D (m*inC-G10D* on pBANG78) or pBANG78-R172A (*minC-R172A* on pBANG78) was transformed into S4 (*min::kan*) or BSM374 (*ftsZ-I374V, min::kan*). A spot test was done following the protocol described in Fig 2 with the following samples: Row 1, S4/ pBANG78-G10D; 2, S4/ pBANG78-R172A; 3, BSM374/pBANG78; 4, BSM374/ pBANG78-G10D; 5, BSM374/ pBANG78-R172A. B: The minimal amount of MinC or MinC mutant proteins to cause uniform filamentation in S4 and BSM374 strains. Plasmid pBANG78 (pBANG59/P*tac::minCD* in the case of sample d) and its derivatives containing the *minC-G10D* or *minC-R172A* mutations were induced with minimal concentrations of IPTG to cause uniform filamentation in the indicated strains in liquid culture. The MinC protein level was determined by immunoblot with the WT strain S3 and Δ*min* strain S4 as controls: a, S3; b, S4/pBANG78-G10D; c, S4/pBANG78-R172A; d, S4/pBANG59; e, BSM374/pBANG78; f, BSM374/ pBANG78-R172A; g, S4 and h, Marker at 28.8KD. The relative protein levels were indicated. *Loading volume for samples a, d and g was 5 fold more that that of samples b, c, e and f (see *materials and methods*).

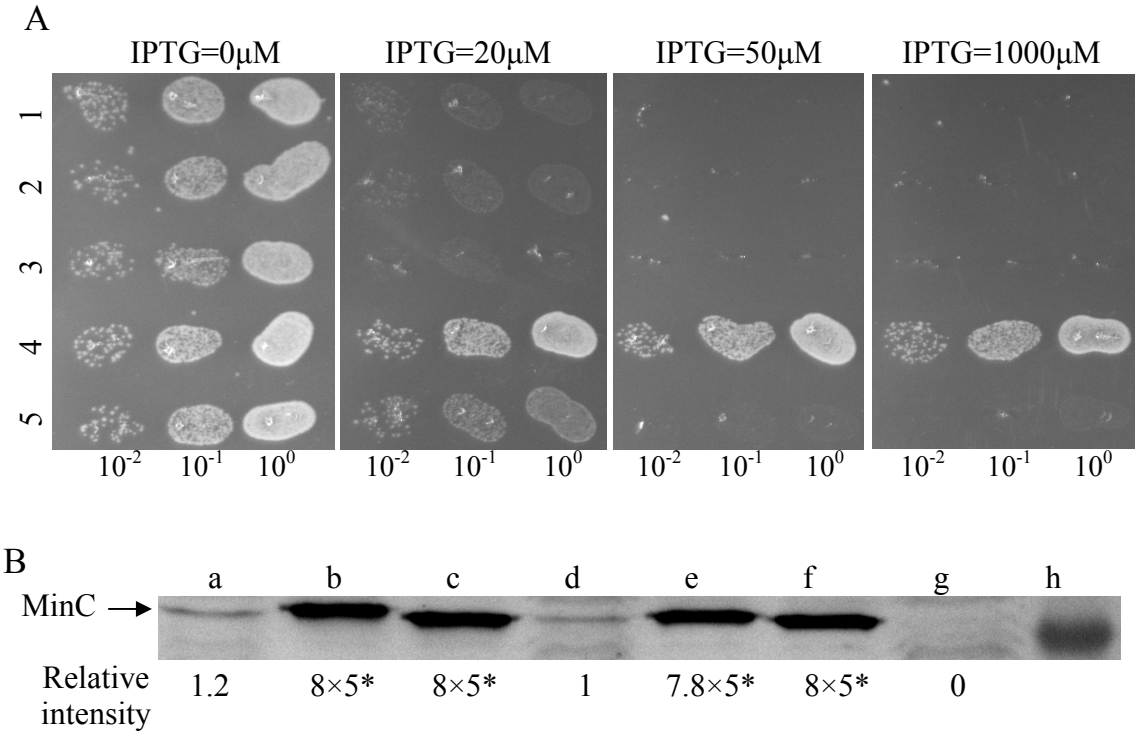
A
IPTG=0μM
IPTG=20μM
IPTG=50μM
IPTG=1000μM
1
2
3
4
5
10-2 10-1 100
10-2 10-1 100
10-2 10-1 100
10-2 10-1 100
B
a b c d e f g h
MinC
Relative intensity
1.2 8×5* 8×5* 1 7.8×5* 8×5* 0

prevented by MalE-MinC^{N} in a concentration dependent manner (data not shown). Together, these results demonstrate that FtsZ-I374V and FtsZ-WT have similar sensitivity to MinC^{N}. Therefore, we conclude that the MinC/MinD resistance of FtsZ-I374V is due to the resistance to MinC^{C}/MinD.

Concentration dependent effect of MinC^{C}/MinD on Z rings

Overproduction of MinC^{C} in the presence of MinD inhibits assembly of Z rings (Shiomi & Margolin, 2007) even though MinC^{C} does not affect the polymerization of FtsZ in vitro (Hu & Lutkenhaus, 2000). MinC^{C} was shown to block the lateral association of FtsZ polymers in vitro and this activity may be responsible for the disruption of the Z ring in vivo (Dajkovic et al., 2008a). However, the importance of lateral interactions between FtsZ polymers in Z-ring assembly remains enigmatic because of the relatively short length of the FtsZ protofilaments and a failure to observe multistranded polymers in vivo by electron cryotomography (Chen & Erickson, 2005, Li *et al.*, 2007). Our finding that the septal localization and division inhibitory action of MinC^{C}/MinD require the region of FtsZ that is also involved in the interaction with FtsA and ZipA raised the possibility that MinC^{C}/MinD could compete with FtsA and ZipA. Such competition may dislodge FtsZ polymers from the membrane thereby disrupting the Z ring. There are at least two discrete steps in the inhibition of cell division by MinC^{C}/MinD. We had already observed that limited induction of GFP-MinC^{C}/MinD caused filamentation, but the fluorescence was present in ring structures (Fig. 14, A1). This result indicated that Z rings were present but they did not support division: the limited expression of GFP-MinC^{C}/MinD prevented Z-ring function without disrupting its formation. Induction of GFP-MinC^{C}/MinD at a higher

Fig. 14. Effect of the induction level of GFP-MinC^{C}/MinD on Z ring assembly. GFP-MinC^{C}/MinD was induced from pHJZ109 at different IPTG concentrations in JS964 (*min::kan*). Samples were taken at different times after induction and subjected to fluorescence microscopy. At the lower IPTG level (A1, cells were induced with IPTG=100 μM for 5 hours), GFP-MinC^{C}/MinD inhibits division but doesn't disrupt the Z rings as the fluorescence is present in rings. However, at the higher IPTG level (cells were induced with IPTG=200 μM), both division and Z ring assembly were blocked (B1: T=1.5 hr; B2: T=3 hr). Images A1' to B2' are the phase contrast pictures of the corresponding fluorescent images A1 to B2.

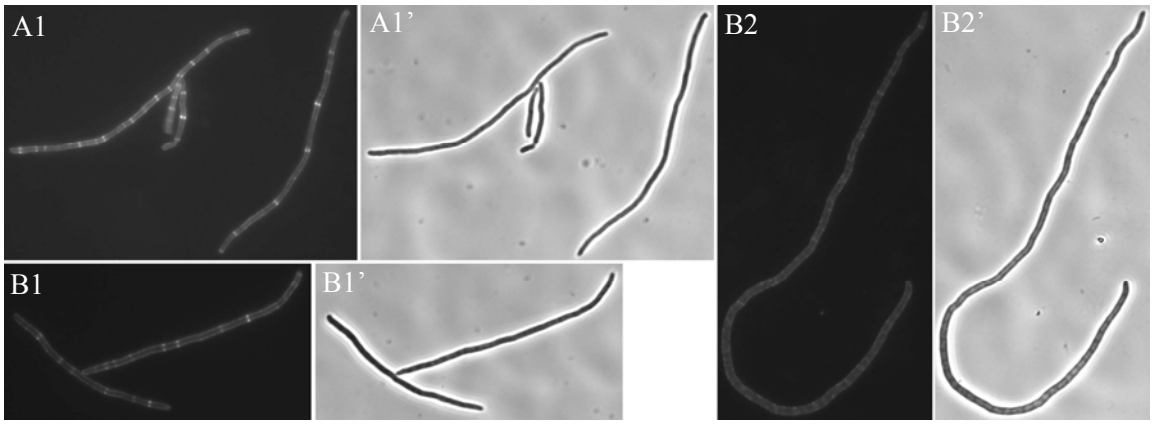
A1
A1’
B2
B2’
B1
B1’

level resulted in filamentation and initial localization to Z rings (Fig. 14, B1) which eventually disappeared (Fig. 14, B2). We reasoned that one possible mechanism by which $MinC^C$/MinD could block Z-ring function is to preferentially displace either FtsA or ZipA from the Z ring. If $MinC^C$/MinD competes more efficiently with one of the two (FtsA or ZipA) for interacting with FtsZ, then overproduction of $MinC^C$/MinD at some level could displace just one of them and not disrupt the ring since the Z ring can form with either FtsA or ZipA (Pichoff & Lutkenhaus, 2002).

To test this, we did immuno-staining to examine the localization of FtsZ, FtsA, ZipA and FtsK proteins in cells over-expressing $MinC^C$/MinD. The localization pattern of FtsK serves as an indicator of the integrity of the Z ring since its septal localization requires FtsZ, FtsA and ZipA (Wang & Lutkenhaus, 1998, Pichoff & Lutkenhaus, 2002). $MinC^C$/MinD was induced in strain S4/pBANG75 (S3, *min::kan* /P_{lac}::*minC*^{C}*D*) with 100 μM IPTG, which is sufficient to cause filamentation and prevent colony formation. At different time points samples were taken and stained using antisera against FtsZ, FtsA, ZipA and FtsK. Before IPTG induction (Fig. 15, T=0 min), most cells had FtsZ and ZipA rings and slightly less contained FtsA and FtsK rings. After one hour induction, most cells still had FtsZ and ZipA rings but only a small portion of the cells had FtsA and FtsK rings (data not shown). Two hours after induction, cells were filamentous but the vast majority contained FtsZ and ZipA rings throughout their length (Fig. 15, Z2 and P2). In contrast, FtsA and FtsK rings were only rarely observed (Fig. 15, A2 and K2). By three hours, ring localization of all 4 proteins was lost (Fig. 15, T=3hr) although FtsZ and ZipA rings were sporadically observed (Fig. 15, Z3 and P3). Interestingly at this time point, FtsZ was present in spiral and ladder-like structures instead of rings. These spiral structures were also observed in other experiments using either GFP-$MinC^C$/MinD or FtsZ-GFP in the presence of

Fig. 15. Effect of $MinC^C$/MinD induction on the localization of FtsZ, FtsA, ZipA and FtsK. $MinC^C$/MinD was induced with 100 μM IPTG in S4 (*min::kan*)/pBANG75. Cells were removed at indicated time points and analyzed by immunofluorescent microscopy using antisera against FtsA (A1-A3), FtsZ (Z1-Z3), ZipA (P1-P3) and FtsK (K1-K3). As a control, S4/pBANG75 cells were treated with cephalexin at 20 μg/mL for 2 hours to generate filamentous cells. The localization of FtsA (A4), FtsZ(Z4), ZipA(P4) and FtsK(K4) in these filaments was also checked by immuno-staining.

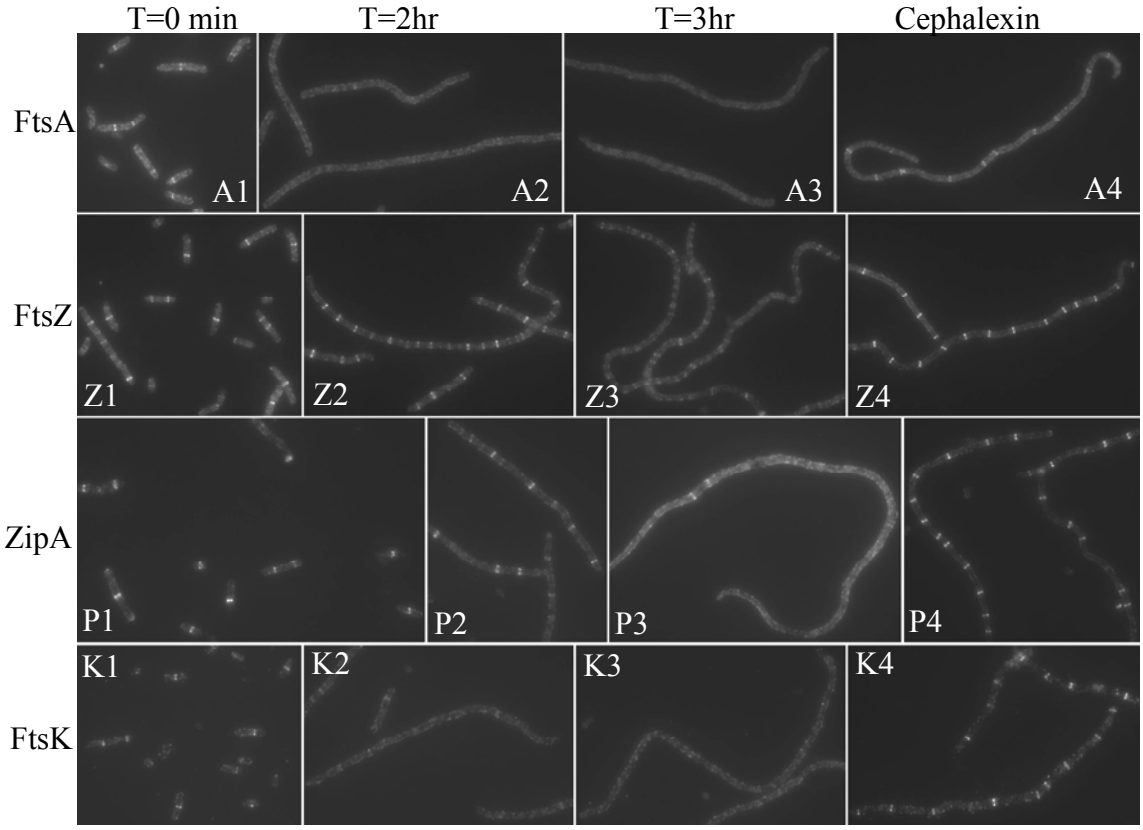
T=0 min
T=2hr
T=3hr
Cephalexin
FtsA
FtsZ
ZipA
FtsK
A1
A2
A3
A4
Z1
Z2
Z3
Z4
P1
P2
P3
P4
K1
K2
K3
K4

overexpressed MinC^{C}/MinD, but only at specific time points. We think these structures are due to the spiraling-out of FtsZ polymers as Z rings are disrupted.

The change in the localization pattern of these proteins upon MinC^{C}/MinD induction is not due to filamentation per se, as filamentous cells of S4/pBANG75 generated by cephalexin treatment, contained all four proteins in ring structures (Fig. 15, cephalexin) although FtsA and FtsK rings were present at a slightly lower number per filament. As another control MinC^{C}/MinD was induced in BSM374 (*ftsZ-I374V*, *min::kan*). The cells did not filament and FtsZ, FtsA, ZipA and FtsK formed rings at similar frequencies (data not shown). This failure of MinC^{C}/MinD to cause filamentation or affect the frequency of these rings in this strain is consistent with the failure of MinC^{C}/MinD to bind to FtsZ-I374V and compete with FtsA and ZipA.

These results clearly demonstrate that overproduction of MinC^{C}/MinD initially displaces FtsA, and therefore FtsK (and presumably other downstream proteins), from the WT Z ring. Later, this overproduction eventually disrupts the Z ring, probably because it also displaces ZipA. This result provides an explanation for the earlier observation that at a low induction level GFP-MinC^{C}/MinD prevented division but still localized to rings (Fig. S3, A1); FtsA was displaced but Z rings still formed with the aid of ZipA. Similarly, The reduced frequency of FtsA rings in S4/pBANG75 at T=0 min (Fig. 15, T=0 min) and in cephalexin treated cells (Fig. 15, cephalexin) is likely due to the basal expression of MinC^{C}/MinD from pBANG75, since S4 and BSM374 contained FtsA rings at a similar frequency in the absence of this plasmid (Fig. 9 and data not shown).

Relative division inhibitory activity of the two domains of MinC.

In the proper context both the N- and the C-terminal domains of MinC have division inhibitory activity, however, the relative efficiency of the two domains and their contribution to the activity of full length MinC/MinD have not been determined. Previous studies have shown that when MinD is not present, MalE-$MinC^N$ is a more potent division inhibitor than MalE-$MinC^C$ (Hu & Lutkenhaus, 2000). The division inhibitory activity of $MinC^C$ is only observed in the presence of MinD (Shiomi & Margolin, 2007). To compare the activity of the two domains of MinC in the same context and under more physiological conditions, we took advantage of the two MinC mutants (MinC-G10D and MinC-R172A) described previously (Hu et al., 1999, Zhou & Lutkenhaus, 2005). The *minC-G10D* and *minC-R172A* mutations significantly reduce the activity of $MinC^N$ and $MinC^C$ respectively, so that the division inhibitory activity of MinC-G10D/MinD is mainly from the $MinC^C$ domain and that of MinC-R172A/MinD is mainly from the $MinC^N$ domain. As shown in Fig. 13A (rows 1 and 2), the two MinC mutants displayed very similar ability to prevent the growth of the FtsZ-WT Δ*min* strain (S4) when expressed with MinD under *lac* promoter; no growth at or above 20 μM IPTG. Western blot analysis further confirmed that the same amount of the mutant MinC proteins was required to cause uniform filamentation in liquid culture (Fig 13, b&c).

The killing efficiency of the two MinC mutants must be significantly lower than WT MinC since WT MinC/MinD on the same vector (pBANG78/P*lac::minCD*) could not be transformed into the S4 strain (data not shown). However, another plasmid (pBANG59) with lower expression of MinC/MinD could be transformed into S4 (Fig 8, row 1). Western analysis of this strain (S4/pBANG59) indicated that the minimal MinC level required to cause uniform

filamentation was slightly less than the MinC level expressed from the chromosome of a wild type strain (Fig. 13B, lane d and a, respectively), consistent with what was reported before (Zhou & Lutkenhaus, 2005). Comparison of the protein levels also indicates that at least 40 times more mutant MinC (MinC-G10D or R-172A) was required to cause uniform filamentation in S4 (Δmin) strain than WT MinC (Fig. 13B, b, c&d), suggesting that each domain of MinC is at least 40 fold less active than full length MinC in blocking division.

We also wanted to compare the effect of the *ftsZ-I374V* mutation to that of the *minC-R172A* mutation to see whether they are equivalent in affecting the responsiveness of FtsZ to MinC/MinD. Both mutations eliminate the toxicity of $MinC^C$/MinD and therefore should have a similar effect. To do this, under the control of an IPTG-inducible promoter, wild type MinC/MinD was expressed in BSM374 (*ftsZ-I374V, min::kan*) and MinC-R172A/MinD was expressed in S4 (*ftsZ-WT, min::kan*) and the IPTG sensitivity of these two strains was compared. As shown in Fig 13A rows 2 and 3, growth of both strains was inhibited at the same IPTG concentration (20 μM). Subsequent analysis showed that the same amount of MinC protein was required for wild type MinC/MinD to cause filamentation in BSM374 (Fig. 13B, lane e) as for MinC-R172A/MinD to cause filamentation in the S4 strain (Fig. 13B, lane c). Thus, WT MinC/MinD has the same toxicity in the FtsZ-I374V strain as MinC-R172A/MinD has in FtsZ-WT strain. This result confirms that FtsZ-I374V is resistant to $MinC^C$/MinD. Consistent with this conclusion, MinC-R172A/MinD is as toxic (Fig. 13A, row 5; 13B, lane f) as wild type MinC/MinD in the FtsZ-I374V strain. Also, MinC-G10D/MinD did not show any detectable toxicity in BSM374 (*ftsZ-I374V, min::kan*) (Fig. 13A, row 4). This latter result was expected since the inhibitory activity of both domains of MinC would be abolished. We also used GFP-MinC/MinD and the corresponding mutants (GFP-MinC-G10D and GFP-MinC-R172A) in

JS964 (Δ*min*) strain to assess the relative toxicity of the two domains of MinC and to compare them to WT MinC. The results were similar to what was shown above with untagged proteins---the two mutant forms of MinC/MinD have very similar division inhibitory activity and are at least 40 fold less active than WT MinC/MinD (data not shown).

Discussion

Focusing on elucidating the molecular mechanism of the division inhibitory activity of $MinC^C$/MinD in this study, we found that localization of $MinC^C$/MinD to the Z ring requires the C terminal conserved tail of FtsZ, an unstructured region which also interacts with FtsA and ZipA (Liu *et al.*, 1999, Ma & Margolin, 1999, Haney et al., 2001). $MinC^C$/MinD bocks cell division in two steps: first $MinC^C$/MinD efficiently displaces FtsA on the Z ring and can therefore block the function of the Z ring; further overproduction of $MinC^C$/MinD eventually disrupts the Z ring, probably because it also displaces ZipA.

Localization of $MinC^C$/MinD to the Z ring.

$MinC^C$/MinD has been shown to localize to the Z ring and this localization depends on $MinC^C$ since a point mutation (R172A) in $MinC^C$ prevents localization of GFP-$MinC^C$/MinD (Zhou & Lutkenhaus, 2005, Johnson et al., 2002). However the component(s) of the Z ring that is directly involved in recruiting $MinC^C$/MinD to the septum was not clearly demonstrated even though there are several lines of evidence suggesting that it is FtsZ: a) localization of $MinC^C$/MinD does not require other known components of the Z ring (FtsA, ZapA or ZipA)

(Johnson et al., 2004); and b) direct interaction between FtsZ and $MinC^C$ has been detected in several assays (Dajkovic et al., 2008a). Our results strongly support that FtsZ directly recruits $MinC^C$/MinD to the septum because we isolated FtsZ mutants that are resistant to $MinC^C$/MinD, the one we studied in detail---FtsZ-I374V fails to recruit $MinC^C$/MinD to the septum, and does not interact with it in vitro.

The role of MinD is still not clear as the targeting of $MinC^C$/MinD to the Z ring is generally thought to be mediated by the FtsZ-$MinC^C$ interaction (Dajkovic et al., 2008a). However, $MinC^C$ is not targeted, nor does it have toxicity, in the absence of MinD (Johnson et al., 2002, Shiomi & Margolin, 2007) and there is no evidence to show that MinD contacts any septal components directly. This is in contrast to DicB, which can also target $MinC^C$ to the Z ring, but does so via an interaction with ZipA. In this case the localization is thought to be a bipartite signal involving both DicB and $MinC^C$ making contacts with ZipA and FtsZ, respectively (Johnson *et al.*, 2004). We examined the targeting of $MinC^C$/DicB to the Z ring in BSM374 (*ftsZ-I374V*, *min::kan*) strain by GFP tagging of $MinC^C$, we found that GFP-$MinC^C$/DicB was still targeted to the Z rings. Consistent with this, and unlike the resistance to MinC/MinD (Fig. 8), BSM374 does not show significant resistance to MinC/DicB (data not shown). This is perhaps not very surprising because of the difference in targeting of $MinC^C$ to the Z ring by MinD and DicB as discussed above. Plus, what is really recognized by FtsZ to achieve the targeting is probably $MinC^C$/MinD or $MinC^C$/DicB complexes but not $MinC^C$ alone. In this sense, it is not surprising if the requirements for FtsZ to recognize these two complexes are not the same since the complexes are different, which can explain why FtsZ-I374V blocks the targeting of $MinC^C$/MinD but allows $MinC^C$/DicB to do so.

One role for MinD is to recruit and concentrate $MinC^C$ on the membrane but there is probably more, since MinD greatly enhances the toxicity of a version of $MinC^C$ ($MinC^C$-MTS) which is targeted to the membrane artificially by addition of a membrane targeting sequence (unpublished data). $MinC^C$-MTS does not show detectable toxicity in the absence of MinD but becomes a potent division inhibitor when MinD is present. This observation is similar to what was observed previously with full length MinC (Johnson et al., 2002). Also, MinDΔ10, which lacks the membrane targeting sequence, increases the toxicity of MinC, but not as well as the full length MinD (Hu & Lutkenhaus, 2001). These results are consistent with MinD enhancing the affinity of $MinC^C$ for FtsZ, and/or performing some other function of which we are unaware.

The last 15-20 residues of FtsZ---a busy region for protein interactions.

FtsZ is one of the most conserved proteins in bacteria, consistent with its critical role in cell division. It consists of a main body ($FtsZ_{1\text{-}320}$ in *E.coli*), which is structurally homologous to tubulin, and an unstructured tail ($FtsZ_{321\text{-}383}$ in *E.coli*), which is less conserved and shows significant variation in length and sequence (Ma & Margolin, 1999, Lowe & Amos, 1998) (Fig. 7). However the last ~15 residues of this tail are highly conserved in FtsZ from most bacteria, suggesting a conserved function for this region. Indeed, this tail is involved in interaction with FtsA and ZipA in *E.coli* and EzrA and SepF (YlmF) in *B.subtilis* (Haney et al., 2001, Singh *et al.*, 2007, Ishikawa *et al.*, 2006). Here, we show that it is also involved in interacting with $MinC^C$/MinD and therefore MinC/MinD. The interaction with FtsA and ZipA is required for Z ring formation, whereas the interaction with EzrA or MinC/MinD has regulatory roles. Because this region is mediating interaction with many proteins, most of the mutants we isolated (D373E,

I374V, L378V) result in small biochemical changes; the mutant proteins must still interact with other proteins (FtsA and ZipA) to function in division. Nonetheless, these subtle changes result in significant resistance to MinC/MinD and are deficient in $MinC^C$/MinD binding. The *ftsZ-I374V* mutation did not affect the interaction between FtsZ and ZipA, however, the interaction with FtsA was possibly reduced. Nonetheless, recruitment of FtsA to the Z ring appeared normal suggesting that there is still a strong enough interaction.

$MinC^C$/MinD disrupts the Z ring in two stages

It was shown previously that MalE-$MinC^C$ inhibits the lateral association of FtsZ polymers in vitro and this activity was proposed to be the basis for the inhibitory activity of $MinC^C$/MinD in vivo (Dajkovic et al., 2008a). Here we show that $MinC^C$/MinD blocks division in two stages. In the first stage $MinC^C$/MinD displaces FtsA from the Z ring. This requires less $MinC^C$/MinD but prevents the recruitment of downstream proteins such as FtsK. As a result the Z ring is nonfunctional for division. At the second stage, requiring more $MinC^C$/MinD, the Z ring is disrupted probably because ZipA is also displaced. The fact that $MinC^C$/MinD displaces FtsA more readily than ZipA could mean that FtsA binds the tail of FtsZ with lower affinity than ZipA or could simply be due to the Z ring containing less FtsA molecules than ZipA (ZipA/FtsA=4/1). We don't have direct evidence to demonstrate that the eventual disintegration of the Z ring by $MinC^C$/MinD is due to the displacement of ZipA. It is possible that inhibition of the lateral association of FtsZ polymers by $MinC^C$/MinD is also a contributing factor.

The observation that the FtsA is displaced from the Z ring more readily than ZipA explains why the Z rings fail to function upon $MinC^C$/MinD induction. The Z rings persist with

the aid of ZipA but do not function since FtsA, FtsK and presumably other cell division proteins are absent. A previous study (Justice *et al.*, 2000), concluded that MinC/MinD prevented the recruitment of FtsA to the Z ring instead of disrupting the Z ring to inhibit division. However, there are several studies showing that MinC/MinD does indeed disrupt the Z ring (Johnson et al., 2002, Pichoff & Lutkenhaus, 2001, Hu et al., 1999) and we find that the integrity of Z rings are much more sensitive to intact MinC/MinD than $MinC^{C}$/MinD. We can not explain the difference between our results and their observations although they obtained different results depending upon the fixation conditions. It's possible that they had a mutation that inactivated the N terminus of MinC in their MinC/MinD construct, making it more or less like $MinC^{C}$/MinD. However, they also reported that overexpression of FtsA reduced the filamentation caused by their MinC/MinD construct but we were unable to find conditions where overexpression of FtsA (despite trying many different expression levels) reduced the filamentation caused by overexpression of $MinC^{C}$/MinD. This is perhaps not so surprising since expression of $MinC^{C}$/MinD at the minimal level required to cause uniform filamentation is unlikely to only displace FtsA but also starts to affect ZipA. Also, overexpression of FtsA would place more FtsA on the Z ring but this can be detrimental since the ratio of these proteins (FtsZ, FtsA , ZipA) must be within a certain window for the normal functioning of the Z ring (Hale & de Boer, 1997, Dai & Lutkenhaus, 1992).

Model for MinC/MinD on Z ring formation.

With the results obtained here and previous studies, we provide details that support a model for the mode of action of MinC/MinD in preventing formation of Z rings (Johnson *et al.*,

2004). As shown in Fig. 16, MinC/MinD localizes to membrane-associated FtsZ polymers through $MinC^{C}$/MinD interacting with the conserved C-terminal tail of FtsZ. By directly contacting FtsZ, MinC/MinD prevents Z ring formation in at least two ways: first, $MinC^{C}$/MinD disrupts the function of the Z ring by interfering with the recruitment of FtsA and possible reducing polymer bundling; second, this targeting of MinC/MinD to the Z ring brings $MinC^{N}$ in close proximity to FtsZ polymers, so that it is near its target. The combination of these two activities makes MinC/MinD a potent division inhibitor.

The resistance of the FtsZ I374V mutant to MinC/MinD suggests that the targeting of MinC/MinD to the Z ring (through $MinC^{C}$/MinD) is very important for its activity; on the other hand the observation that the presence of the *ftsZ I374V* allele (BSZ374 strain) in a wild type background (min^{+}) results in very few minicells almost argues against this. When we compare the division inhibitory activity of the two domains of MinC (by employing mutations that inactivate either domain in the context of MinC/MinD), we found that they have the same efficiency in blocking division and preventing colony formation. Each domain, however, is much less efficient than full length MinC/MinD (Fig 13), suggesting that the two parts of MinC work synergistically to achieve maximum activity. The importance of the two domains of MinC is further highlighted by the observation that the *min* operon containing the *minC-G10D* or the *minC-R172A* mutations on a single copy plasmid can not prevent minicell formation (Zhou & Lutkenhaus, 2005).

Why the FtsZ-I374V mutant does not make minicells is not clear. We think one possible reason is that, as we have shown, FtsZ-I374V is still sensitive to $MinC^{N}$. The presence of MinE in the cell concentrates MinC/MinD at the poles through the oscillation and the high polar

Fig. 16. Model for the inhibitory action of MinC/MinD on Z ring assembly. Under physiological conditions any attempt to make polar Z rings is prevented by MinC/MinD concentrated at the poles through the Min oscillation. MinC/MinD in the polar zone binds to ZipA and FtsA decorated FtsZ polymers located at the membrane before a complete Z ring is formed through the $MinC^{C}$/MinD-FtsZ interaction and displaces primarily FtsA. The binding of MinC/MinD to the tail of FtsZ also brings $MinC^{N}$ close to FtsZ polymers, resulting in breakage of the FtsZ polymers. The combination of these activities ensures that no polar Z rings can be made in the cell and therefore guarantees the precision of cytokinesis. IM: inner membrane.

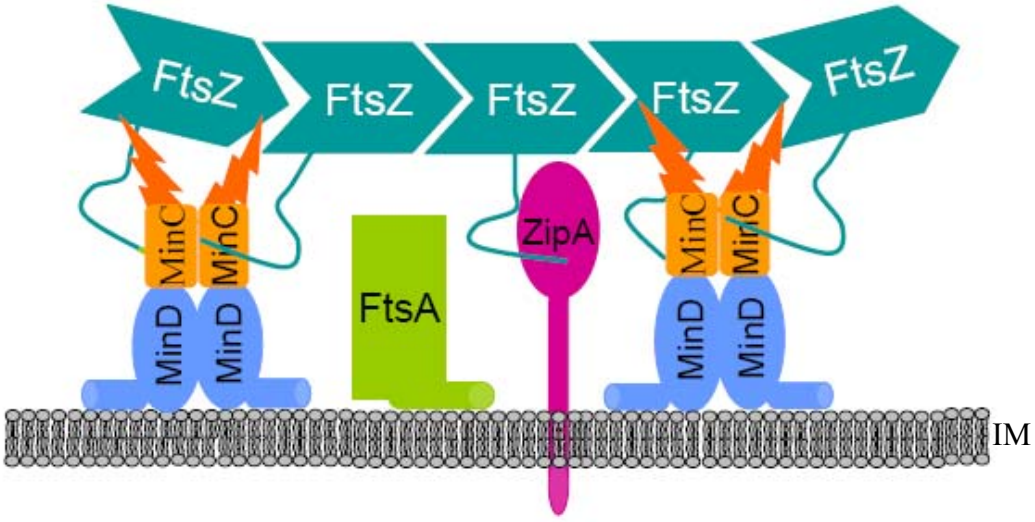
FtsZ
FtsZ
FtsZ
FtsZ
FtsZ
MinC
MinC
MinC
MinC
ZipA
FtsA
MinD
MinD
MinD
MinD
IM

concentration of $MinC^N$ (as part of MinC) may disrupt the polar Z rings. Consistent with FtsZ-I374V being sensitive to $MinC^N$, we have shown that expression of MinC/MinD at a higher level prevents the growth of BSM374 (Fig 13, row 3). However, this can not be the only reason as we have shown in Fig. 13 that BSM374 (*ftsZ-I374V*, *min::kan*) has the same sensitivity to WT MinC/MinD as S4 (*ftsZ*-WT, *min::kan*) has to MinC-R172A/MinD. This result indicates that the two mutations (*ftsZ-I374V* and *minC-R172A*) are similar in affecting the responsiveness of FtsZ to MinC/MinD. Nevertheless, MinC-R172A can not block minicell formation in FtsZ-WT strain (Zhou & Lutkenhaus, 2005) whereas WT MinC efficiently prevents minicell formation in FtsZ-I374V strain. The fact that BSZ374 strain is not making minicells does not necessarily mean that the targeting of MinC/MinD to the Z ring is not required for its function at physiological levels (can be deduced from the effect of MinC-R172A). At overexpressed levels the two domains of MinC can function separately but combining them results in an inhibitor that works synergistically to ensure the disruption of polar Z rings. In this sense, it will be interesting to know whether minicells are formed if a $MinC^N$ resistant *ftsZ* allele is present on the chromosome.

Chapter IV: Examination of the interaction between FtsZ and MinC^N in *E. coli* suggests how MinC disrupts Z rings

Abstract

In the previous study we examined the MinC^C/MinD-FtsZ interaction and the effect of MinC^C/MinD on Z rings. As discussed above, along with MinD, the C-terminal domain of MinC (MinC^C) competes with FtsA, and to a less extent with ZipA, for interaction with the C-terminal tail of FtsZ to block division. In this study we explored the interaction between N-terminal domain of MinC (MinC^N) and FtsZ and tried to extend our understanding of the inhibitory mechanism of MinC^N. A search for mutations in *ftsZ* that confer resistance to MinC^N identified an α-helix at the interface of FtsZ subunits as being critical for the activity of MinC^N. Focusing on one such mutant FtsZ-N280D, we showed that it greatly reduced the FtsZ-MinC interaction and was resistant to MinC^N both *in vivo* and *in vitro*. With these results, an updated model for the action of MinC on FtsZ is proposed: MinC interacts with FtsZ to disrupt two interactions, FtsZ-FtsA/ZipA and FtsZ-FtsZ, both of which are essential for Z ring formation and function.

Introduction

The N-terminal domain of MinC is believed to be the anti-FtsZ part of MinC for a long time because: 1) it is able to block cell division *in vivo* when overexpressed, even in the absence of MinD (Hu & Lutkenhaus, 2000); 2) it prevents the sedimentation of FtsZ polymers *in vitro* as efficiently as full length MinC and 3) the ability of MinC to interact with FtsZ and block FtsZ polymer sedimentation is greatly reduced by the MinC-G10D mutation, which is in the N terminal part of MinC. However the molecular mechanism by which $MinC^N$ antagonizes FtsZ polymer assembly is still not very clear. $MinC^N$ blocks the sedimentation of FtsZ but it does not seem to affect the GTPase activity of FtsZ. This is somewhat a conundrum because if the block of FtsZ sedimentation by $MinC^N$ is due to the inhibition of polymerization as originally proposed, then the GTPase activity of FtsZ should be affected (activated or reduced) by $MinC^N$ since the GTPase activity is associated with polymerization. Recently in a more careful study using the FRAP (Fluorescence Recovery After Photobleaching) analysis, it was shown that $MinC^N$ does not affect the amount of FtsZ that is in the polymer form, which means that the association of FtsZ subunits to make the polymer is not affected by $MinC^N$. Subsequent EM (Electron Microscopy) studies indicate that FtsZ polymers do exist but they are much shorter when $MinC^N$ (or MinC) is present. Because of these observations, it is thought that $MinC^N$ acts after polymerization to shorten FtsZ polymers (Dajkovic et al., 2008a).

In order to get more insight into the affect and mechanism of $MinC^N$ on FtsZ, we examined the interaction between $MinC^N$ and FtsZ from the FtsZ side in this study. We took a genetic approach to isolate FtsZ mutants that are specifically resistant to $MinC^N$. A couple of such mutants were obtained and a detailed study of one of these mutants indicates how $MinC^N$

interacts with FtsZ. Taken together the data obtained from this and previous studies, we proposed a more detailed mechanism of how MinC antagonizes Z ring formation.

Results

Mutations mapping to two regions of FtsZ confer resistance to MinC/MinD.

In the previous study, we screened an FtsZ mutant library for resistance to $MinC^C$/MinD and identified four such mutants which altered the C-terminal tail of FtsZ (FtsZ - D373E, I374V, L378V and K380M) (Shen & Lutkenhaus, 2009). Since MinC has two functional domains that affect FtsZ differently (Hu & Lutkenhaus, 2000, Shiomi & Margolin, 2007), we screened the same FtsZ mutant library with full length MinC/MinD, hoping to identify additional mutants, some of which might be resistant to $MinC^N$. This approach is possible since resistance to one domain of MinC results in a loss of synergy between the two domains of MinC and therefore confers some level of resistance to MinC/MinD (Shen & Lutkenhaus, 2009). To do this, we introduced the plasmid (pBANG59/P*tac::minCD*) expressing MinC/MinD under IPTG control into the strain (S7/*W3110 ftsZ*^{0} *min::kan recA::*Tn*10*) containing the mutagenzied *ftsZ* library and selected with 1 mM IPTG (cells with WT *ftsZ* are unable to form colonies at or above 0.1 mM IPTG). Survivors were isolated and mutations in *ftsZ* were identified.

Sequence analysis revealed that these MinC/MinD resistant mutants contain mutations that primarily alter amino acids in two regions of FtsZ (Fig. 17A): the extreme C-terminus of FtsZ (including *ftsZ*-I374V and *ftsZ*-L378V, which were previously identified in the screen using $MinC^C$/MinD) and an α-helix [H-10 helix (Oliva *et al.*, 2004)] (*ftsZ-R271G, ftsZ-E276D* and

ftsZ-N280S) that lies at the end of the FtsZ molecule opposite the GTP-binding site (Fig. 17B). Mutants in this latter group are likely to be resistant to $MinC^N$, since the $MinC^C$/MinD resistant mutations map to the extreme C-terminus of FtsZ (Shen & Lutkenhaus, 2009). We also found another mutation (*ftsZ*-L205M) that conferred resistance to MinC/MinD but it mapped to a third location on FtsZ. However, its resistance is probably due to a decreased GTPase of the mutant protein because this altered residue: 1) is located in the T7 loop [Fig.17B, pink and (Oliva et al., 2004)] of FtsZ, which is involved in GTP hydrolysis (Lowe & Amos, 1998); and 2) is very close to the residue altered in the *ftsZ2* mutant (FtsZ-D212G) that is known to be resistant to MinC/MinD and has reduced GTPase activity (Dai et al., 1994, Bi & Lutkenhaus, 1990). A reduction in the GTPase activity of FtsZ appears to be a common mechanism of resistance to division inhibitors such as SulA and MinC (Dajkovic et al., 2008a, Dajkovic et al., 2008b). The reduced GTPase activity slows down polymer disassembly, which shifts the equilibrium to assembled polymers and reduces the sensitivity to these inhibitors. For this reason (and its MinC/MinD resistance is intermediate) the FtsZ-L205M mutant was not studied further.

Isolation of FtsZ mutants resistant to $MinC^N$.

Before studying any of the above potential $MinC^N$ resistant mutants in detail, we performed another screen looking for $MinC^N$ resistant mutants in a more direct way. We did a PCR random mutagenesis of the *ftsZ*-I374V allele and constructed an *ftsZ*-I374V mutant library using the same method as in the previous study. Since FtsZ-I374V shows some resistance to MinC/MinD (a strain carrying this mutation survives following induction of MinC/MinD from

Fig 17. FtsZ mutants that confer resistance to MinC/MinD. A) A spot test to check the MinC/MinD sensitivity of FtsZ mutants. The plasmid (pBANG59/P*tac::minC/minD*) expressing MinC/MinD was introduced into an *ftsZ*^{0} strain (S7/ W3110, *ftsZ*^{0}, *min::kan*, *recA*::Tn*10*) complemented with the indicated alleles of *ftsZ* present on a plasmid (pBANG112). One colony of each strain was resuspended in 900 µl of LB medium, serially diluted by 10 and 3 µl from each dilution was spotted on plates (with Spc and Amp) with or without IPTG (as indicated) and incubated overnight at 37°C. MinC-R172A serves as a control. B) Location of the residues on FtsZ molecule altered by mutations examined in this study. The structure of the FtsZ dimer from *M. jannaschii* (PBD ID# 1W5B) is shown. The residues corresponding to those mutated in *E.coli* and studied here are indicated. FtsZ-N280 is in red, FtsZ-R271 and FtsZ-E276 are in blue and FtsZ-L205 is in pink. GTP is green.

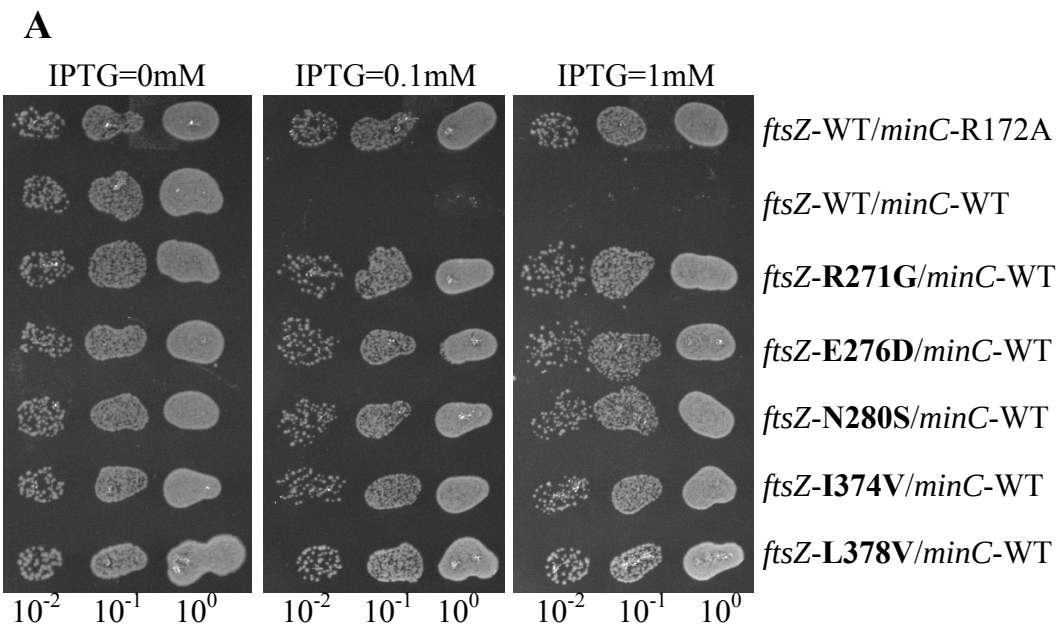
A
IPTG=0mM
IPTG=0.1mM
IPTG=1mM
ftsZ-WT/minC-R172A
ftsZ-WT/minC-WT
ftsZ-R271G/minC-WT
ftsZ-E276D/minC-WT
ftsZ-N280S/minC-WT
ftsZ-I374V/minC-WT
ftsZ-L378V/minC-WT
10-2 10-1 100
10-2 10-1 100
10-2 10-1 100

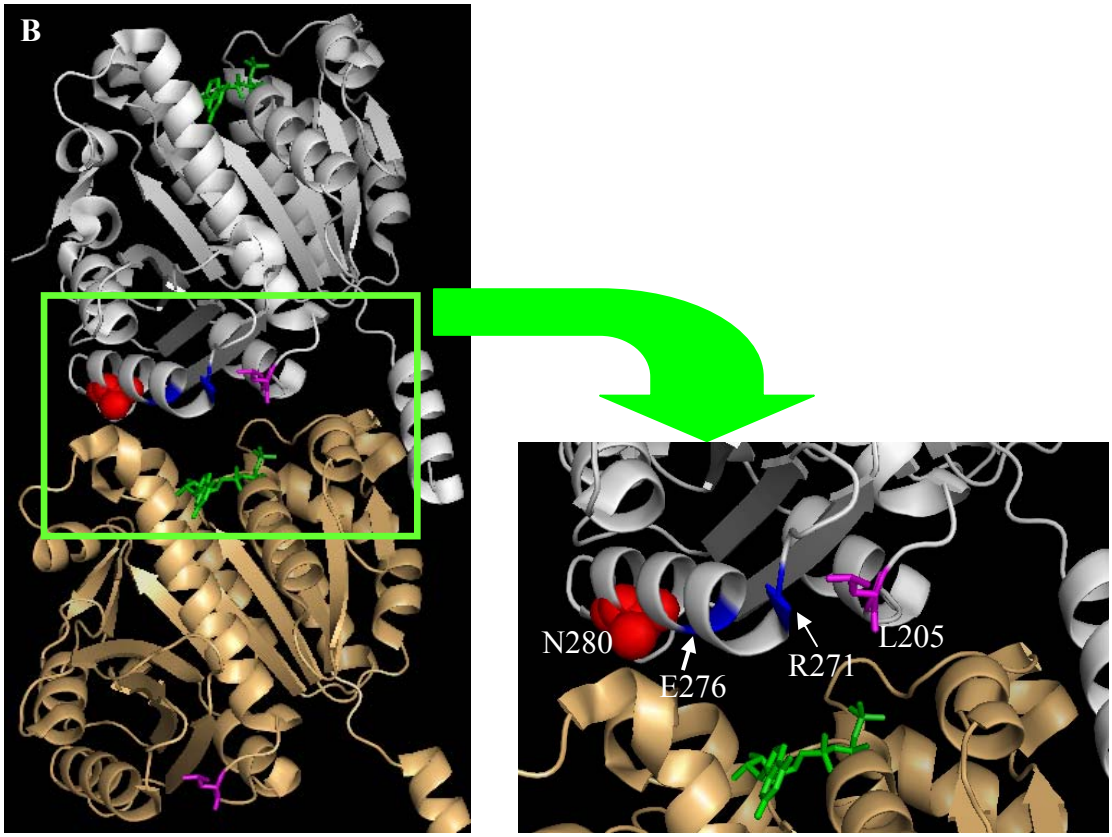
B
N280
E276
R271
L205

the plasmid pBANG59), the resultant library was screened using plasmid pBANG78 /P*lac::minCD,* which prevents the *ftsZ*-I374V strain from forming colonies at IPTG ≥ 25 μM. This plasmid produces a higher level of MinC/MinD than the one (pBANG59) used above to screen the WT-*ftsZ* based library.

Mutants surviving this selection are expected to have the *ftsZ*-I374V mutation that confers resistance to $MinC^C$/MinD and an additional mutation(s) conferring resistance to $MinC^N$. Surprisingly, using this approach we only obtained two mutants, both of which contained the *ftsZ-I374V* mutation and a mutation that altered residue N280 (*ftsZ-N280D* and *ftsZ-N280T*, both were obtained multiple times). A mutation altering residue N280 (*ftsZ-N280S*), as well as two additional mutations altering residues in helix H-10 (*ftsZ-R271G* and *ftsZ-E276D*), was obtained in the previous screen using the mutagenized *ftsZ*-WT allele and selecting with a lower level of MinC/MinD (Fig. 17A). Together, these results suggest that the H-10 helix of FtsZ is critical for the activity of $MinC^N$. Notice that this α-helix lies at the interface of FtsZ subunits in the polymer [Fig. 17B and (Oliva et al., 2004)], which may be a clue in understanding how $MinC^N$ attacks FtsZ.

Characterization of the FtsZ-N280D mutant.

The above analysis indicated the importance of the N280 residue of FtsZ in the $MinC^N$-FtsZ interaction. Comparison of all the potential $MinC^N$ resistant mutations (*ftsZ-R271G, ftsZ-E276D* and the various *ftsZ*-N280 mutations in the absence of the *ftsZ-I374V* mutation) indicated that *ftsZ-N280D* shows the most MinC/MinD resistance (data not shown) and was therefore chosen for subsequent studies. To assess the effect of this mutation on the cell phenotype, we first placed it onto the chromosome at the native *ftsZ* locus using the lambda RED

recombineering system (Datsenko & Wanner, 2000) as described before (Shen & Lutkenhaus, 2009). We also recombined the allele containing the two mutations (*ftsZ-I374V* + *ftsZ-N280D* - referred to as *ftsZ23*) to the chromosome. The resultant strains were designated BSZ280D (*ftsZ-N280D*) and BSZ23 (*ftsZ23*). Once we got these strains, a western blot analysis was done to determine the stability and abundance of the FtsZ mutant proteins in corresponding strains. As shown in Fig. 18, the FtsZ protein level in all the mutants is the same as in the WT strain, indicating none of the mutant proteins have a stability problem.

The morphology of the BSZ280D strain was similar to the FtsZ-WT strain except that the average cell length of the BSZ280D strain is slightly longer due to the occasional long cells it produces (Table 6). It did not produce minicells although it had a slightly broader cell length distribution. Inactivation of the Min system in BSZ280D resulted in minicell formation and caused mild filamentation [on average cells were 2-3 fold longer compared to typical min^- cells such as S4 (Table 6)] in early exponential phase but not in stationary phase. This is likely due to the FtsZ-N280D mutant having somewhat compromised FtsZ activity even though it is still able to complement an $ftsZ^o$ strain and support division (see later). The mild filamentation was not obvious in the Min^+ strain BSZ280D (most of these cells are very close to WT cells even though occasionally it produces very long cells, which makes the average cell length longer that the WT strain), indicating that the Min system is having a positive effect in this strain. One possibility is that by eliminating polar Z rings, the Min system makes more FtsZ molecules available for assembly of the midcell Z ring. Such activity may compensate for the compromised FtsZ activity caused by the *ftsZ-N280D* mutation. This scenario suggests that the FtsZ-N280D mutant is still responding to MinC/MinD to some extent, which is discussed later.

Fig. 18. Western blot detecting the stability and abundance of FtsZ in different mutants. Grow the indicated strains to OD_{600}=0.4 and then harvest the cells. The whole cell lysate was used in an immunoblot analysis to determine the stability and abundance of FtsZ mutants in corresponding strains. For each sample, the loading volume is equivalent to the lysate of 200μl OD_{600}=0.4 cells. 1: S3, 2: BSZ280D, 3:BSZ374V, 4:BSZ23, 5: S18/pBANG112, 6: S18/pBANG112-280D, 7: S18/pBANG112-374V, 8: S18/pBANG112-23, M: protein marker.

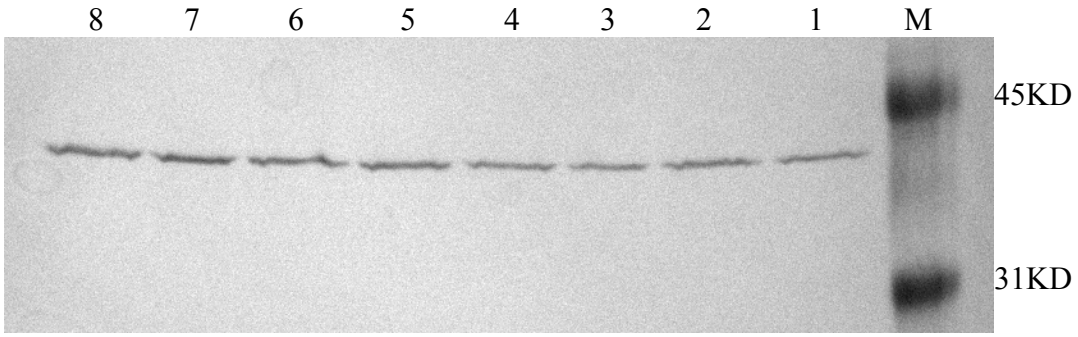
8
7
6
5
4
3
2
1
M
45KD
31KD

Table 6. Characterization of FtsZ mutant strains. All measurements are done with exponentially growing cultures at OD_{600}=0.45.

	S3	BSZ280D	BSZ374V	BSZ23	S4	BSM280D	BSM374V	BSM23
Ave. length (range)/μm	3.9 (2.5-7.1)	6.0 (3.2-17.0)	4.0 (2.4-10.3)	8.6 (2.7-29.6)	6.5 (2.3-23.5)	13.2 (3.2-59.3)	5.7 (2.1-18.8)	13.2 (3.2-51.5)
% of polar divisions	0	0	0	21	29	38	19.5	28

In contrast to BSZ374V [which was described previously (Shen & Lutkenhaus, 2009)] and BSZ280D, the BSZ23 strain produces many minicells [about 20-25% of the total constrictions are at the poles in an exponentially growing culture (Table 6)] and has the typical heterogeneous cell length distribution observed in Min$^-$ strains. It also displays the mild filamentation phenotype in exponential growth phase that was observed with the BSM280D strain (Table 6). Inactivation of the Min system in the BSZ23 strain did not detectably change the morphology or minicelling phenotype except that it further increases the average cell length slightly (Table 6). Together, these results indicate that the presence of the *ftsZ-I374V* + *ftsZ-N280D* mutations in a strain completely suppresses the activity of the Min system.

FtsZ-N280D and FtsZ-I374V are resistant to the N and C terminal domains of MinC respectively.

Having the various mutations (*ftsZ-N280D, ftsZ-I374V* and *ftsZ-23*) on the chromosome in a Δ*min* background allowed us to confirm their MinC/MinD resistance. An *ftsZ*-WT strain (S4/*ftsZ*-WT *min::kan*) containing the *minC/minD* low expression plasmid (pBANG59 /*Ptac::minCD*) fails to form colonies at or above 50 μM IPTG (Fig. 19). However, the mutant strains (BSM280D/*ftsZ-N280D min::kan*; BSM374V/*ftsZ-I374V min::kan*; BSM23/*ftsZ-23 min::kan*) harboring the same plasmid survive at 1 mM IPTG, indicating all mutants have significant MinC/MinD resistance.

As discussed above, mutations (such as *ftsZ2*) that decrease the GTPase activity of FtsZ confer resistance to the division inhibitors MinC/MinD and SulA. As an initial test to determine whether the increased MinC/MinD resistance of these mutants might be due to reduced GTPase activity of these mutant proteins, we checked their SulA sensitivity. None of the mutant strains displayed increased resistance to SulA (Fig. 20). In fact, BSZ280D and BSZ23 were slightly

Fig 19. FtsZ-N280D and FtsZ-I374V display significant resistance to MinC/MinD. Following the protocol described in Fig 17, a spot test was done using the indicated strains harboring the plasmid pBANG59 (P*tac::minC/minD*).

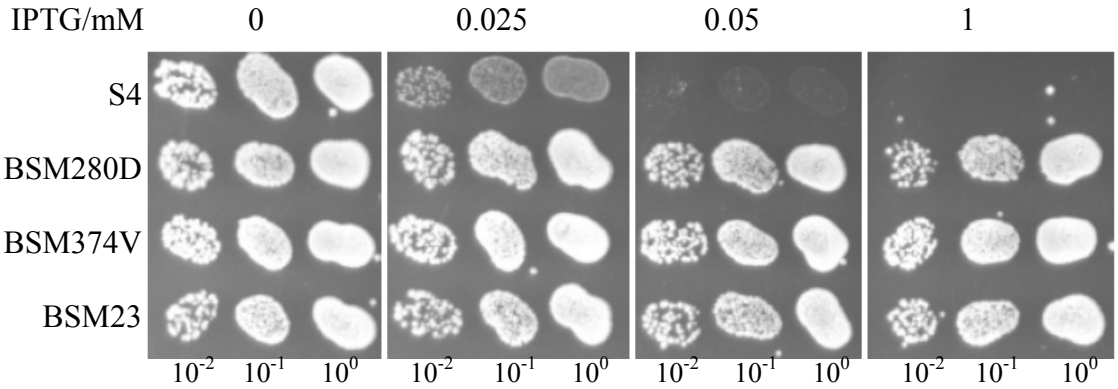
IPTG/mM
0
0.025
0.05
1
S4
BSM280D
BSM374V
BSM23
10^{-2} 10^{-1} 10^{0}
10^{-2} 10^{-1} 10^{0}
10^{-2} 10^{-1} 10^{0}
10^{-2} 10^{-1} 10^{0}

Fig 20. SulA sensitivity test. The indicated strains harboring the plasmid pBS31(P*trc::sulA*) were spot tested on plates containing different IPTG concentrations.

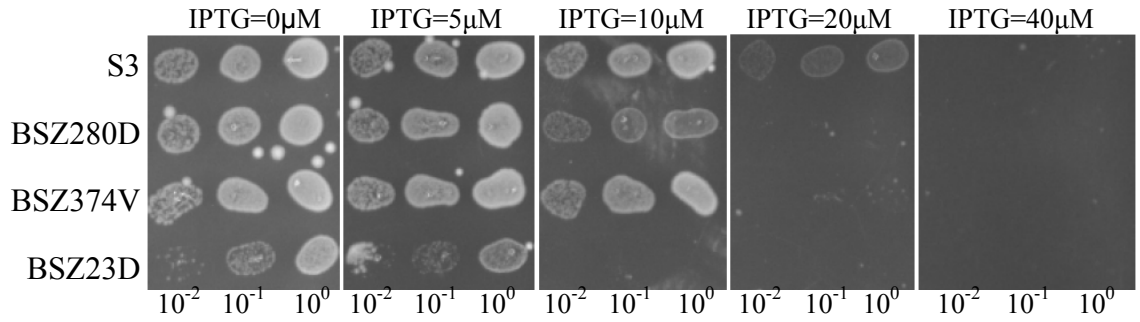
IPTG=0μM
IPTG=5μM
IPTG=10μM
IPTG=20μM
IPTG=40μM
S3
BSZ280D
BSZ374V
BSZ23D
10-2 10-1 100
10-2 10-1 100
10-2 10-1 100
10-2 10-1 100
10-2 10-1 100

more sensitive to SulA than the wild type strain. This may be due to the *ftsZ-N280D* mutation compromising FtsZ activity. Nonetheless, these data suggest that the GTPase activity of these mutant proteins was not significantly reduced *in vivo*.

As described previously, FtsZ-I374V is resistant to $MinC^C$ but still sensitive to $MinC^N$ (Shen & Lutkenhaus, 2009). To see how FtsZ-N280D responds to the two domains of MinC, we used two *minC* mutations, *minC-G10D* and *minC-R172A*, that eliminate the toxicity of the N and C terminal domains of MinC respectively (Hu et al., 1999, Zhou & Lutkenhaus, 2005). As shown in Fig. 21, when the two MinC mutants (along with MinD) are expressed from a plasmid (pBANG78) under the control of an IPTG-inducible promoter, they prevent colony formation of the FtsZ-WT strain (S4/S3 *min::kan*) at about the same level (20 μM IPTG), indicating the two domains of MinC have similar toxicity as reported previously (Shen & Lutkenhaus, 2009). When these MinC mutants are expressed in the FtsZ-N280D strain (BSM280D/BSZ280D *min::kan*), only MinC-G10D/MinD is toxic (Fig. 21). MinC-G10D/MinD prevents colony formation of this strain slightly more efficiently than in the FtsZ-WT strain, indicating the FtsZ-N280D mutant is a little more susceptible to $MinC^C$/MinD compared to FtsZ-WT. This was further confirmed using $MinC^C$/MinD (Fig. 22) and is probably due to the reduced activity of the FtsZ-N280D protein. In contrast, expression of MinC-R172A/MinD was unable to prevent colony formation of the FtsZ-N280D mutant, indicating this FtsZ mutant is resistant to $MinC^N$. Taken together, these results demonstrate that the FtsZ-N280D mutant is resistant to $MinC^N$ but still sensitive to $MinC^C$. Also, the resistance of this mutant to the low level of MinC/MinD observed in Fig. 19 must be due to its resistance to $MinC^N$. This behavior is just the opposite of the FtsZ-I374V mutant, which is resistant to $MinC^C$ but sensitive to $MinC^N$. As expected, neither domain of MinC is able to prevent colony formation in a strain containing *ftsZ23* (Fig. 21). This allele also

Fig 21. FtsZ-N280D and FtsZ-I374V are resistant to the N- and C-terminal domains of MinC respectively. The plasmid pBANG78 (P*lac::minC/minD*) or derivatives containing the *minC* alleles *minC-G10D* or *minC-R172A* was introduced into the indicated strains and a spot test was done as described above. pBANG78 produces a higher level of MinC/MinD than pBANG59 due to a higher copy number of the plasmid and a stronger ribosome binding site for MinC translation.

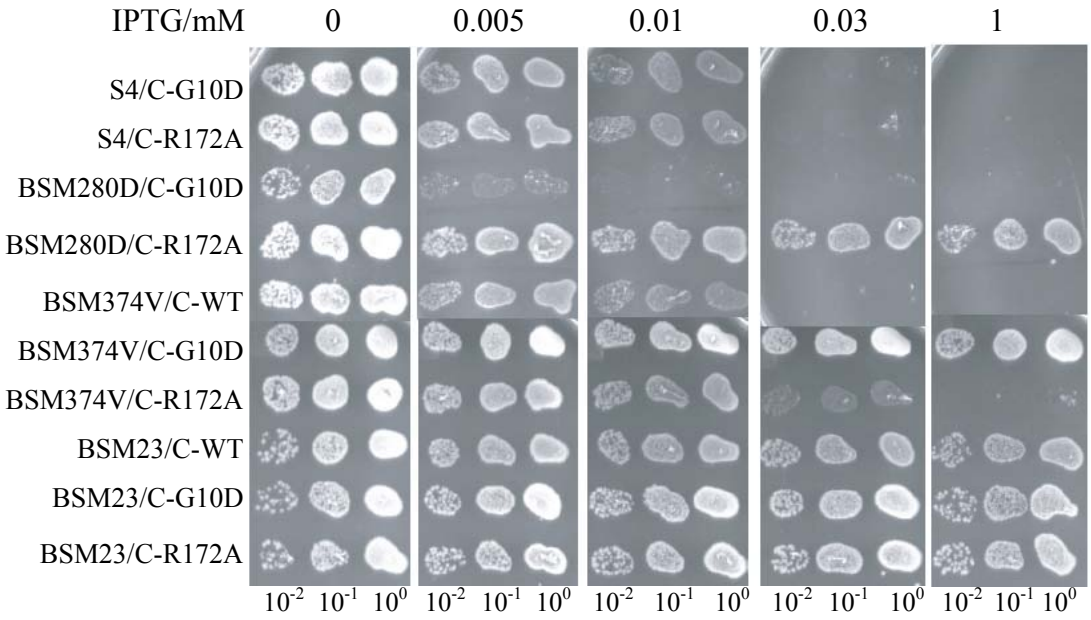
IPTG/mM
0
0.005
0.01
0.03
1
S4/C-G10D
S4/C-R172A
BSM280D/C-G10D
BSM280D/C-R172A
BSM374V/C-WT
BSM374V/C-G10D
BSM374V/C-R172A
BSM23/C-WT
BSM23/C-G10D
BSM23/C-R172A
10^{-2} 10^{-1} 10^{0}

Fig. 22. MinC^{C}/MinD sensitivity test of the FtsZ mutant strains. Indicated strains containing the plasmid pBANG75 (P*lac::minC^{C}/minD*) expressing MinC^{C}/MinD (Shen & Lutkenhaus, 2009) were spot tested on plates with different IPTG concentrations.

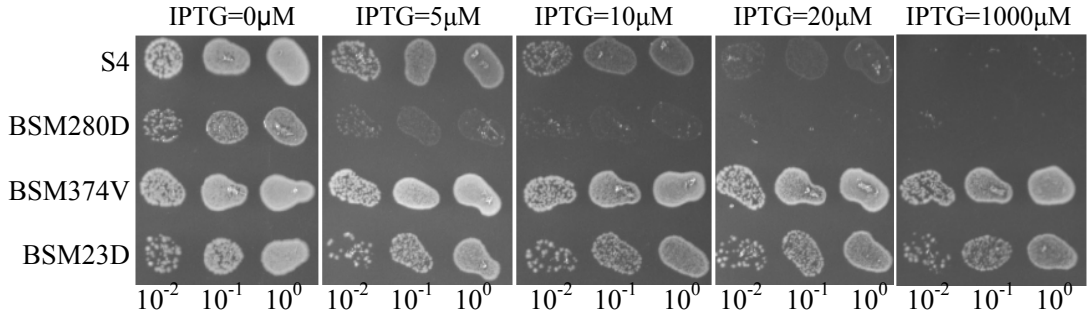
IPTG=0μM
IPTG=5μM
IPTG=10μM
IPTG=20μM
IPTG=1000μM
S4
BSM280D
BSM374V
BSM23D
10-2 10-1 100
10-2 10-1 100
10-2 10-1 100
10-2 10-1 100
10-2 10-1 100

confers resistance to a high level of full length MinC/MinD. The conclusion from these studies is that FtsZ-N280D and FtsZ-I374V are resistant to the N and C terminal domains of MinC respectively and that combining the two mutations renders cells completely resistant to MinC/MinD.

GFP-MinC/MinD localizes to the Z rings in the FtsZ-N280D mutant.

GFP-MinC^{C}/MinD was previously shown to localize to the Z ring and this was dependent upon the C-terminal tail of FtsZ (Shen & Lutkenhaus, 2009, Zhou & Lutkenhaus, 2005, Johnson et al., 2004). In contrast, localization of GFP-MinC/MinD to Z rings is difficult to observe (Johnson et al., 2002); it is very toxic and disrupts Z rings and causes filamentation before the fluorescent signal is observed. However, it should be possible to observe GFP-MinC/MinD at the Z ring in the FtsZ-N280D mutant because it displays significant resistance to MinC/MinD (due to resistance to MinC^{N}) but does not affect the interaction between MinC^{C}/MinD and FtsZ.

To confirm this, we introduced the plasmid pBANG85 (*Ptrc::gfp-minCD*) expressing GFP-MinC/MinD under IPTG control into the *ftsZ^{0}* strain S7 (W3110 *ftsZ^{0} min::kan recA::Tn10*) containing derivatives of pBANG112 expressing various alleles of *ftsZ* and examined the fluorescent signal at different IPTG concentrations. We used this approach since this plasmid (pBANG85) could not be introduced into the control strain S4 (S3 *min::kan*) due to the toxicity associated with the basal expression of GFP-MinC/MinD. In strain S7/pBANG112 FtsZ is produced from the plasmid and the level is slightly higher than the chromosomal level (about 1.5-2 fold, Fig. 18), which allows introduction of the pBANG85 plasmid. As shown in Fig. 23A', when GFP-MinC/MinD is expressed in the FtsZ-WT strain (S7/pBANG112), it causes

filamentation even at a very low induction level (IPTG=2.5 μM) where the fluorescence can barely be detected. The weak signal appears to be largely on the membrane. However, very occasionally weak fluorescent bands are observed suggestive of GFP-MinC/MinD association with Z rings in the process of being dismantled (arrow in Fig. 23A'). Induction of GFP-MinC/MinD at an intermediate level (IPTG=7.5 μM) in the FtsZ-N280D mutant strain (S7/pBANG112-*ftsZ N280D*) results in strong fluorescent bands indicative of localization to Z rings (Fig. 23B'). When induced at a higher level, GFP-MinC/MinD disrupts the Z ring and causes filamentation and therefore fails to localize (data not shown). These results are consistent with FtsZ-N280D being resistant to $MinC^N$ but sensitive to $MinC^C$/MinD. As a control, GFP-MinC/MinD was induced in the FtsZ-23 strain (S7/pBANG112-*ftsZ23*) at the same level as in the FtsZ-N280D mutant. As shown in Fig. 23C', the flourescence is on the membrane but does not localize to Z rings (in a fraction of these cells the GFP also accumulates as spots along the cell membrane but the basis for this phenomenon is not known). This lack of localization is consistent with what we observed with the FtsZ-I374V mutant (Shen & Lutkenhaus, 2009). Together, these results confirm that the localization of MinC/MinD to the Z ring is dependent upon the $MinC^C$/MinD-FtsZ interaction and that the *ftsZ-N280D* mutation is resistant to the action of $MinC^N$.

FtsZ-N280D has reduced interaction with MinC and $MinC^N$ in vitro.

The increased resistance of the FtsZ-N280D mutant to MinC/MinD and $MinC^N$ *in vivo* prompted us to check if the FtsZ-MinC and FtsZ-$MinC^N$ interactions are altered by this mutation *in vitro*. To this end, we did three tests.

Fig 23. GFP-MinC/MinD localization in FtsZ mutant strains. GFP-MinC/MinD was induced from the plasmid pBANG85 (P*trc::gfp-minC/minD*) in the *ftsZ*^{0} strain S7 (W3110, *ftsZ*^{0}, *min::kan*, *recA*::Tn*10*) complemented with indicated alleles of *ftsZ* on plasmid pBANG112. Diluted (1/1000) overnight cultures were induced with IPTG (2.5 μM for FtsZ-WT and 7.5 μM for others) and grown to OD_{600}≈0.4. Cells were then subjected to fluorescence microscopy. Representative fluorescence micrographs (A'-C') and the corresponding phase contrast images (A-C) are shown.

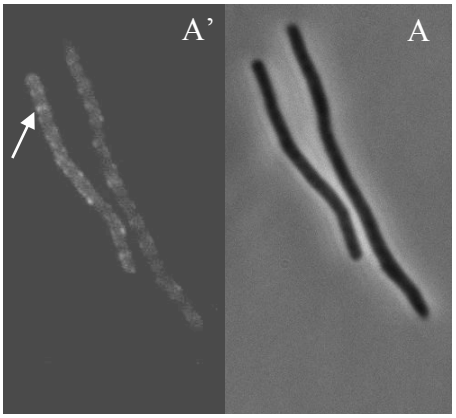

FtsZ-WT

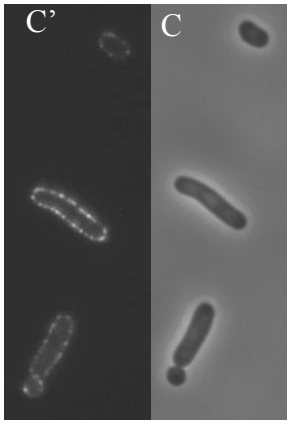

FtsZ-23

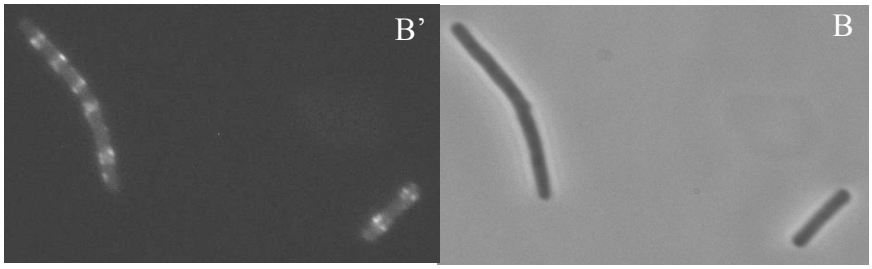

FtsZ-280D

First, we did a sedimentation assay to test the ability of MinC and $MinC^N$ to antagonize FtsZ polymer assembly. We purified the FtsZ-N280D and FtsZ-23 proteins and tested the effect of MinC or $MinC^N$ in a sedimentation assay as described previously (Hu et al., 1999). In a preliminary sedimentation assay containing 5 μM FtsZ and 1mM GTP (or GDP as control) in polymerization buffer, these proteins (FtsZ wild type and mutants including FtsZ-I374V isolated previously) had very similar polymerization efficiencies with GTP and did not assemble with GDP (data not shown). We also checked the GTPase of these mutants using a NADH-coupled enzymatic assay (Chen & Erickson, 2009). The FtsZ-N280D mutant has decreased GTPase activity that is ~60% of the wild type protein (Fig. 24). The GTPase activity of FtsZ23 is similar to that of FtsZ-N280D whereas the GTPase of FtsZ-I374V is comparable to the WT protein. By assaying the GTPase activity at various protein concentrations we determined that the FtsZ-N280D mutant has a modest assembly deficiency [the critical concentration for polymerization of this mutant is around 2.5 μM, which is about 1.5 μM higher than the WT protein (Fig. 24)]. This is perhaps not too surprising as this mutation alters a residue in the H-10 helix, which is at the interface between FtsZ subunits (Fig. 17B). Importantly, this mutant is slightly more sensitive to SulA than the FtsZ-WT *in vivo* and is as sensitive to MalE-SulA as FtsZ-WT *in vitro* (data not shown). These results indicate that MalE-SulA blocks FtsZ-N280D assembly as efficiently as FtsZ-WT assembly, which means that at this concentration (5 μM) FtsZ-N280D is turning over fast enough to respond to inhibitors such as SulA. Therefore, we used this concentration (5 μM) for the tests with MinC described below.

To test how the *ftsZ-N280D* mutation affects the interaction between FtsZ and MinC or $MinC^N$, we did a sedimentation assay as described previously (Hu & Lutkenhaus, 2000) in which increasing amounts of MalE-$MinC^N$ were added to the FtsZ polymerization reaction. As shown

Fig 24. GTPase activity of FtsZ-WT and FtsZ-N280D assayed at different protein concentrations. Using the NADH coupled enzymatic assay (Chen & Erickson, 2009), the GTPase of FtsZ was determined in the standard polymerization buffer (50mM MES, 50mM KCl, 10mM $MgCl_2$, pH=6.5) containing 0.5mM GTP with a gradient of FtsZ protein concentrations. The assay was done at 25°C.

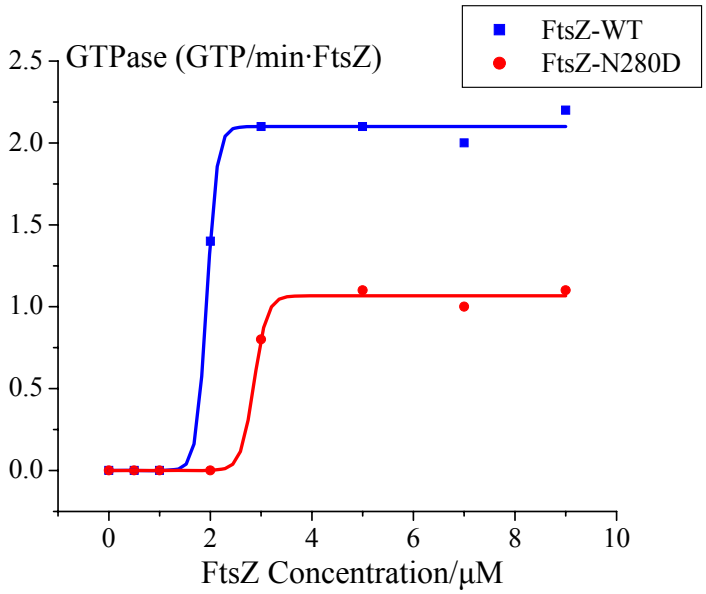
FtsZ-WT
FtsZ-N280D
GTPase (GTP/min·FtsZ)
2.5
2.0
1.5
1.0
0.5
0.0
0
2
4
6
8
10
FtsZ Concentration/μM

in Fig. 25A, the amount of FtsZ-WT in the pellet decreases as the MalE-MinC^N concentration increases, which is consistent with what was reported before (Hu & Lutkenhaus, 2000) and indicates that MinC^N is blocking FtsZ sedimentation. However, when the FtsZ-N280D mutant protein was used in this test, the amount of FtsZ in the pellet was not affected by the amount of MalE-MinC^N in the reaction (Fig. 25B). We also did this test with MalE-MinC; the result is the same as with MalE-MinC^N---the sedimentation of FtsZ-WT but not FtsZ-N280D is inhibited by MalE-MinC in a concentration dependent manner (data not shown). These results demonstrate that FtsZ-N280D has significant resistance to MinC and MinC^N *in vitro*.

Second, we performed a far western blot to examine the interaction between FtsZ and MinC or MinC^N. For this test, MalE-MinC or MalE-MinC^N was run on a native PAGE gel, transferred to a nitrocellulose membrane which was then incubated with 5 μM FtsZ (WT or the N280D mutant) and the FtsZ bound to MalE-MinC or MalE-MinC^N was detected using typical western blot methodology. The results in Fig. 26 demonstrate that an interaction between MalE-MinC or MalE-MinC^N and FtsZ-WT can be detected in this assay. However, the interaction with FtsZ-N280D is greatly reduced, demonstrating a decreased interaction between FtsZ-N280D and MinC or MinC^N. MalE-SulA was used in the test to serve as a positive control since both of them (FtsZ-WT and FtsZ-N280D) show similar sensitivity to SulA (Fig S2). The result shows that FtsZ-N280D binds MalE-SulA as efficiently as FtsZ-WT (Fig 26), which indicates that the decreased signal for MinC/MinC^N with FtsZ-N280D is not due to poorer antibody detection of the FtsZ-N280D protein but due to the decreased interaction between them.

Third, we did a biosensor assay to examine the affinity between FtsZ and MinC. FtsZ-WT and FtsZ-N280D were biotinylated and immobilized to sensor chips containing covalently linked streptavidin. MalE-MinC at various concentrations was then injected and the response

Fig. 25. FtsZ-N280D is insensitive to the action of $MinC^N$ *in vitro*. A sedimentation assay was used to test the effect of MalE-$MinC^N$ on the assembly of FtsZ-WT and FtsZ-N280D. The reactions containing FtsZ (5 μM) and an increasing amount of MalE-$MinC^N$ in polymerization buffer were initiated with the addition of 1mM GTP (or GDP as control, lane1). After 5 min the reactions were centrifuged and the pellet of each reaction was analyzed by SDS-PAGE. The final concentration of MalE-$MinC^N$ was 0, 2.5, 5, 10 and 20 μM in reactions of lanes 2 to 6 respectively. * : the more than background accumulation of MalE-$MinC^N$ in the pellets is due to a nonspecific association of MalE-$MinC^N$ with FtsZ because: when 16 μM heat-inactivated FtsZ-N280D was used in the sedimentation assay (heat inactivation was confirmed by the failure to respond to GTP in the sedimentation assay) we observed the same amount of FtsZ-N280D in the pellet as with reactions containing active FtsZ-N280D (5 μM) and GTP. We assume that the FtsZ-N280D in the pellet following heat inactivation is due to nonspecific aggregation. If MalE-$MinC^N$ at various concentrations was present in these reactions we observed the same amount of MalE-$MinC^N$ in the pellets (using either 16 μM heat-inactivated FtsZ-N280D with GDP or 5 μM active FtsZ-N280D with GTP), indicating it was nonspecifically associated with the pelleted FtsZ.

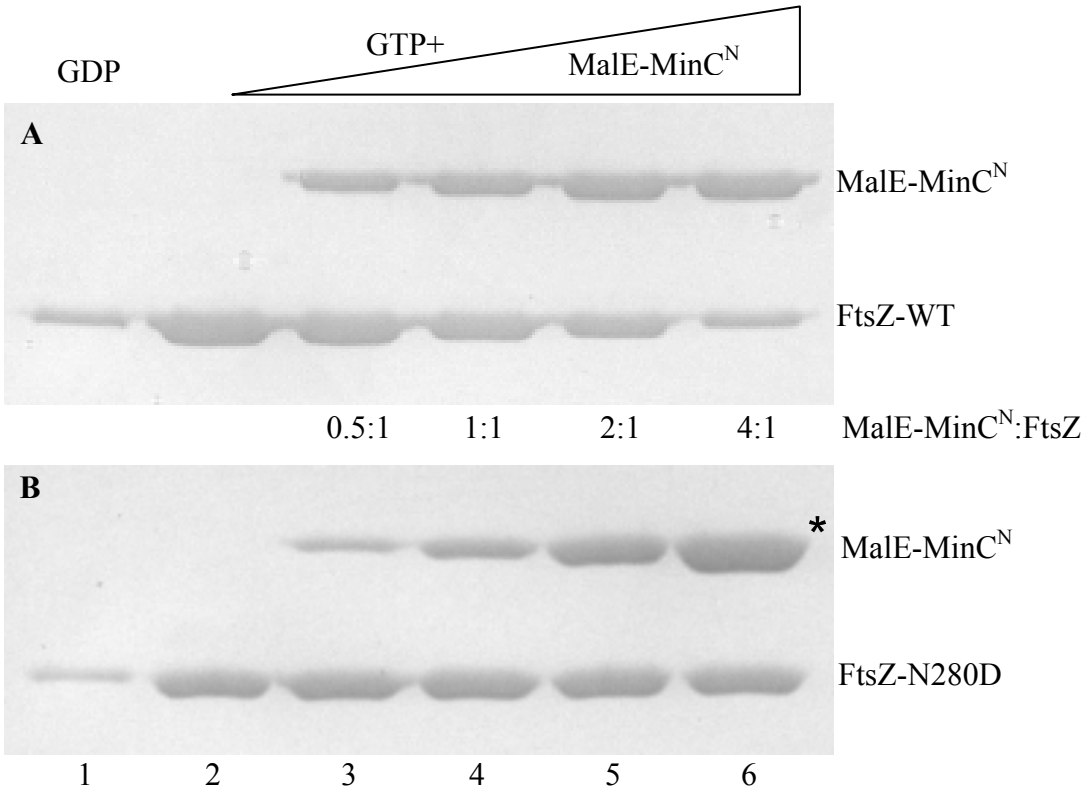
GDP
GTP+
MalE-MinC^N
A
MalE-MinC^N
FtsZ-WT
0.5:1
1:1
2:1
4:1
MalE-MinC^N:FtsZ
B
*
MalE-MinC^N
FtsZ-N280D
1
2
3
4
5
6

Fig. 26. FtsZ-N280D displays decreased interaction with MinC and $MinC^N$. Purified MalE-MinC or MalE-$MinC^N$ (or MalE-SulA as control, about 1 μg protein in each lane) was run on native PAGE gel and transferred to a nitrocellulose membrane. The membrane was blocked with milk and then incubated with 5 μM FtsZ (WT or the FtsZ-N280D mutant) in FtsZ polymerization buffer. After several washes the membrane was blotted with FtsZ antiserum and detected with an AP-conjugated secondary antibody.

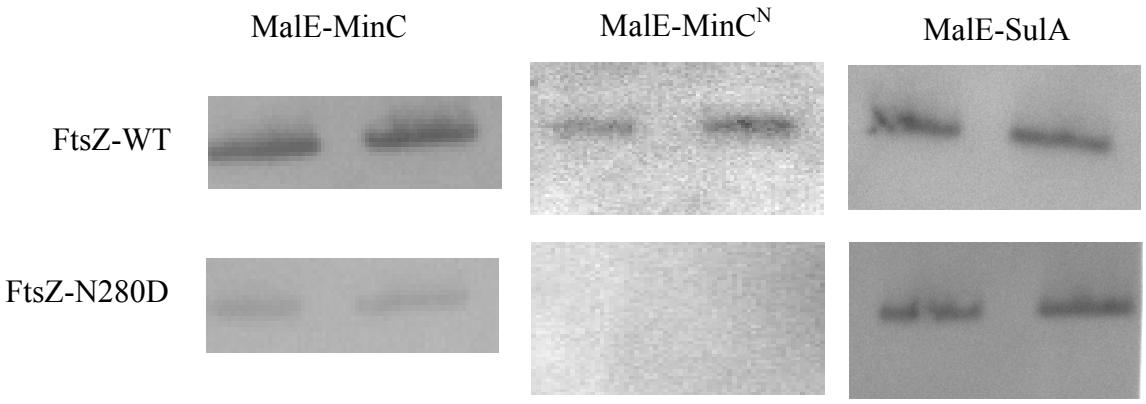
MalE-MinC
MalE-MinC^{N}
MalE-SulA
FtsZ-WT
FtsZ-N280D

was analyzed. The calculated K_D is about 6 μM for WT FtsZ. However, we were unable to calculate a K_D for the FtsZ-N280D mutant because its affinity for MinC is beyond the detection range (10 pM-100 μM) of the system (Fig. 27). This means that the K_D of FtsZ-N280D for MinC is above 100 μM, which is significantly higher than for FtsZ-WT, confirming a decreased interaction between FtsZ-N280D and MinC.

FtsZ-23 is synthetic lethal with SlmA.

As mentioned above, the mutant strains BSZ280D and BSZ374V do not produce minicells even though they have some resistance to MinC/MinD. This suggests that these FtsZ mutants are still responding to MinC/MinD effectively so that topological regulation by the Min system is occurring (each mutant retains responsiveness to one of the two domains of MinC). However for the FtsZ-N280D mutant, the non-minicelling phenotype may not be that informative as it has reduced FtsZ activity [as evidenced by the increased critcal concentration (Fig. 24)]. This reduced activity might counteract its MinC/MinD resistance in minicell production. To test this under conditions where FtsZ activity is not limiting we used an *ftsZ*^{0} strain (S18/W3110 *ftsZ*^{0} *min*$^+$ *recA::Tn10*) complemented with different *ftsZ* alleles present on a plasmid (pBANG112). As mentioned above, this plasmid expresses about 1.5-2 fold of the chromosomal level FtsZ (Fig.18) and therefore could counteract the reduced FtsZ activity caused by mutations such as *ftsZ-N280D*. Consistent with the higher level of FtsZ provided by the plasmid, minicells are observed and about 5% of the total constrictions are polar when wild type FtsZ is present (S18/pBANG112) (Fig. 28). With *ftsZ-N280D* the number of minicells increases and about 25-30% of the total constrictions are at the poles. These results indicate that the Min

Fig 27. Biosensor assay testing the affinity between FtsZ and MalE-MinC. Biotinylated FtsZ (WT or the N280D mutant) was immobilized onto the SA chip surface. MalE-MinC at various concentrations (1, 2, 4, 8, 16, 32μM) was injected and the signals were analyzed by the BIAevaluation program. More details can be found in the *experimental procedures*. In the case of FtsZ-N280D, these is no stable MinC binding as evidenced by the decreasing signal in the MalE-MinC injecting phase. For this reason, the disassociation signal (washing) was not shown.

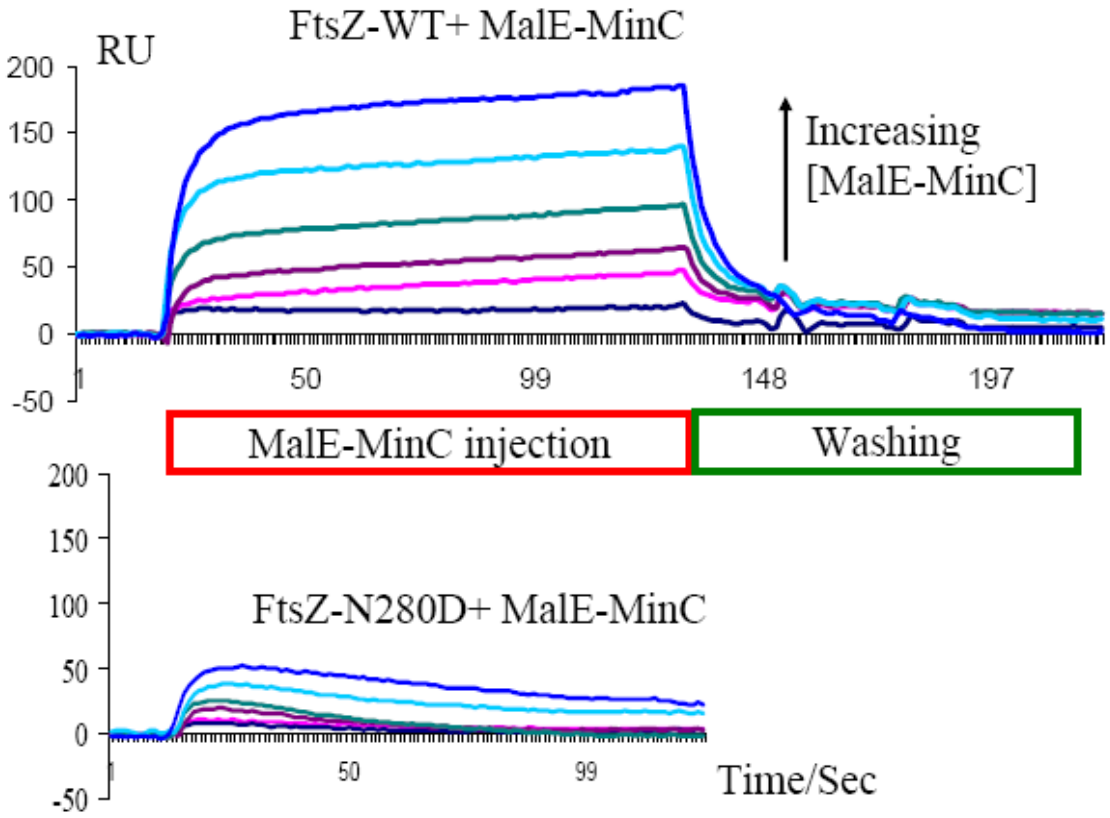
FtsZ-WT+ MalE-MinC
RU
200
150
100
50
0
-50
1
50
99
148
197
Increasing
[MalE-MinC]
MalE-MinC injection
Washing
200
150
100
50
0
-50
FtsZ-N280D+ MalE-MinC
1
50
99
Time/Sec

Fig 28. Polar divisions caused by *ftsZ* mutations. To assess to what extent the various *ftsZ* mutations impair Min function, polar constrictions were quantitated in an *ftsZ*^{0} strain (S18/W3110 *ftsZ*^{0} *recA:Tn10*) complemented with the indicated *ftsZ* alleles on a plasmid (pBANG112). The Δ*min* strain S7/pBANG112 (W3110 *ftsZ*^{0} *min::kan recA::Tn10*/*ftsZ*-WT) was included as a control. Cells were grown to OD_{600}≈0.4, fixed with 0.2% glutaraldehyde and the total number of constrictions (polar and medial) quantified by phase-contrast microscopy. The numbers presented here are the percentage of obvious polar constrictions out of the total number of constrictions.

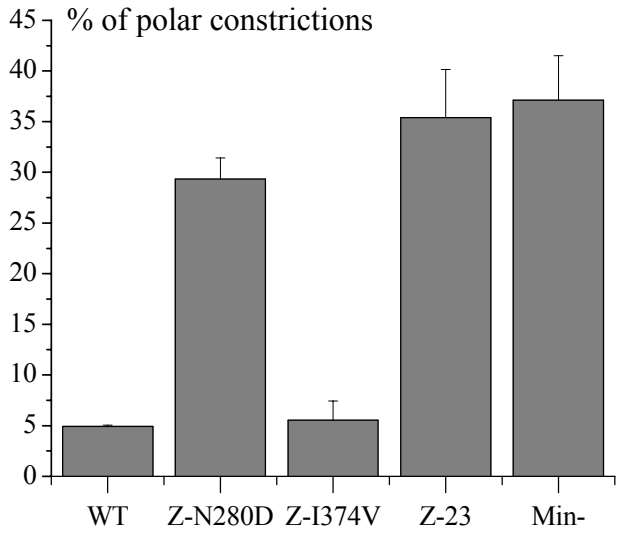
% of polar constrictions
45
40
35
30
25
20
15
10
5
0
WT
Z-N280D
Z-I374V
Z-23
Min-

system is less effective in this mutant. With *ftsZ-23*, about 35% of constrictions are polar, similar to the Δ*min* strain. In contrast, with *ftsZ*-I374V the fraction of polar divisions is similar to what is observed with FtsZ-WT strain.

As an alternative approach to examine the interaction of the *ftsZ* alleles and Min, we determined if they were synthetic lethal with loss of *slmA*. It is known that inactivation of *slmA* is lethal if cells do not have a functional Min system (Bernhardt & de Boer, 2005). If the *ftsZ* mutations disrupt the Min function to a significant extent they should be synthetic lethal with loss of *slmA*. This approach was facilitated by the observation that the *min slmA* double mutant is lethal at low temperature (≤30ºC) but not at high temperature (42 ºC) (S. Du and J. Lutkenhaus, unpublished data). Since it is known that increased FtsZ can suppress this lethality, we suspect that the FtsZ protein level or activity is increased at high temperature. The *slmA::cat* allele was introduced into strains with different *ftsZ* alleles in the *min*$^+$ or Δ*min* background by P1 phage mediated transduction and transductants were selected with chloramphenicol at 42 ºC. The transductants were then restreaked at 30ºC and their growth was monitored. As expected, none of the strains containing the *slmA::cat* allele (regardless of the *ftsZ* allele, either *ftsZ*-WT, *ftsZ-N280D*, *ftsZ-I374V* or *ftsZ-23*) were able to form isolated colonies at 30 ºC in the Δ*min* background (data not shown). In the *min*$^+$ background, only the strain containing the *ftsZ23* allele displayed synthetic lethalality with loss of *slmA* (Fig. 29). The failure of the FtsZ-23 mutant to grow without *slmA* even in the presence of Min further indicates that the Min system is ineffective in cells containing these two *ftsZ* mutations and is consistent with the minicelling phenotype conferred by the *ftsZ23 a*llele. However, the growth of strains carrying either of the single *ftsZ* mutations (*ftsZ-N280D* or *ftsZ-I374V*) indicates that Min function is not totally absent

Fig 29. FtsZ-23 is synthetic lethal with inactivation of *slmA* at low temperature. One colony of each of the strains: S3 *slmA::cat* (*ftsZ-WT*), BSZ280D *slmA::cat* (*ftsZ-N280D*), BSZ374V *slmA::cat*(*ftsZ-I374V*) and BSZ23 *slmA::cat* (*ftsZ-23*) was picked from a plate grown at 42°C and streaked on an LB plate and grown at 30°C for about 20 hours.

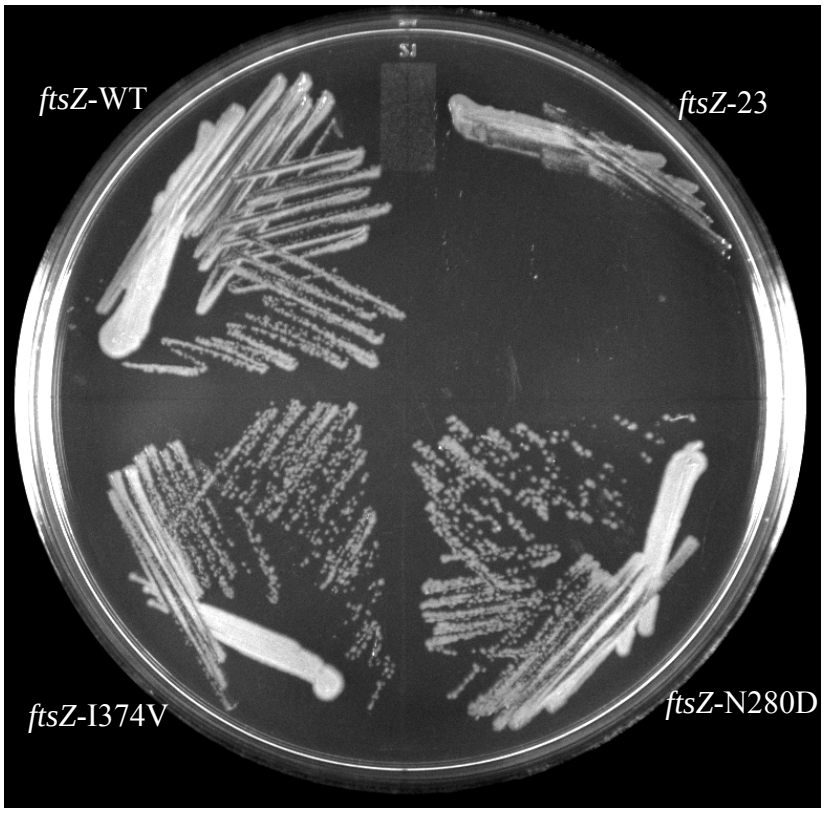
ftsZ-WT
ftsZ-23
ftsZ-I374V
ftsZ-N280D

in these strains. This finding is consistent with the non-minicelling phenotype of the BSZ280D and BSZ374V mutants.

Discussion

MinC (or more precisely $MinC^N$) prevents the pelleting of FtsZ polymers in sedimentation assays (Hu et al., 1999) without significantly affecting the GTPase activity of FtsZ (confirmed here using the NADH coupled enzymatic assay), suggesting that MinC does not affect FtsZ polymerization *per se*. FRET studies actually indicate that the amount of FtsZ in the polymer form is unaffected by MinC, although EM studies showed that MinC results in shorter polymers (Dajkovic et al., 2008a). Dajkovic *et al* showed that MinC reduces the mechanical stability of FtsZ polymer networks (Dajkovic et al., 2008a), which may explain why FtsZ polymers pellet less efficiently when MinC is present. This activity is largely due to $MinC^N$ since $MinC^C$ does not affect the pelleting of FtsZ polymers even though it also decreases the elasticity of FtsZ networks by preventing FtsZ polymer bundling (Dajkovic et al., 2008a, Hu & Lutkenhaus, 2000). It was postulated that $MinC^N$ weakens the longitudinal interaction between FtsZ subunits in the polymer and therefore causes loss of polymer stiffness and induces polymer shortening (Dajkovic et al., 2008a). But how such activity is achieved is largely unknown.

Our results from this study indicate that residues located on one face of the H-10 helix that lies at the interface of two FtsZ subunits within an FtsZ polymer are critical for the FtsZ-$MinC^N$ interaction. The location of these residues is consistent with the above idea that $MinC^N$ weakens the longitudinal interaction between FtsZ subunits. The FtsZ-N280D mutant was studied in detail. This protein has slightly decreased FtsZ activity *in vivo* and a small deficiency

in the GTPase activity *in vitro* due to weaker interaction between FtsZ subunits as evidenced by a small increase in the critical concentration for polymerization. This is consistent with the involvement of the H-10 helix in the interaction between FtsZ subunits (Oliva et al., 2004). Nonetheless, FtsZ-N280D is resistant to $MinC^N$ *in vivo* and the sedimentation of FtsZ-N280D polymers is insensitive to $MinC^N$ *in vitro*. The resistance to $MinC^N$ is specific since FtsZ-N280D displays slightly increased sensitivity to SulA and $MinC^C$/MinD. The reduced interaction between FtsZ-N280D and MinC/$MinC^N$ provides a basis for its $MinC^N$ resistance [notice that the affinity (K_D) of the FtsZ-MinC interaction was about 6 μM in this study, which is different from what was reported before (≈1μM, (Hu et al., 1999)). This difference may be due to the use of two different systems to assess the interaction]. One interpretation of our data is that $MinC^N$ attacks the FtsZ dimer interface at the H-10 helix to break FtsZ polymers.

The H-10 helix is very close to the SulA binding site on FtsZ [represented by the F268 residue (Bi & Lutkenhaus, 1990, Dajkovic et al., 2008b)]. However, the mechanisms by which $MinC^N$ and SulA inhibit FtsZ ring formation are fundamentally different. SulA blocks the FtsZ GTPase and inhibits FtsZ polymerization, whereas $MinC^N$ does not (Mukherjee *et al.*, 1998, Hu et al., 1999, Dajkovic et al., 2008a, Dajkovic et al., 2008b). Instead, $MinC^N$ causes FtsZ polymer shortening but the basis for this activity was not clear. The results obtained from this study prompt us to propose a model for the action of $MinC^N$ based upon the following observations: 1) $MinC^N$ shortens FtsZ polymers but does not affect the GTPase or polymerization of FtsZ *per se* (Dajkovic et al., 2008a), 2) the GTPase of FtsZ is actually required for the inhibitory activity of $MinC^N$ (Dajkovic et al., 2008a), 3) FtsZ polymers contain a significant amount of subunits in the GDP form [up to 50% at [GTP]>100 μM) (Chen & Erickson, 2009)] and 4) the *ftsZ-N280D* mutation decreases the interaction between FtsZ (GDP form) and MinC.

In our model MinC binds to polymerized FtsZ through the $MinC^C$/MinD interaction with the conserved tail of FtsZ regardless of the nucleotide bound to FtsZ. This binding brings $MinC^N$ in close proximity to the FtsZ polymer, although the H-10 helix may or may not be fully accessible to $MinC^N$ (see Fig. 30). If GTP is at the FtsZ dimer interface (Fig. 30, No.2), the strong FtsZ-FtsZ interaction retains the H-10 helix at the FtsZ dimer interface so that it is less exposed to the FtsZ-$MinC^N$ interaction. However, if GDP is present (Fig. 30, No.1), the H-10 helix becomes available for $MinC^N$ binding and the polymer is then severed by $MinC^N$. This process may be aided by the curvature of FtsZ filaments or thermal fluctuations. After breaking the FtsZ polymer, $MinC^N$ (or MinC) binding does not affect the rate of the FtsZ subunit release from the polymer (if it is in the GDP form, Fig. 30 No.3) or the GTP hydrolysis rate (if it is in the GTP form, Fig. 30 No.4). In this way, MinC/$MinC^N$ attacks and shortens the FtsZ polymers without significantly affecting the GTPase.

To test the possibility that the FtsZ interface containing GDP is the preferred target for $MinC^N$, we generated GDP containing polymers by using DEAE-dextran (Mukherjee & Lutkenhaus, 1994, Trusca *et al.*, 1998) and checked to see how MinC or $MinC^N$ affects these polymers in a sedimentation assay. We did not observe cosedimentation of MinC/$MinC^N$ with these polymers nor did we detect a decrease in the amount of FtsZ polymer. However, this test is not conclusive since it is possible that the DEAE-dextran may coat the FtsZ polymer and block the interaction with MinC/$MinC^N$. More sophisticated strategies are required to estimate this possibility. Alternatively, an approach that is closer to the physiological situation where both FtsZ polymer and $MinC^N$ (as part of MinC/MinD) are on the membrane may be necessary to examine the effect of $MinC^N$ on FtsZ.

Fig. 30. A model for the action of MinC on Z ring formation. This model is modified from the previous model (Shen & Lutkenhaus, 2009) with a focus on the activity of $MinC^N$ on FtsZ polymers. In this model it is assumed that FtsZ polymers undergo treadmilling, i.e. the addition of GTP bound subunits to the polymer is at the "+" end (GTP bound end) and the release of GDP bound subunits is from the "-"end. MinC (along with MinD, which is omitted in this figure) attaches to FtsZ polymers through the $MinC^C$/MinD-FtsZ interaction, which disrupts the FtsZ-FtsA and/or FtsZ-ZipA interactions and displaces these Z ring promoting factors from FtsZ polymers. $MinC^N$ (as part of MinC) breaks the FtsZ polymers by attacking the interface between two FtsZ subunits through interaction with the H-10 helix at the FtsZ dimer interface. We assume that this helix becomes available for $MinC^N$ binding if the dimer interface has GDP bound (No.1) but not if GTP is present (No.2). Therefore, $MinC^N$ only attacks FtsZ interfaces with GDP bound between the two subunits. We also assume that MinC binding does not affect the release of GDP bound subunits (No.3) nor the hydrolysis of GTP at GTP containing subunits (No.4).

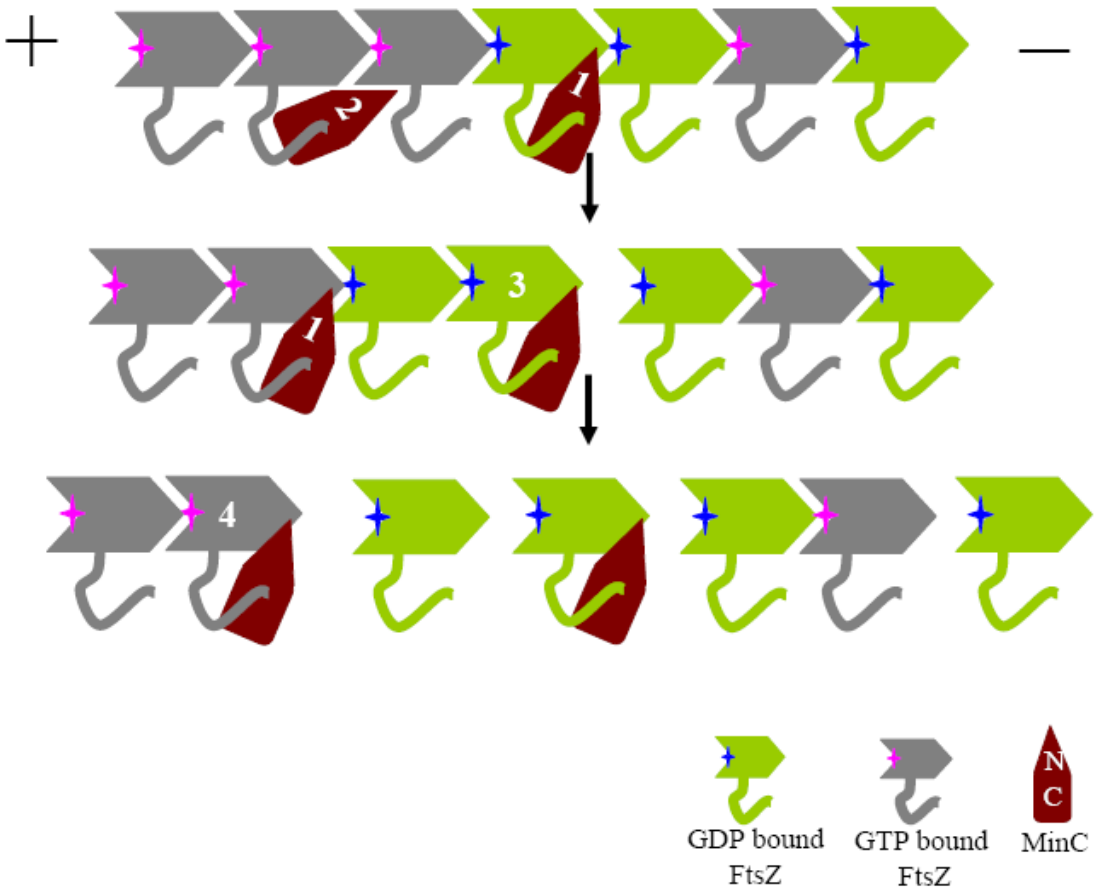
+
−
1
2
1
3
4
N
C
GDP bound FtsZ
GTP bound FtsZ
MinC

The BSZ23 strain, containing both *ftsZ* mutations (*ftsZ-I374V* and *ftsZ-N280D*), produces minicells and behaves essentially like a min^{-} strain, indicating that the Min system is totally ineffective. A puzzling observation is that the FtsZ single mutants (BSZ374V and BSZ280D) do not produce minicells even though they display some resistance to MinC/MinD. One possible explanation for the non-minicelling phenotype of the BSZ374V and BSZ280D strains is that their MinC/MinD resistance is insufficient (clearly not as great as BSZ23). If so, this would indicate that resistance to just one domain of MinC is not sufficient to produce minicells. However, mutations in MinC that inactivate either domain (MinC-G10D or MinC-R172A) cause minicell production [(Zhou & Lutkenhaus, 2005) and unpublished data from M. Wissel and J.Lutkenhaus].

When we compare the effect of *minC* (for example *minC-R172A*) and *ftsZ* mutations (such as *ftsZ-I374V*) on the responsiveness of FtsZ to MinC in a colony forming assay, they are very similar (Fig. 21). Yet *minC* mutations cause minicell production but *ftsZ* mutations do not. Therefore, the degree of MinC/MinD resistance may not be able to explain everything. For the BSZ280D strain, the non-minicelling phenotype may in part be due to the decreased FtsZ activity compromising the MinC/MinD resistance. When we complement an *ftsZ*^{0} strain with the *ftsZ-N280D* allele from a plasmid (which makes slightly more than chromosomal level FtsZ), it leads to significant minicell production (Fig. 28). In contrast, the same strain complemented with *ftsZ-I374V* does not produce more minicells than the strain with *ftsZ*-WT. These data suggest that MinC^{N} may play a more important role in blocking polar Z ring formation under normal conditions. On the other hand, the MinC/MinD resistance of the *ftsZ-I374V* allele is at least similar (if not greater than) to the *ftsZ-N280D* allele (Fig. 21, the plasmid pBANG78 expressing wild-type MinC/MinD can be introduced into the BSM374V strain but not the BSM280D strain

because the basal level of MinC/MinD is too toxic). However, the FtsZ-N280D strain makes minicells if the FtsZ activity is not a limiting factor, whereas FtsZ-I374V does not. This is another case where the extent of MinC/MinD resistance does not correlate with the minicelling phenotype. Therefore, we believe that there must be something we do not understand regarding the spatial regulation of cell division by the Min system, which deserves further investigation.

Chapter V: Differential MinC/MinD sensitivity between polar and mid-cell Z rings

Abstract

In *E. coli* the Z ring has the potential to assemble anywhere in the cell but is restricted to midcell by the action of negative regulatory systems including the Min system. The current model for the action of the Min system is that the MinC/MinD division inhibitory complex is evenly distributed on the membrane and can disrupt Z rings formed anywhere in the cell, however, MinE spatially regulates MinC/MinD by restricting it to the cell poles and thus protects the midcell for Z ring formation. This model predicts that Z rings formed at different cellular locations have equal sensitivity to MinC/MinD in the absence of MinE. However here we show evidence that differential MinC/MinD sensitivity between polar and internal Z rings (midcell ones in normal sized cells and the ones between nucleoids in longer cells) exists even when there is no MinE. MinC/MinD at proper level is able to block minicell production in Δmin strains without increasing the cell length, indicating that polar Z rings are preferentially blocked. In the FtsZ-I374V strain, wild type morphology can be easily achieved with MinC/MinD in the absence of MinE. We also show that MinC/MinD at proper induction level can rescue the lethal phenotype of min slmA double deletion strains. We believe the mechanism behind this is that by eliminating polar Z rings (or FtsZ structures), MinC/MinD frees up FtsZ molecules to assemble Z rings at internal sites and therefore rescues the division and growth of these cells. Taken together, these data indicate that polar Z rings are more susceptible to MinC/MinD than midcell Z rings, either because the midcell Z rings are better protected from the action of MinC/MinD or MinC/MinD is working more efficiently at cell poles even in the absence of MinE.

Introduction

One of the questions left behind from the previous two studies is why the two FtsZ mutant strains (BSZ374 and BSZ280D) do not make minicells even though they have significant MinC/MinD resistance (Shen & Lutkenhaus, 2010, Shen & Lutkenhaus, 2009). This is particularly true for the BSZ374 strain. Whereas for the BSZ280D strain, as we discussed above, the reduced activity of the mutant FtsZ protein partially counteracts its MinC/MinD resistance and therefore limits minicell production. However, it is very hard to believe that this is the only reason for the non-minicelling phenotype of the BSZ280D strain because the vast majority of the BSZ280D cells are perfectly wild-type like. This question becomes more obvious when we compare the two FtsZ mutations (FtsZ-I374V and FtsZ-N280D) with mutations in MinC that affect the MinC-FtsZ interaction similarly (MinC-R172A and MinC-G10D respectively). Strains containing MinC mutations make minicells but not those with FtsZ mutations. This is puzzling and no suitable explanation was apparent. However, one observation we had may be a clue for the understanding of this conundrum.

In the earlier studies, we accidentally found that in the BSM374 strain (*ftsZ-I374V, min::kan*), Z rings formed at different positions of the cell show different sensitivity to MinC/MinD with the polar ones being more susceptible than the ones at midcell. This observation is contradictory to the current view of the action of the Min system (Fig. 31) in which it is generally assumed that all Z rings are equivalent. Initially we were concerned that this phenomenon was unique to the FtsZ-I374V mutant strain. However, further examination reported herein reveals this also occurs in other strains. In addition, we are able to provide supporting evidence from other studies.

Fig. 31. Current model for the action of the Min system. A: when cells don't have MinE, MinC and MinD interact with each other to form a nonspecific division inhibitor which is capable of blocking Z ring formation at all potential division sites. Therefore the cells fail to divide and grow into extremely long filaments and eventually die. B: in WT cells when MinE is present, cell division occurs in the middle of the cell but not at poles because MinE gives topological specificity to the MinC/MinD division inhibitor complex so that it is working only at cell poles. As a result, the midcell space is protected from the action of MinC/MinD and therefore permissive for Z ring formation. C: as a prediction from the current model for Min, when MinC/MinD is induced in a Δmin strain, it will either block all the divisions and cause severe filamentation if it is induced to a high enough level or result in incomplete inhibition of division and allow sporadic divisions at internal and polar positions if the induction level is intermediate.

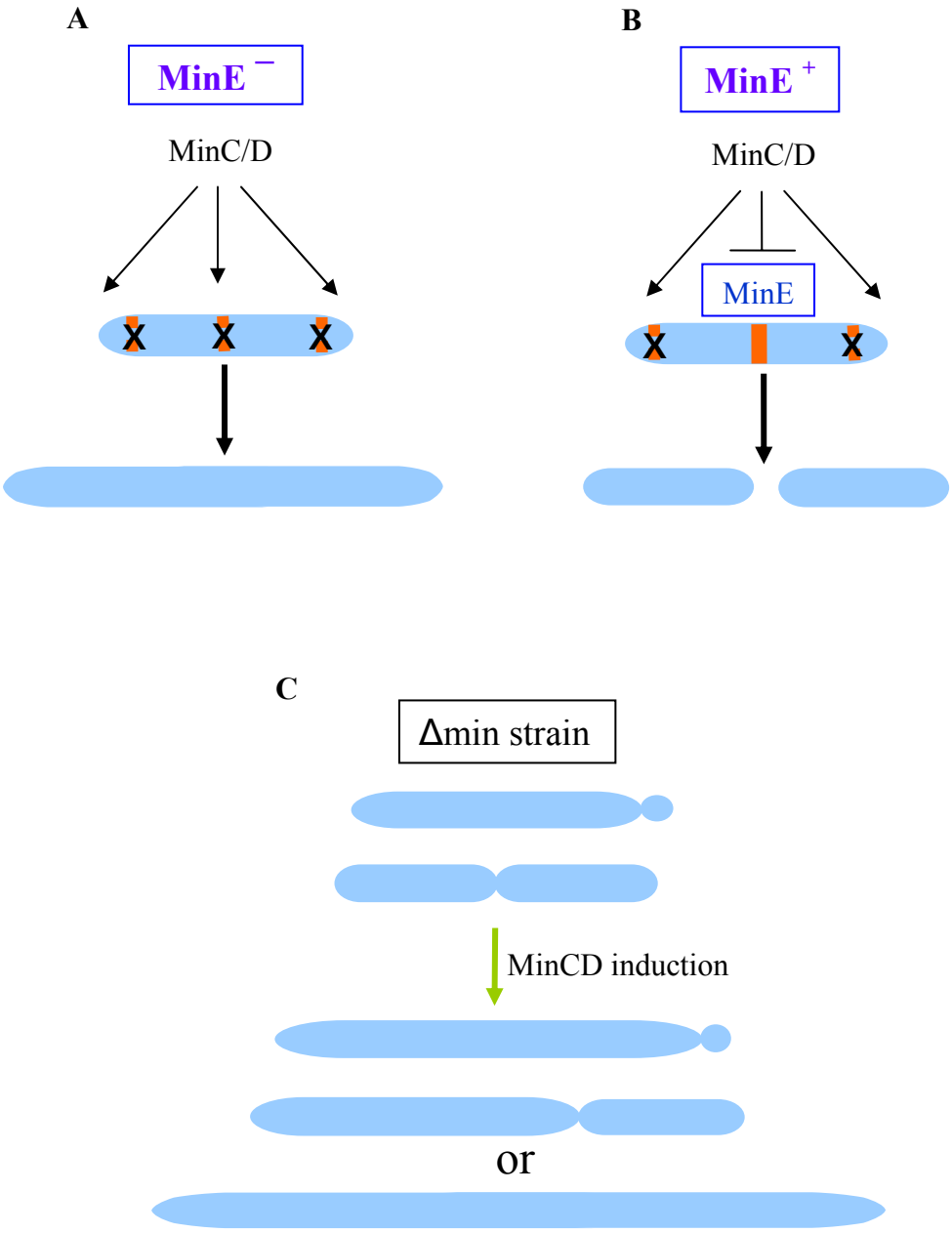
A
MinE −
MinC/D
B
MinE +
MinC/D
MinE
C
Δmin strain
MinCD induction
or

As illustrated in Fig. 31, the current view on the Min system suggests that Z rings formed at any position in the cell have equally sensitivity to MinC/MinD in the absence of MinE, the topological regulator of the Min system (de Boer et al., 1989, de Boer et al., 1992b). In a Δmin strain, Z ring assemble randomly at poles or internal positions of the cell. No difference has been reported in terms of the composition of the polar and midcell Z rings and divisomes. Therefore if MinC/MinD is expressed in a Δmin strain, both polar and internal divisions should occur until the MinC/MinD level reaches high enough to completely block all divisions. However, during the course of the above studies, we found a situation where induction of MinC/MinD at intermediate levels only blocks the polar divisions, which means that polar Z rings are more sensitive to MinC/MinD than internal Z rings. Here, we extend this study and the results lead us to conclude that it is a general phenomenon that polar Z rings are more susceptible to MinC/MinD than the Z rings formed at internal positions in the cell. Although a general phenomenon, we observed that the differential MinC/MinD sensitivity of polar and internal Z rings is particularly pronounced in the strain with FtsZ-I374V. In this strain expression of MinC/MinD can readily lead to a WT phenotype in the absence of the spatial regulator MinE.

Result

Bypass of MinE for the spatial regulation of cytokinesis by MinC/MinD in the FtsZ-I374V strain.

When checking the MinC/D resistance of the FtsZ-I374V mutant as described in Fig. 8 and Fig. 19, we observed that there is an IPTG dependent morphology change of the strain BSM374/pBANG59 (*ftsZ-I374V, min::kan*/P*lac::minCD*): with no or very low IPTG induction

of MinC/MinD, this strain behaves like a typical Δmin strain, which is what's expected. As the IPTG concentration increases to 50 ~ 100μM, the cells still have the characteristic heterogeneous cell length distribution of normal Δmin strains but they did not make any minicells. At this stage the average cell length and the cell length distribution are very similar as the same strain without IPIG induction, indicating that internal divisions are not affected by this level of MinC/MinD, even though the polar divisions are almost completely blocked as evidenced by loss of minicell production. When we further increase the IPTG concentration to 1mM to induce more MinC/MinD, the cells completely turned into wild-type morphology with a cell length distribution similar to Min^+ WT cells and division only occurring at midcell (Fig. 32). Immuno-staining analysis indicates that these cells do not have any detectable polar Z rings (data not shown). This is very surprising because these cells do not have MinE to direct MinC/MimD to the cell poles, yet the evidence clearly indicates that MinC/MinD is eliminating polar Z rings while not disturbing midcell Z rings. Thus, the proper level of MinC/MinD is as effective as the fully intact Min system in spatially regulating Z ring formation in the FtsZ-I374V strain. This morphological change is truly dependent upon MinC/MinD because it did not happen in the presence of a MinC mutation G10D (data not shown), which reduces the activity of the N terminal part of MinC significantly. These data clearly demonstrate that polar Z rings are more susceptible to MinC/MinD than internal/midcell Z rings in the BSM374 strain and the requirement of MinE for the spatial regulation of Min can be bypassed under this situation.

Fig. 32. Effect of MinC/MinD induction on the BSM374 strain. MinC/MinD expression is under an IPTG-inducible promoter control from the plasmid pBANG59. BSM374 bearing this plasmid was grown in LB medium (supplemented with Spc) with or without 1mM IPTG to OD_{600}=0.4. The cultures were then subjected to microscopy analysis. The BSZ374 strain serves as a control. A: cell length distribution of the indicated strains. B-D: representative images showing the morphology of indicated cells. B: BSZ374, C: BSM374/pBANG59 in the presence of 1mM IPTG, D: BSM374/pBANG59 without IPTG induction.

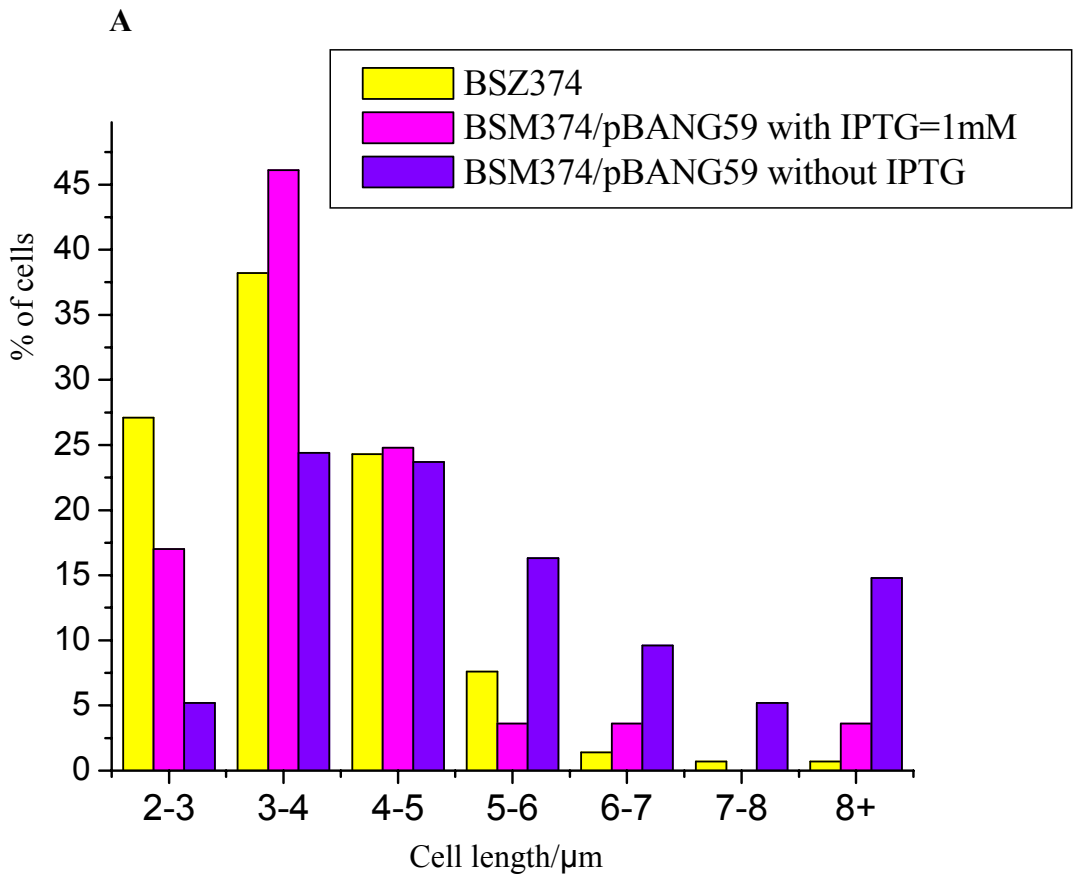
A
BSZ374
BSM374/pBANG59 with IPTG=1mM
BSM374/pBANG59 without IPTG
% of cells
0
5
10
15
20
25
30
35
40
45
2-3
3-4
4-5
5-6
6-7
7-8
8+
Cell length/μm

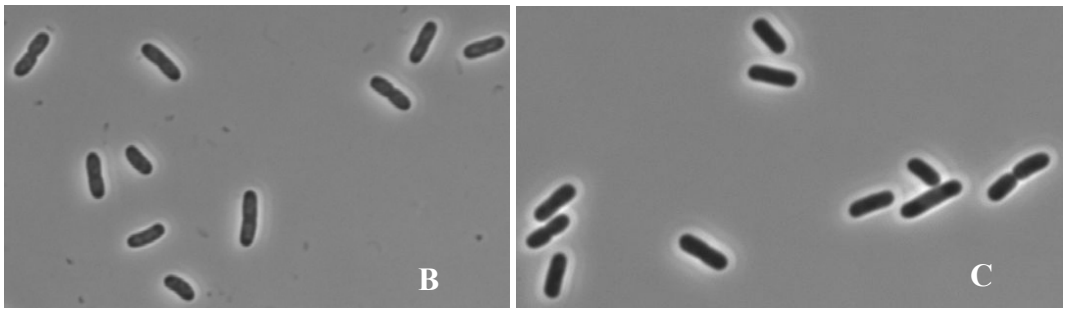
B
C

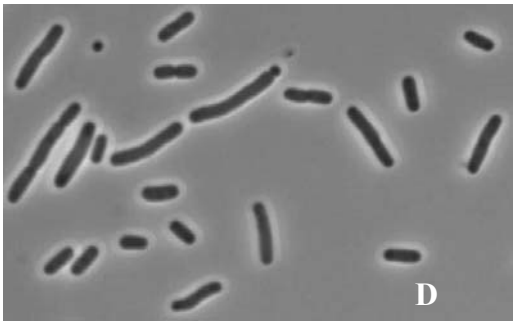
D

Differential MinC/MinD sensitivity between polar and midcell Z rings exists in a variety of strains.

When we first observed the above phenotype we worried that it was a unique property of the FtsZ-I374V mutant due to some unknown effect from this mutation or there was something unexpected in the MinC/MinD expression plasmid PBANG59. To exclude these possibilities we first repeated the above analysis with different MinC/MinD constructs, some of which were made in this study for this purpose (such as PBANG76 /P*lac::minCD* on pGB2) and some were made previously by other people (such as λDB173/P*lac::minCD* on a lambda vector). For all the constructs we tried we got very similar results to what we observed with pBANG59 (Table. 7). With λDB173, we were unable to restore the WT-like morphology of BSM374 since MinC/MinD could not be induced to a sufficient level. However with other constructs where sufficient MinC/MinD could be produced, we were able to restore the WT-like morphology. Nonetheless, with all of these constructs we were able to find appropriate induction levels where minicell formation was prevented without causing filamentation, indicating that polar and internal divisions are differentially affected by MinC/MinD.

One plasmid (pBANG78) we employed, which can produce higher levels of MinC/MinD, allowed us to observe an even wider change in morphology during the course of MinC/MinD induction than that observed with pBANG59. With no IPTG induction BSM374/pBANG78 behaved like a typical Δmin strain even though less minicells are produced, probably because of the high basal MinC/MinD level from this plasmid (this basal level is enough to kill an FtsZ-WT Δmin strain such as S4). When grown in medium with 5-10μM IPTG, the cells are very close to WT-like, they divide in the middle, show less heterogeneity in cell length and the majority of

Table. 7. MinC/MinD can block minicell formation without causing filamentation in Δmin strains. For all the studies, the strains with the indicated constructs were grown in liquid culture supplemented with IPTG at a variety of concentrations to OD_{600}≈0.4. Samples are then fixed with 0.2% glutaraldehyde and subjected to microscopy analysis. *: the conditions listed here are the range of IPTG concentrations that efficiently block minicell formation (less than 1% of the total constrictions are at the poles) but do not cause any kind of filamentation, i.e. the average cell length is not longer and the cell length distribution is not broader. (minicells are not included in the cell length analysis).

Table. 7. Stop minicell formation in Δmin strains by MinC/MinD.

Strain	Construct	Conditions that stop minicell formation*
S4	pBANG59 (P*lac::minCD*)	IPTG=20-25μM
	pBS31 (P*trc::sulA*)	none
	pBANG61 (P*lac::minD*)	none
	pBANG55 (P*trc::minC-MTS*)	IPTG= 40-60μM
	pHJZ117 (P*lac::minC*)	none
	pBANG78-G10D (P*lac::minC*$_{G10D}$*D*)	IPTG=5-10μM
	pBANG78-R172A (P*lac::minC*$_{R172A}$*D*)	IPTG=5-10μM
BSM374	pBANG59 (P*lac::minCD*)	IPTG=50-1000μM
	pBANG78-G10D (P*lac::minC*$_{G10D}$*D*)	IPTG>200μM
	pBANG78-R172A (P*lac::minC*$_{R172A}$*D*)	IPTG=10-15μM
	pBANG78 (P*lac::minCD*)	IPTG=5-10μM
	pBANG76 (P*lac::minCD*)	IPTG>500μM
	λDB173 (P*lac::minCD*)	IPTG>100μM
BSM280D	pBANG59 (P*lac::minCD*)	IPTG≈100μM
BSM23	pBANG59 (P*lac::minCD*)	none

cells are indistinguishable from regular WT cells. If MinC/MinD is induced to an even higher level with IPTG>20μM, cells become filamentous and eventually get killed. These results demonstrate that the IPTG dependent morphological change of BSM374/pBANG59 observed previously is not due to something special other than minCD on the plasmid PBANG59 because all other MinC/MinD constructs have similar impacts. We also sequenced all the constructs used in this study to confirm their sequence information.

To see whether this phenomenon is unique to the FtsZ-I374V mutant strain, we did similar tests in other strains with different genetic backgrounds. First we tested two FtsZ-WT strains S4 (W3110, *leu::tn10, min::kan*) and S22 (MG1655, *min::kan*). Both strains containing the plasmid pBANG59 displayed similar morphological changes upon MinC/MinD induction. With low or no IPTG induction a typical Min^{-} phenotype is observed. As the MinC/MinD level is increased, minicell production was gradually reduced but the cells did not get any longer. In contrast to the FtsZ-I374V strain, this elimination of minicell production without an increase in cell length only occurred over a very narrow range of MinC/MinD induction [for example, IPTG = 20-25 μM for S4/pBANG59] (Table. 7). In this narrow range minicell formation was completely blocked but the strain still had the same cell length distribution as a typical Δmin strain. If the induction of MinC/MinD is above this window, filamentation started to occur. These results indicate that MinC/MinD can stop minicell formation in these two FtsZ-WT strains without causing any filamentation. However, in these two cases the range of MinC/MinD induction that blocks minicell production before causing filamentation is in a very narrow range (IPTG = 20-25 μM for S4/pBANG59 in contrast to IPTG= 50-1000 μM for BSM374/pBANG59). In addition, no MinC/MinD induction level was found that restored these Δmin cells to a WT like morphology. This is probably due to the fact that FtsZ-WT is much more sensitive to

MinC/MinD than FtsZ-I374V. The broader MinC/MinD induction range that blocks minicell formation without inducing filamentation in the FtsZ-I374V mutant suggests that the difference in MinC/MinD sensitivity between polar and internal Z rings is much greater in this mutant than in FtsZ-WT strains (discussed later).

We also examined two other FtsZ mutant strains BSM280D and BSM23 for their response to MinC/MinD. BSM280D/PBANG59 responds to MinC/MinD induction in a similar way as S4/pBANG59, but the minimal IPTG concentration required to stop minicell formation in this strain is higher than in the S4/pBANG59 strain (Table. 7). Even though there seems to be a small range of MinC/MinD induction that blocks minicell formation without causing significant filamentation, we have to clarify that such tests in this strain offer less reliable information. This is because: the key point in these tests is the existence of MinC/MinD induction levels that stop minicell production without causing any filamentation. Unfortunately, the BSM280D strain without any plasmid displayed a mild filamentation phenotype and broader cell length distribution compared to regular Δmin strain such as S4 (Table. 6). Therefore such a test in this strain is more difficult. Nevertheless our results seem to indicate that the differential MinC/MinD sensitivity between polar and internal Z rings also exists in the BSM280D strain.

In contrast to the strains tested so far, BSM23/pBANG59 was not affected by MinC/MinD induction. Minicells are produced at all IPTG concentrations and there is no significant change in morphology during the course of MinC/MinD induction. This is consistent with this strain being insensitive to MinC/MinD due to the presence of ftsZ23 which is resistant to both domains of MinC (Fig. 21). It also supports our conclusion that the prevention of minicell production in the other strains is indeed due to the action of MinC/MinD.

We also used plasmids expressing MinC alone, MinD alone or SulA in the S4 strain to serve as controls for the above analysis. Expression of MinD alone in this strain has little effect on minicell formation or cell length distribution, indicating that MinD by itself does not affect division at any position. Induction of MinC alone or SulA in the S4 strain does change the cell morphology, however, neither of them can block minicell formation without causing filamentation. They do stop minicell production at high levels but by the time they stop the minicell formation, almost all divisions are blocked and cells are getting filamentous, indicating that MinC alone or SulA can not distinguish Z rings at polar and internal positions. One potential explanation for this is that: both MinC and SulA are in the cytoplasm. They target the cytoplasmic FtsZ (monomer and/or polymer forms) that are the precursors of Z rings. These precursors are unlikely to be presorted and differentially directed to specific locations in the cell but are probably shared by all potential Z rings. Therefore when MinC or SulA is induced to decrease the supply of Z ring precursors, polar and internal Z rings are equally affected.

Our results indicate that MinC on the membrane (recruited by MinD) can differentiate between polar and internal Z rings whereas MinC in the cytoplasm can not, it behaves as a nonspecific inhibitor, similar to SulA. As one approach to explore this difference, we made a plasmid (pBANG55) expressing MinC with a membrane targeting sequence fused to its C terminus (MinC-MTS) and induced this construct in the S4 strain. Surprisingly and in contrast to MinC in the cytoplasm, MinC-MTS induction in the S4 strain caused similar morphological changes as MinC/MinD induction; minicell production was blocked at intermediate induction without affecting the cell length distribution (Table. 7). This result means that MinC-MTS can also differentiate polar and internal Z rings. This result also suggests that MinD is not absolutely required for MinC to distinguish internal Z rings from polar Z rings and that its role is to place

MinC on the membrane. The same line of observation also suggests that MinC in the cytoplasm and MinC on the membrane affect FtsZ differently.

MinC/MinD is able to rescue the growth defect of min slmA double mutants.

As discussed in the last chapter, neither min nor slmA is essential. However, inactivation of both is lethal at low temperatures (≤ 30 °C) because the cells fail to assemble functional Z rings and therefore cannot divide. The synthetic lethal phenotype of the min and slmA double mutant can be rescued by a couple of conditions: high temperature, culture in minimal medium or extra FtsZ (Bernhardt & de Boer, 2005). If the double mutant is grown in minimal medium such as M9 or grown in rich medium at high temperature such as 42 °C, the cells are able to divide and form regular colonies. In rich medium at low temperatures such as 30 °C, a one to two fold increase of FtsZ can also rescue the growth of the cells. It seems like the problem of the min slmA double mutant at low temperature is that the FtsZ molecules in the cell are spread out among many incomplete FtsZ structures [Du and Lutkenhaus, unpublished data; (Bernhardt & de Boer, 2005)]. In the absence of these inhibitors the dispersed FtsZ is unable to make functional Z rings. Therefore increasing the FtsZ level in the cell by supplying extra FtsZ can rescue the growth of these cells. In addition, it is likely that growing the double mutant at high temperature or in minimal medium also increases the FtsZ protein level or activity and therefore restores the growth.

We wanted to test whether MinC/MinD at proper levels can rescue the growth of the min slmA mutant. The hypothesis behind this is: if MinC/MinD can distinguish polar Z rings from midcell Z rings and selectively disrupt polar ones, it may free the FtsZ molecules from cell poles

so that enough FtsZ is available to assemble Z rings at internal spaces. If so, it may be able to rescue the growth of the double mutant. To test this possibility, we introduced the plasmid expressing MinC/MinD (PBANG84/P*trc::minCD*) into four different min slmA mutants and examined their growth over the course of MinC/MinD induction. As shown in Fig. 33, low induction levels of MinC/MinD can rescue the growth of S14 (W3110 *min::kan slmA::cat*) at 30°C but high levels killed it. In the case of S16 (*BSZ374 min::kan slmA::cat*), high levels (IPTG≥ 50μM) of MinC/MinD can rescue and low levels can not. For S19 (*BSZ280D min::kan slmA::cat*), it seemed like a broad range of MinC/MinD level can partially rescue the growth. As for S20 (*BSZ23 min::kan slmA::cat*), no condition was found to be able to efficiently rescue colony formation with this plasmid, even though the MinC/MinD induction does help the growth a little bit but never to the point where cells can form isolated colonies.

Microscopic examination revealed that when growth is efficiently rescued by MinC/MinD, the cells are close to (if not less heterogeneous than) typical Δmin cells in morphology and cell length, but they do not make minicells. This is in consistent with our idea that MinC/MinD eliminates polar Z rings/FtsZ structures to increase the FtsZ supply for making internal Z rings. This result is also consistent with the notion that extra FtsZ is the key for rescuing the growth of these cells, although in this case the increase in FtsZ is due to local redistribution rather than an overall increase in the level of FtsZ. Interestingly, if these double mutants are rescued by extra FtsZ or growth at high temperature, they are producing minicells (even though not as many as regular Δmin strains), which is different than rescue by MinC/MinD, further confirming that the rescue by MinC/MinD is due to the elimination of polar Z rings/FtsZ structures.

Fig. 33. Rescue of min slmA double mutants by MinC/MinD. The plasmid pBANG84 (P*trc::minCD*) was transformed into the indicated min slmA strains and the cells grown on LB plates with Spc at 42 °C. Then one colony from each strain (harboring the plasmid pBANG84) was subject to a spot test on LB plates (with Spc) containing different IPTG concentrations at 30 °C. 1: S14 (*W3110 min::kan slmA::cat*)/pBANG84; 2: S16 (*BSZ374 min::kan slmA::cat*)/pBANG84; 3: S19 (*BSZ280D min::kan slmA::cat*)/pBANG84; 4: S20 (*BSZ23 min::kan slmA::cat*)/pBANG84.

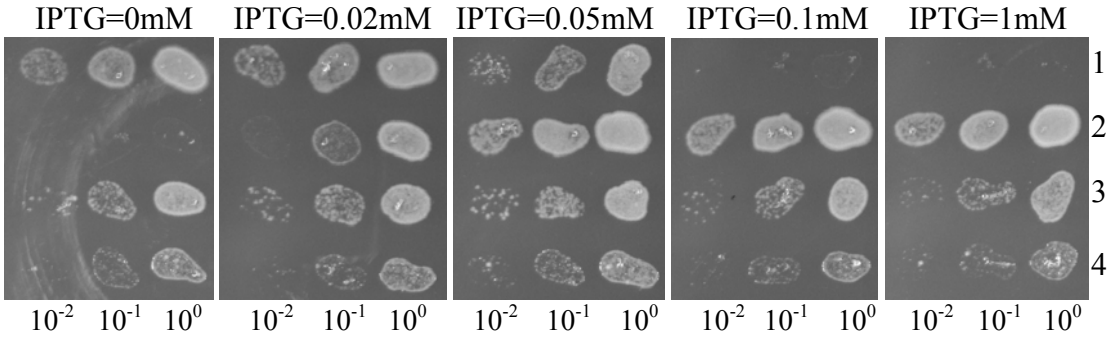
IPTG=0mM
IPTG=0.02mM
IPTG=0.05mM
IPTG=0.1mM
IPTG=1mM
1
2
3
4
10-2 10-1 100
10-2 10-1 100
10-2 10-1 100
10-2 10-1 100
10-2 10-1 100

Discussion

In this study, we show evidence that in *E. coli* cells, polar divisions are more susceptible to MinC/MinD even in the absence of MinE. First, a limited level of MinC/MinD is able to completely block minicell formation in several Δmin strains without causing any filamentation, indicating that polar divisions are efficiently blocked under these situations but internal divisions are not affected. Immuno-staining analyses confirmed that MinC/MinD is working at the level of Z ring formation to differentially affect divisions at different positions. Second, proper levels of MinC/MinD induction can rescue the growth of min slmA double mutants at low temperature. This is very surprising if we do not consider the differential MinC/MinD sensitivity between polar and internal Z rings. Extra FtsZ was shown to rescue these double mutants (Bernhardt & de Boer, 2005). It seems like the problem of these mutants is the inability to assemble functional Z rings due to FtsZ being spread among multiple incomplete Z ring structures in the absence of these Z ring regulators. If extra FtsZ is needed to help these cells grow, how can MinC/MinD, a potent inhibitor of Z ring assembly, rescue the growth of these mutants? We believe this is because, consistent with the first observation, proper levels of MinC/MinD selectively disrupt the polar Z rings (or FtsZ polymer structures near cell poles before a polar Z ring is made) and artificially increase the FtsZ available for internal Z ring assembly as the FtsZ molecules released from the polar Z rings/FtsZ structures are now squeezed to internal spaces.

Among all the strains tested, BSM374 seems to have the greatest difference in MinC/MinD sensitivity between polar and middle Z rings. A broad range of MinC/MinD induction levels can stop minicell production in this strain without causing filamentation; at high levels, MinC/MinD can completely revert these cells to a WT-like morphology. Thus, the

function of MinE can be totally bypassed to achieve spatial regulation of Z ring assembly in this strain. Interestingly, the minimal MinC/MinD level required to stop minicell production is not much higher in the BSM374 strain than in the FtsZ-WT Strain S4 (Table. 7), which means that the polar Z rings in BSM 374 do not have much more resistance to MinC/MinD than those in the S4 strain. Again this is something unexpected because the BSM374 strain displayed significant MinC/MinD resistance compared to the S4 strain in the killing assay (Fig. 8 and 19). These seemingly contradictory observations actually support our idea that polar and internal Z rings have different sensitivity to MinC/MinD, although the extent of difference can vary in different strains. In the killing assay, what we are really measuring is the sensitivity of internal Z rings to MinC/MinD because this is what determines the viability of the cells. Since the BSM374 strain survives high levels of MinC/MinD induction, it indicates that internal Z rings in this strain have great resistance to MinC/MinD. But as evidenced by the ability of low level of MinC/MinD to block minicell formation in this strain (BSM374), the polar Z rings do not have much more MinC/MinD resistance than the polar Z rings in the S4 strain. These comparisons clearly demonstrate that a big difference in MinC/MinD sensitivity between polar and internal Z rings exists in the BSM374 strain. However, it is not clear why the difference is much greater in the BSM374 strain than in any other strains.

MinC-MTS, like MinC/MinD is able to selectively block polar divisions but WT-MinC by itself can not. This implies that MinD is not absolutely required but that MinC has to be on the membrane to differentiate polar and internal Z rings. MinC has two functional domains and it seems like both domains are able to differentially affect polar and internal Z rings as evidenced by the ability of MinC/MinD to block minicell formation in BSM374 and BSM280D strains. This is further confirmed by the fact that both $MinC^{G10D}$/MinD and $MinC^{R172A}$/MinD (two

mutant forms of MinC/MinD that reduce tha activity of $MinC^N$ and $MinC^C$ respectively) are able to (even though higher levels than WT-MinC/MinD are required) block minicell production in the S4 strain without causing filamentation. Although both domains of MinC are able to get rid of polar Z rings, $MinC^N$ seems to play a more important role because in the min slmA double mutant rescue assay shown in Fig. 33, WT-MinC/MinD and $MinC^{R172A}$/MinD can efficiently rescue the strain S14 (*ftsZ-WT min::kan slmA::cat*) as well as S16 (*ftsZ-I374V min::kan slmA::cat*), indicating that an active $MinC^N$ is sufficient. However, if $MinC^{G10D}$/MinD is used to rescue the growth of S14, it can greatly improve the growth but never work as effectively as WT-MinC/MinD or $MinC^{R172A}$/MinD because the cells are ubable to form robust single colonies. Additionally, similar results were obtained when we used $MinC_{R172A}$/MinD, $MinC_{G10D}$/MinD or even WT-MinC/MinD to rescue the strain S19 (*ftsZ-N280D min::kan slmA::cat*). These data suggest that $MinC^N$ is playing a critical role in the rescue of these double mutants because when the action of $MinC^N$ is reduced (by mutations on MinC or FtsZ), the rescue is never very efficient.

It is interesting to know the molecular basis for the differential MinC/MinD sensitivity between polar and midcell Z rings. Potentially there are at least two possibilities: either MinC/MinD is working more efficiently at cell poles even in the absence of MinE or the middle of the cell is a preferred place for Z ring assembly and midcell Z rings are better protected against the attack of MinC/MinD. In support of the first possibility, cardiolipin (CL) was shown to be enriched at *E. coli* cell poles (Mileykovskaya & Dowhan, 2000, Koppelman *et al.*, 2001) and MinD seems to have higher affinity for CL than other phospholipids such as phosphatidylglycerol (PG). This implies that MinC/MinD may prefer to localize to and be concentrated at cell poles. However, fluorescent microscopy analysis on GFP-MinD and GFP-

MinC/MinD (or GFP-MinC^{C}/MinD) in Δmin cells revealed that the GFP signal was not enriched at cell poles but evenly on the membrane (Shen & Lutkenhaus, 2009, Zhou & Lutkenhaus, 2003). Additionally, as discussed above, MinD does not seem to be absolutely required for MinC to selectively disrupt the polar Z rings because MinC-MTS can do it efficiently in the absence of MinD. This MinC-MTS fusion seems to be evenly on the membrane too as revealed by GFP tagging at the N terminus (data not shown). All these observations suggest that MinC/MinD may not be significantly enriched at cell poles and the polar accumulation of MinC or MinC/MinD, if there is any, may not be required for MinC or MinC/MinD to preferentially disrupt polar Z rings. However, this does not completely rule out the possibility that MinC or MinC/MinD is working more efficiently at cell poles. There could be a polarly localized factor(s) that activates or increases the affinity of MinC for FtsZ at cell poles and such factors may not have to enrich MinC at poles in any way.

In Δmin strains, the Z rings are predicted to randomly form at polar and internal positions because the frequency of polar divisions (about 30% of total divisions) in these cells is in consistent with such a "random formation" model based on calculations from the heterogeneous cell length distribution of these cells (for example: a cell with one length unit has one middle and two polar positions for potential Z ring formation; a cell with two length units will have three middle and two polar positions and a cell with three length units will have five middle and two polar positions for potential Z ring assembly, etc). Such a model then predicts that the mid point of the cell is not more preferred for Z ring assembly in the absence of the Min system. However, this may or may not the real case in the cell; experimental data fitting a model does not mean that the model is correct. For instance, when the min slmA double mutant is grown at 42°C or at 30°C with extra FtsZ supply, not too many minicells are produced and the majority (above 90%)

of the divisions (and Z rings too as revealed by immuno-staining) are between nucleoids at internal positions. This seems to suggest that middle/internal spaces are preferred for Z ring assembly and subsequent division. As for the possibility that internal Z rings are better protected against MinC/MinD, we think it's possible even though there is no evidence indicating that this is the case. If it is true, there must be novel factors (proteins, special biophysical properties of the middle area of the cell, etc) involved to differentiate the midcell Z rings from polar Z rings.

In *B. subtilis*, MinJ-DivIVA seems to block the action of MinC/MinD on constricting Z rings/septa under physiological conditions. MinC/MinD is localized to the Z ring/septum through MinJ-DivIVA late during division but it never disrupts the Z ring (Edwards & Errington, 1997). However in the absence of MinJ or DivIVA, MinC/MinD disrupts them and therefore causes filamentation (Bramkamp et al., 2008, Patrick & Kearns, 2008). So during division, MinJ-DivIVA works to protect the constricting Z rings from being disrupted by MinC/MinD. There is a fundamental difference between the Min systems in *E. coli* and *B. subtilis*, *E. coli* has MinE does not have the MinJ-DivIVA system. However, similar factors may exist to better protect the midcell Z rings against MinC/MinD in *E. coli* and it will be interesting to figure out the identity of these factors. Nevertheless, even if such factors exist, their protection is limited because the internal Z rings can be disrupted by MinC/MinD easily.

Chapter VI: Conclusions and discussions

Critical to our understanding of the spatial regulation of cytokinesis by the Min system is the mechanism of action of MinC, an inhibitor of Z ring formation (de Boer *et al.*, 1989, Hu et al., 1999). MinC has two structural domains (Hu & Lutkenhaus, 2000, Cordell et al., 2001), each of which can interact with FtsZ and block cell division, although the separated domains are much less active than the intact MinC (Shen & Lutkenhaus, 2009). However, it was not very clear how each domain of MinC interacts with FtsZ and the molecular mechanism by which each domain antagonizes FtsZ. The isolation of mutations in *ftsZ* in these studies allows discrimination of the interaction between FtsZ and the two domains of MinC. Residues in the extreme C-terminus of FtsZ (represented by I374) are critical for $MinC^{C}$/MinD-FtsZ interaction (Shen & Lutkenhaus, 2009) whereas residues in the H-10 helix containing N280 are essential for $MinC^{N}$-FtsZ interaction. By targeting different regions of FtsZ the two domains of MinC affect different aspects of Z ring formation to achieve synergy in disrupting Z rings.

Our findings that the two domains of MinC depend upon different regions of FtsZ suggest that they antagonize Z ring assembly by different mechanisms. $MinC^{N}$ has been shown to be able to block Z ring assembly and cell division in vivo and prevent FtsZ polymer sedimentation in vitro. It always puzzles people because $MinC^{N}$ disrupts FtsZ sedimentation without significantly affecting its GTPase. The GTPase activity of FtsZ requires FtsZ polymerization; no affect on the GTPase of FtsZ indicates that $MinC^{N}$ does not affect the de novo polymerization process. Alternatively, people suggest that $MinC^{N}$ may work after FtsZ polymer assembly. Evidence has been reported to support that $MinC^{N}$ does not reduce the amount of FtsZ in the polymer form but shortens the FstZ polymers significantly. Our results

showing that $MinC^N$ interacts with the H-10 helix of FtsZ puts more insight into the mechanism of $MinC^N$ attacking FtsZ polymers. The H-10 helix including the N280 residue critical for the $MinC^N$-FtsZ interaction is at the FtsZ dimer interface. $MinC^N$ binds to this H-10 helix at the dimerization interface of FtsZ subunits in a polymer to break and shorten the FtsZ polymer. Since $MinC^N$ is not able to break FtsZ polymers assembled with GMPCPP (a non-hydrolysable analogue of GTP) and $MinC^N$ does not affect the GTPase activity of FtsZ (if assembled with GTP), we propose that $MinC^N$ only attacks FtsZ dimer interfaces with GDP bound. In support of this, a significant fraction (can be up to 50%) of the subunits in FtsZ polymers are in the GDP form. GTP hydrolysis in the polymer weakens the FtsZ-FtsZ interaction and may expose the H-10 helix for $MinC^N$ binding and therefore allow $MinC^N$ to act as a wedge and sever the FtsZ polymer. In this way, $MinC^N$ frequently attacks and shortens the FtsZ polymers without affecting its GTPase significantly.

In contrast to $MinC^N$, $MinC^C$ does not affect cell division and FtsZ polymer assembly by itself. However, in the presence of MinD, $MinC^C$ is also able to inhibit cell division but the source of this toxicity was a mystery. Through isolating mutations in FtsZ that confer resistance to $MinC^C$/MinD, we realized that the extreme C terminal tail of FtsZ is critical for the inhibitory activity of $MinC^C$/MinD. This tail of FtsZ is very conserved in sequence and functions to attach FtsZ polymers to the membrane through interaction with FtsA and ZipA. Because $MinC^C$/MinD interacts with the same region of FstZ as FtsA and ZipA do, overproduction of $MinC^C$/MinD competes with and displaces FtsA and/or ZipA from the Z ring to inhibit division since the FtsA-FtsZ and ZipA-FtsZ interactions are essential for the formation and functionality of the Z ring. Careful examination revealed that $MinC^C$/MinD antagonizes the Z ring in a concentration dependent manner. At low concentrations, it displaces FtsA from the Z ring so that downstream

proteins are not recruited and the ring can not constrict. At higher concentrations, it probably also displaces ZipA and completely disrupts the Z ring (Shen & Lutkenhaus, 2009). $MinC^C$ has also been shown to block the lateral association of FtsZ polymers, which could contribute to the toxicity of $MinC^C$ too; however, this activity of $MinC^C$ does not require MinD.

In WT cells when full length MinC/MinD is present, any attempt to make polar Z rings is prevented by MinC/MinD concentrated at the poles through the Min oscillation. MinC/MinD localizes to membrane-associated FtsZ polymers through $MinC^C$/MinD interacting with the conserved C-terminal tail of FtsZ. By directly contacting FtsZ, $MinC^C$/MinD may compete with and release FtsA and/or ZipA from these FtsZ polymers so that they can not organize into Z rings; more importantly, this targeting of MinC/MinD to membrane-anchored FtsZ polymers brings $MinC^N$ in close proximity to these polymers, so that it is near its target. $MinC^N$ then breaks and destroys these polymers. The combination of these two activities makes MinC/MinD a potent division inhibitor.

During the course of this study, we accidentally found that the polar Z rings in the cell are more sensitive to MinC/MinD than midcell Z ring even in the absence of MinE. If MinC/MinD is induced in a Δmin strain, it will selectively disrupt the polar Z rings first, and later the midcell Z rings. The molecular basis of this differential MinC/MinD sensitivity between polar and midcell Z rings is currently unknown. But it is important to notice the existence of such a phenomenon because it may be a clue for understanding some undetermined aspects of Z ring assembly in the cell and/or the spatial regulation of cytokinesis by Min. It may also offer some insights to explain the non-minicelling phenotype of the two FtsZ mutants (BSZ374 and BSZ280D). If polar and midcell Z rings have different sensitivity to MinC/MinD, then the requirements for MinC/MinD to disrupt them may not be exactly the same. For example, the

interaction between $MinC^C$/MinD and FtsZ that is affected by the FtsZ-I374V mutation is important for MinC/MinD to work on midcell Z rings (as evidenced by MinC/MinD resistance of this mutant strain) but may not be so critical for it to destroy the polar Z rings (evidenced by no minicell production of the same mutant).

Our finding that polar and internal Z rings have differential sensitivity to MinC/MinD was unexpected. However, a consequence of this differential sensitivity is that expression of MinC/MinD in the absence of MinE can eliminate polar Z rings and minicell formation without inhibiting internal Z rings and causing filamentation. In an FtsZ-WT strain, this only occurres within a very narrow window of MinC/MinD induction and wild type morphology is not achieved. However, in a strain with FtsZ-I374V the differential sensitivity between polar and internal Z rings is magnified. This magnification is due to increased resistance of internal FtsZ-I374V rings to MinC/MinD but the sensitivity of polar Z rings is relatively unchanged. As a result a wide range of expression levels of MinC/MinD without MinE could suppress minicell formation in the FtsZ-I374V Δmin cells without affecting internal rings. At an intermediate level of MinC/MinD expression, minicell formation was suppressed and the complete wild type morphology was achieved. Thus, spatial regulation of Z ring assembly was obtained, not by pushing MinC/MinD to the poles though oscillation, but by an FtsZ mutation that markedly altered the differential sensitivity of internal and polar Z rings to MinC/MinD. This raises the question of why such a complex oscillation arose through evolution when a single mutation in FtsZ can achieve the same result without oscillation.

References

Adams, D. W. & J. Errington, (2009) Bacterial cell division: assembly, maintenance and disassembly of the Z ring. *Nat Rev Microbiol* **7**: 642-653.

Adler, H. I., W. D. Fisher, A. Cohen & A. A. Hardigree, (1967) MINIATURE escherichia coli CELLS DEFICIENT IN DNA. *Proc Natl Acad Sci U S A* **57**: 321-326.

Anderson, D. E., F. J. Gueiros-Filho & H. P. Erickson, (2004) Assembly dynamics of FtsZ rings in Bacillus subtilis and Escherichia coli and effects of FtsZ-regulating proteins. *J Bacteriol* **186**: 5775-5781.

Beall, B. & J. Lutkenhaus, (1991) FtsZ in Bacillus subtilis is required for vegetative septation and for asymmetric septation during sporulation. *Genes Dev* **5**: 447-455.

Bernhardt, T. G. & P. A. de Boer, (2005) SlmA, a nucleoid-associated, FtsZ binding protein required for blocking septal ring assembly over Chromosomes in E. coli. *Mol Cell* **18**: 555-564.

Bi, E. & J. Lutkenhaus, (1990) Analysis of ftsZ mutations that confer resistance to the cell division inhibitor SulA (SfiA). *J Bacteriol* **172**: 5602-5609.

Bi, E. & J. Lutkenhaus, (1993) Cell division inhibitors SulA and MinCD prevent formation of the FtsZ ring. *J Bacteriol* **175**: 1118-1125.

Bi, E. F. & J. Lutkenhaus, (1991) FtsZ ring structure associated with division in Escherichia coli. *Nature* **354**: 161-164.

Bramhill, D. & C. M. Thompson, (1994) GTP-dependent polymerization of Escherichia coli FtsZ protein to form tubules. *Proc Natl Acad Sci U S A* **91**: 5813-5817.

Bramkamp, M., R. Emmins, L. Weston, C. Donovan, R. A. Daniel & J. Errington, (2008) A novel component of the division-site selection system of Bacillus subtilis and a new mode of action for the division inhibitor MinCD. *Mol Microbiol* **70**: 1556-1569.

Bramkamp, M. & S. van Baarle, (2009) Division site selection in rod-shaped bacteria. *Curr Opin Microbiol* **12**: 683-688.

Chen, Y., K. Bjornson, S. D. Redick & H. P. Erickson, (2005) A rapid fluorescence assay for FtsZ assembly indicates cooperative assembly with a dimer nucleus. *Biophys J* **88**: 505-514.

Chen, Y. & H. P. Erickson, (2005) Rapid in vitro assembly dynamics and subunit turnover of FtsZ demonstrated by fluorescence resonance energy transfer. *J Biol Chem* **280**: 22549-22554.

Chen, Y. & H. P. Erickson, (2009) FtsZ filament dynamics at steady state: subunit exchange with and without nucleotide hydrolysis. *Biochemistry* **48**: 6664-6673.

Corbin, B. D., X. C. Yu & W. Margolin, (2002) Exploring intracellular space: function of the Min system in round-shaped Escherichia coli. *EMBO J* **21**: 1998-2008.

Cordell, S. C., R. E. Anderson & J. Lowe, (2001) Crystal structure of the bacterial cell division inhibitor MinC. *EMBO J* **20**: 2454-2461.

Dai, K. & J. Lutkenhaus, (1991) ftsZ is an essential cell division gene in Escherichia coli. *J Bacteriol* **173**: 3500-3506.

Dai, K. & J. Lutkenhaus, (1992) The proper ratio of FtsZ to FtsA is required for cell division to occur in Escherichia coli. *J Bacteriol* **174**: 6145-6151.

Dai, K., A. Mukherjee, Y. Xu & J. Lutkenhaus, (1994) Mutations in ftsZ that confer resistance to SulA affect the interaction of FtsZ with GTP. *J Bacteriol* **176**: 130-136.

Dajkovic, A., G. Lan, S. X. Sun, D. Wirtz & J. Lutkenhaus, (2008a) MinC spatially controls bacterial cytokinesis by antagonizing the scaffolding function of FtsZ. *Curr Biol* **18**: 235-244.

Dajkovic, A. & J. Lutkenhaus, (2006) Z ring as executor of bacterial cell division. *J Mol Microbiol Biotechnol* **11**: 140-151.

Dajkovic, A., A. Mukherjee & J. Lutkenhaus, (2008b) Investigation of regulation of FtsZ assembly by SulA and development of a model for FtsZ polymerization. *J Bacteriol* **190**: 2513-2526.

Datsenko, K. A. & B. L. Wanner, (2000) One-step inactivation of chromosomal genes in Escherichia coli K-12 using PCR products. *Proc Natl Acad Sci U S A* **97**: 6640-6645.

de Boer, P., R. Crossley & L. Rothfield, (1992a) The essential bacterial cell-division protein FtsZ is a GTPase. *Nature* **359**: 254-256.

de Boer, P. A., R. E. Crossley, A. R. Hand & L. I. Rothfield, (1991) The MinD protein is a membrane ATPase required for the correct placement of the Escherichia coli division site. *EMBO J* **10**: 4371-4380.

de Boer, P. A., R. E. Crossley & L. I. Rothfield, (1989) A division inhibitor and a topological specificity factor coded for by the minicell locus determine proper placement of the division septum in E. coli. *Cell* **56**: 641-649.

de Boer, P. A., R. E. Crossley & L. I. Rothfield, (1990) Central role for the Escherichia coli minC gene product in two different cell division-inhibition systems. *Proc Natl Acad Sci U S A* **87**: 1129-1133.

de Boer, P. A., R. E. Crossley & L. I. Rothfield, (1992b) Roles of MinC and MinD in the site-specific septation block mediated by the MinCDE system of Escherichia coli. *J Bacteriol* **174**: 63-70.

Drew, D. A., M. J. Osborn & L. I. Rothfield, (2005) A polymerization-depolymerization model that accurately generates the self-sustained oscillatory system involved in bacterial division site placement. *Proc Natl Acad Sci U S A* **102**: 6114-6118.

Ebersbach, G., E. Galli, J. Moller-Jensen, J. Lowe & K. Gerdes, (2008) Novel coiled-coil cell division factor ZapB stimulates Z ring assembly and cell division. *Mol Microbiol* **68**: 720-735.

Edwards, D. H. & J. Errington, (1997) The Bacillus subtilis DivIVA protein targets to the division septum and controls the site specificity of cell division. *Mol Microbiol* **24**: 905-915.

Erickson, H. P., D. W. Taylor, K. A. Taylor & D. Bramhill, (1996) Bacterial cell division protein FtsZ assembles into protofilament sheets and minirings, structural homologs of tubulin polymers. *Proc Natl Acad Sci U S A* **93**: 519-523.

Feucht, A., I. Lucet, M. D. Yudkin & J. Errington, (2001) Cytological and biochemical characterization of the FtsA cell division protein of Bacillus subtilis. *Mol Microbiol* **40**: 115-125.

Fu, X., Y. L. Shih, Y. Zhang & L. I. Rothfield, (2001) The MinE ring required for proper placement of the division site is a mobile structure that changes its cellular location during the Escherichia coli division cycle. *Proc Natl Acad Sci U S A* **98**: 980-985.

Geissler, B., D. Elraheb & W. Margolin, (2003) A gain-of-function mutation in ftsA bypasses the requirement for the essential cell division gene zipA in Escherichia coli. *Proc Natl Acad Sci U S A* **100**: 4197-4202.

Goehring, N. W. & J. Beckwith, (2005) Diverse paths to midcell: assembly of the bacterial cell division machinery. *Curr Biol* **15**: R514-526.

Gonzalez, J. M., M. Velez, M. Jimenez, C. Alfonso, P. Schuck, J. Mingorance, M. Vicente, A. P. Minton & G. Rivas, (2005) Cooperative behavior of Escherichia coli cell-division protein FtsZ assembly involves the preferential cyclization of long single-stranded fibrils. *Proc Natl Acad Sci U S A* **102**: 1895-1900.

Gregory, J. A., E. C. Becker & K. Pogliano, (2008) Bacillus subtilis MinC destabilizes FtsZ-rings at new cell poles and contributes to the timing of cell division. *Genes Dev* **22**: 3475-3488.

Gueiros-Filho, F. J. & R. Losick, (2002) A widely conserved bacterial cell division protein that promotes assembly of the tubulin-like protein FtsZ. *Genes Dev* **16**: 2544-2556.

Hale, C. A. & P. A. de Boer, (1997) Direct binding of FtsZ to ZipA, an essential component of the septal ring structure that mediates cell division in E. coli. *Cell* **88**: 175-185.

Hale, C. A., H. Meinhardt & P. A. de Boer, (2001) Dynamic localization cycle of the cell division regulator MinE in Escherichia coli. *EMBO J* **20**: 1563-1572.

Hale, C. A., A. C. Rhee & P. A. de Boer, (2000) ZipA-induced bundling of FtsZ polymers mediated by an interaction between C-terminal domains. *J Bacteriol* **182**: 5153-5166.

Handler, A. A., J. E. Lim & R. Losick, (2008) Peptide inhibitor of cytokinesis during sporulation in Bacillus subtilis. *Mol Microbiol* **68**: 588-599.

Haney, S. A., E. Glasfeld, C. Hale, D. Keeney, Z. He & P. de Boer, (2001) Genetic analysis of the Escherichia coli FtsZ.ZipA interaction in the yeast two-hybrid system. Characterization of FtsZ residues essential for the interactions with ZipA and with FtsA. *J Biol Chem* **276**: 11980-11987.

Harry, E., L. Monahan & L. Thompson, (2006) Bacterial cell division: the mechanism and its precison. *Int Rev Cytol* **253**: 27-94.

Hirota, Y., A. Ryter & F. Jacob, (1968) Thermosensitive mutants of E. coli affected in the processes of DNA synthesis and cellular division. *Cold Spring Harb Symp Quant Biol* **33**: 677-693.

Howard, M. & K. Kruse, (2005) Cellular organization by self-organization: mechanisms and models for Min protein dynamics. *J Cell Biol* **168**: 533-536.

Hu, Z., E. P. Gogol & J. Lutkenhaus, (2002) Dynamic assembly of MinD on phospholipid vesicles regulated by ATP and MinE. *Proc Natl Acad Sci U S A* **99**: 6761-6766.

Hu, Z. & J. Lutkenhaus, (1999) Topological regulation of cell division in Escherichia coli involves rapid pole to pole oscillation of the division inhibitor MinC under the control of MinD and MinE. *Mol Microbiol* **34**: 82-90.

Hu, Z. & J. Lutkenhaus, (2000) Analysis of MinC reveals two independent domains involved in interaction with MinD and FtsZ. *J Bacteriol* **182**: 3965-3971.

Hu, Z. & J. Lutkenhaus, (2001) Topological regulation of cell division in E. coli. spatiotemporal oscillation of MinD requires stimulation of its ATPase by MinE and phospholipid. *Mol Cell* **7**: 1337-1343.

Hu, Z. & J. Lutkenhaus, (2003) A conserved sequence at the C-terminus of MinD is required for binding to the membrane and targeting MinC to the septum. *Mol Microbiol* **47**: 345-355.

Hu, Z., A. Mukherjee, S. Pichoff & J. Lutkenhaus, (1999) The MinC component of the division site selection system in Escherichia coli interacts with FtsZ to prevent polymerization. *Proc Natl Acad Sci U S A* **96**: 14819-14824.

Hu, Z., C. Saez & J. Lutkenhaus, (2003) Recruitment of MinC, an inhibitor of Z-ring formation, to the membrane in Escherichia coli: role of MinD and MinE. *J Bacteriol* **185**: 196-203.

Huang, J., C. Cao & J. Lutkenhaus, (1996) Interaction between FtsZ and inhibitors of cell division. *J Bacteriol* **178**: 5080-5085.

Huang, K. C., Y. Meir & N. S. Wingreen, (2003) Dynamic structures in Escherichia coli: spontaneous formation of MinE rings and MinD polar zones. *Proc Natl Acad Sci U S A* **100**: 12724-12728.

Huisman, O., R. D'Ari & S. Gottesman, (1984) Cell-division control in Escherichia coli: specific induction of the SOS function SfiA protein is sufficient to block septation. *Proc Natl Acad Sci U S A* **81**: 4490-4494.

Ishikawa, S., Y. Kawai, K. Hiramatsu, M. Kuwano & N. Ogasawara, (2006) A new FtsZ-interacting protein, YlmF, complements the activity of FtsA during progression of cell division in Bacillus subtilis. *Mol Microbiol* **60**: 1364-1380.

Johnson, J. E., L. L. Lackner & P. A. de Boer, (2002) Targeting of (D)MinC/MinD and (D)MinC/DicB complexes to septal rings in Escherichia coli suggests a multistep mechanism for MinC-mediated destruction of nascent FtsZ rings. *J Bacteriol* **184**: 2951-2962.

Johnson, J. E., L. L. Lackner, C. A. Hale & P. A. de Boer, (2004) ZipA is required for targeting of DMinC/DicB, but not DMinC/MinD, complexes to septal ring assemblies in Escherichia coli. *J Bacteriol* **186**: 2418-2429.

Justice, S. S., J. Garcia-Lara & L. I. Rothfield, (2000) Cell division inhibitors SulA and MinC/MinD block septum formation at different steps in the assembly of the Escherichia coli division machinery. *Mol Microbiol* **37**: 410-423.

Kelly, A. J., M. J. Sackett, N. Din, E. Quardokus & Y. V. Brun, (1998) Cell cycle-dependent transcriptional and proteolytic regulation of FtsZ in Caulobacter. *Genes Dev* **12**: 880-893.

Koppelman, C. M., T. Den Blaauwen, M. C. Duursma, R. M. Heeren & N. Nanninga, (2001) Escherichia coli minicell membranes are enriched in cardiolipin. *J Bacteriol* **183**: 6144-6147.

Lackner, L. L., D. M. Raskin & P. A. de Boer, (2003) ATP-dependent interactions between Escherichia coli Min proteins and the phospholipid membrane in vitro. *J Bacteriol* **185**: 735-749.

Lara, B., A. I. Rico, S. Petruzzelli, A. Santona, J. Dumas, J. Biton, M. Vicente, J. Mingorance & O. Massidda, (2005) Cell division in cocci: localization and properties of the Streptococcus pneumoniae FtsA protein. *Mol Microbiol* **55**: 699-711.

Li, Z., M. J. Trimble, Y. V. Brun & G. J. Jensen, (2007) The structure of FtsZ filaments in vivo suggests a force-generating role in cell division. *EMBO J* **26**: 4694-4708.

Liu, Z., A. Mukherjee & J. Lutkenhaus, (1999) Recruitment of ZipA to the division site by interaction with FtsZ. *Mol Microbiol* **31**: 1853-1861.

Loose, M., E. Fischer-Friedrich, J. Ries, K. Kruse & P. Schwille, (2008) Spatial regulators for bacterial cell division self-organize into surface waves in vitro. *Science* **320**: 789-792.

Low, H. H., M. C. Moncrieffe & J. Lowe, (2004) The crystal structure of ZapA and its modulation of FtsZ polymerisation. *J Mol Biol* **341**: 839-852.

Lowe, J., (1998) Crystal structure determination of FtsZ from Methanococcus jannaschii. *J Struct Biol* **124**: 235-243.
Lowe, J. & L. A. Amos, (1998) Crystal structure of the bacterial cell-division protein FtsZ. *Nature* **391**: 203-206.
Lowe, J., H. Li, K. H. Downing & E. Nogales, (2001) Refined structure of alpha beta-tubulin at 3.5 A resolution. *J Mol Biol* **313**: 1045-1057.
Lutkenhaus, J., (2007) Assembly dynamics of the bacterial MinCDE system and spatial regulation of the Z ring. *Annu Rev Biochem* **76**: 539-562.
Lutkenhaus, J., B. Sanjanwala & M. Lowe, (1986) Overproduction of FtsZ suppresses sensitivity of lon mutants to division inhibition. *J Bacteriol* **166**: 756-762.
Ma, X., D. W. Ehrhardt & W. Margolin, (1996) Colocalization of cell division proteins FtsZ and FtsA to cytoskeletal structures in living Escherichia coli cells by using green fluorescent protein. *Proc Natl Acad Sci U S A* **93**: 12998-13003.
Ma, X. & W. Margolin, (1999) Genetic and functional analyses of the conserved C-terminal core domain of Escherichia coli FtsZ. *J Bacteriol* **181**: 7531-7544.
Margolin, W., (2002) Bacterial sporulation: FtsZ rings do the twist. *Curr Biol* **12**: R391-392.
Margolin, W., (2005) FtsZ and the division of prokaryotic cells and organelles. *Nat Rev Mol Cell Biol* **6**: 862-871.
Meinhardt, H. & P. A. de Boer, (2001) Pattern formation in Escherichia coli: a model for the pole-to-pole oscillations of Min proteins and the localization of the division site. *Proc Natl Acad Sci U S A* **98**: 14202-14207.
Michie, K. A. & J. Lowe, (2006) Dynamic filaments of the bacterial cytoskeleton. *Annu Rev Biochem* **75**: 467-492.
Mileykovskaya, E. & W. Dowhan, (2000) Visualization of phospholipid domains in Escherichia coli by using the cardiolipin-specific fluorescent dye 10-N-nonyl acridine orange. *J Bacteriol* **182**: 1172-1175.
Mosyak, L., Y. Zhang, E. Glasfeld, S. Haney, M. Stahl, J. Seehra & W. S. Somers, (2000) The bacterial cell-division protein ZipA and its interaction with an FtsZ fragment revealed by X-ray crystallography. *EMBO J* **19**: 3179-3191.
Moy, F. J., E. Glasfeld, L. Mosyak & R. Powers, (2000) Solution structure of ZipA, a crucial component of Escherichia coli cell division. *Biochemistry* **39**: 9146-9156.
Mukherjee, A., C. Cao & J. Lutkenhaus, (1998) Inhibition of FtsZ polymerization by SulA, an inhibitor of septation in Escherichia coli. *Proc Natl Acad Sci U S A* **95**: 2885-2890.
Mukherjee, A., K. Dai & J. Lutkenhaus, (1993) Escherichia coli cell division protein FtsZ is a guanine nucleotide binding protein. *Proc Natl Acad Sci U S A* **90**: 1053-1057.
Mukherjee, A. & J. Lutkenhaus, (1994) Guanine nucleotide-dependent assembly of FtsZ into filaments. *J Bacteriol* **176**: 2754-2758.
Mukherjee, A. & J. Lutkenhaus, (1998a) Dynamic assembly of FtsZ regulated by GTP hydrolysis. *EMBO J* **17**: 462-469.
Mukherjee, A. & J. Lutkenhaus, (1998b) Purification, assembly, and localization of FtsZ. *Methods Enzymol* **298**: 296-305.
Mulder, E. & C. L. Woldringh, (1989) Actively replicating nucleoids influence positioning of division sites in Escherichia coli filaments forming cells lacking DNA. *J Bacteriol* **171**: 4303-4314.
Oliva, M. A., S. C. Cordell & J. Lowe, (2004) Structural insights into FtsZ protofilament formation. *Nat Struct Mol Biol* **11**: 1243-1250.

Oosawa, F. & M. Kasai, (1962) A theory of linear and helical aggregations of macromolecules. *J Mol Biol* **4**: 10-21.
Osawa, M., D. E. Anderson & H. P. Erickson, (2008) Reconstitution of contractile FtsZ rings in liposomes. *Science* **320**: 792-794.
Patrick, J. E. & D. B. Kearns, (2008) MinJ (YvjD) is a topological determinant of cell division in Bacillus subtilis. *Mol Microbiol* **70**: 1166-1179.
Pichoff, S. & J. Lutkenhaus, (2001) Escherichia coli division inhibitor MinCD blocks septation by preventing Z-ring formation. *J Bacteriol* **183**: 6630-6635.
Pichoff, S. & J. Lutkenhaus, (2002) Unique and overlapping roles for ZipA and FtsA in septal ring assembly in Escherichia coli. *EMBO J* **21**: 685-693.
Pichoff, S. & J. Lutkenhaus, (2005) Tethering the Z ring to the membrane through a conserved membrane targeting sequence in FtsA. *Mol Microbiol* **55**: 1722-1734.
Pichoff, S. & J. Lutkenhaus, (2007) Identification of a region of FtsA required for interaction with FtsZ. *Mol Microbiol* **64**: 1129-1138.
Quardokus, E., N. Din & Y. V. Brun, (1996) Cell cycle regulation and cell type-specific localization of the FtsZ division initiation protein in Caulobacter. *Proc Natl Acad Sci U S A* **93**: 6314-6319.
Raskin, D. M. & P. A. de Boer, (1997) The MinE ring: an FtsZ-independent cell structure required for selection of the correct division site in E. coli. *Cell* **91**: 685-694.
Raskin, D. M. & P. A. de Boer, (1999a) MinDE-dependent pole-to-pole oscillation of division inhibitor MinC in Escherichia coli. *J Bacteriol* **181**: 6419-6424.
Raskin, D. M. & P. A. de Boer, (1999b) Rapid pole-to-pole oscillation of a protein required for directing division to the middle of Escherichia coli. *Proc Natl Acad Sci U S A* **96**: 4971-4976.
Rothfield, L., A. Taghbalout & Y. L. Shih, (2005) Spatial control of bacterial division-site placement. *Nat Rev Microbiol* **3**: 959-968.
Rueda, S., M. Vicente & J. Mingorance, (2003) Concentration and assembly of the division ring proteins FtsZ, FtsA, and ZipA during the Escherichia coli cell cycle. *J Bacteriol* **185**: 3344-3351.
Sanchez, M., A. Valencia, M. J. Ferrandiz, C. Sander & M. Vicente, (1994) Correlation between the structure and biochemical activities of FtsA, an essential cell division protein of the actin family. *EMBO J* **13**: 4919-4925.
Shen, B. & J. Lutkenhaus, (2009) The conserved C-terminal tail of FtsZ is required for the septal localization and division inhibitory activity of MinC(C)/MinD. *Mol Microbiol* **72**: 410-424.
Shen, B. & J. Lutkenhaus, (2010) Examination of the interaction between FtsZ and $MinC^N$ in E. coli suggests how MinC disrupts Z rings. *Mol Microbiol* **75**: 1285-1298.
Shiomi, D. & W. Margolin, (2007) The C-terminal domain of MinC inhibits assembly of the Z ring in Escherichia coli. *J Bacteriol* **189**: 236-243.
Singh, J. K., R. D. Makde, V. Kumar & D. Panda, (2007) A membrane protein, EzrA, regulates assembly dynamics of FtsZ by interacting with the C-terminal tail of FtsZ. *Biochemistry* **46**: 11013-11022.
Small, E., R. Marrington, A. Rodger, D. J. Scott, K. Sloan, D. Roper, T. R. Dafforn & S. G. Addinall, (2007) FtsZ polymer-bundling by the Escherichia coli ZapA orthologue, YgfE, involves a conformational change in bound GTP. *J Mol Biol* **369**: 210-221.

Stricker, J., P. Maddox, E. D. Salmon & H. P. Erickson, (2002) Rapid assembly dynamics of the Escherichia coli FtsZ-ring demonstrated by fluorescence recovery after photobleaching. *Proc Natl Acad Sci U S A* **99**: 3171-3175.

Trusca, D., S. Scott, C. Thompson & D. Bramhill, (1998) Bacterial SOS checkpoint protein SulA inhibits polymerization of purified FtsZ cell division protein. *J Bacteriol* **180**: 3946-3953.

Van De Putte, P., D. Van & A. Roersch, (1964) The Selection of Mutants of Escherichia Coli with Impaired Cell Division at Elevated Temperature. *Mutat Res* **106**: 121-128.

van den Ent, F. & J. Lowe, (2000) Crystal structure of the cell division protein FtsA from Thermotoga maritima. *EMBO J* **19**: 5300-5307.

Varma, A., K. C. Huang & K. D. Young, (2008) The Min system as a general cell geometry detection mechanism: branch lengths in Y-shaped Escherichia coli cells affect Min oscillation patterns and division dynamics. *J Bacteriol* **190**: 2106-2117.

Wang, L. & J. Lutkenhaus, (1998) FtsK is an essential cell division protein that is localized to the septum and induced as part of the SOS response. *Mol Microbiol* **29**: 731-740.

Weart, R. B., A. H. Lee, A. C. Chien, D. P. Haeusser, N. S. Hill & P. A. Levin, (2007) A metabolic sensor governing cell size in bacteria. *Cell* **130**: 335-347.

Weart, R. B. & P. A. Levin, (2003) Growth rate-dependent regulation of medial FtsZ ring formation. *J Bacteriol* **185**: 2826-2834.

Weiss, D. S., J. C. Chen, J. M. Ghigo, D. Boyd & J. Beckwith, (1999) Localization of FtsI (PBP3) to the septal ring requires its membrane anchor, the Z ring, FtsA, FtsQ, and FtsL. *J Bacteriol* **181**: 508-520.

Wu, L. J. & J. Errington, (2004) Coordination of cell division and chromosome segregation by a nucleoid occlusion protein in Bacillus subtilis. *Cell* **117**: 915-925.

Wu, L. J., S. Ishikawa, Y. Kawai, T. Oshima, N. Ogasawara & J. Errington, (2009) Noc protein binds to specific DNA sequences to coordinate cell division with chromosome segregation. *EMBO J* **28**: 1940-1952.

Yu, X. C. & W. Margolin, (1999) FtsZ ring clusters in min and partition mutants: role of both the Min system and the nucleoid in regulating FtsZ ring localization. *Mol Microbiol* **32**: 315-326.

Zhou, H. & J. Lutkenhaus, (2003) Membrane binding by MinD involves insertion of hydrophobic residues within the C-terminal amphipathic helix into the bilayer. *J Bacteriol* **185**: 4326-4335.

Zhou, H. & J. Lutkenhaus, (2005) MinC mutants deficient in MinD- and DicB-mediated cell division inhibition due to loss of interaction with MinD, DicB, or a septal component. *J Bacteriol* **187**: 2846-2857.